1986

Iron-sulfur cluster assembly in aqueous media

William Charles Stevens
Iowa State University

Stevens, William Charles

IRON-SULFUR CLUSTER ASSEMBLY IN AQUEOUS MEDIA

Iowa State University PH.D. 1986

Iron-sulfur cluster assembly in aqueous media

by

William Charles Stevens

A Dissertation Submitted to the

Graduate Faculty in Partial Fulfillment of the

Requirements for the Degree of

DOCTOR OF PHILOSOPHY

Department: Chemistry
Major: Inorganic Chemistry

Approved:

Signature was redacted for privacy.

In Charge of Major Work

Signature was redacted for privacy.

For the Major Department

Signature was redacted for privacy.

For the Graduate College

Iowa State University
Ames, Iowa

1986

TABLE OF CONTENTS

INTRODUCTION

Iron-Sulfur Proteins

The discovery of iron-sulfur proteins in the years surrounding 1960 heralded an area of considerable interest and activity which persists today in biochemistry and inorganic chemistry at seemingly unabating intensity. As Holm has remarked,[1] "With the possible exception of heme proteins no class of metalloproteins has been as thoroughly investigated in the last decade as the nonheme iron-sulfur proteins...."

In 1958, San Pietro and Lang[2] discovered a protein they named Photosynthetic Pyridine Nucleotide Reductase (PPNR). Isolated from spinach chloroplasts in 1962 by Appella and San Pietro,[3] PPNR was the subject of the first quantitative estimation of iron and sulfur content by Fry and San Pietro[4] the same year. Also in 1962, Mortenson, Valentine and Carnahan[5] isolated an iron-sulfur protein, which they named "ferredoxin", from the bacterium Clostridium pasteurianum. This protein was crystallized in a pure state by Tagawa and Arnon[6] in 1962 who also applied the name "ferredoxin" to PPNR from spinach chloroplasts. All these iron-containing proteins, plus High-Potential Iron Protein (HiPIP) isolated from the bacterium Chromatium vinosum in 1963 by Bartsch,[7] also contain the inorganic or "acid-labile" sulfur first noticed by Massey in 1957 as H_2S evolved upon acidification of succinate dehydrogenase.[8] The last member to be

admitted to the class of iron-sulfur proteins was rubredoxin, first isolated in 1965 from C. pasteurianum by Lovenberg and Sobel,[9a,b] which contains no acid-labile sulfur.

Iron-sulfur proteins are widely distributed in nature, participating in photosynthesis, nitrogen fixation, hydrogen metabolism, sulfate reduction, methanogenesis, etc., their chief role being one of electron transport. Rubredoxins contain the tetrahedral $[Fe(S\text{-}cys)_4]$ (S-cys denotes a coordinated, deprotonated cysteine amino acid) active site 1 and are found in numerous anaerobic and aerobic bacteria. In most cases, its physiological role has not been established, as is the case with many HiPIPs.

Ferredoxins are of two major types. The green plant ferredoxins have 2 as their active site; however, [2Fe-2S] proteins are also found in the adrenal glands of animals and in bacteria. The four-iron, four-sulfur active site 3 is shared by bacterial ferredoxins and high-potential iron proteins. Indeed, it has recently been decided that the term "ferredoxin" should encompass both types of proteins irrespective of their reduction potentials.

Though a variety of oxidation levels appear accessible to these active sites, only one redox couple for each protein is physiologically relevant as these proteins undergo only a one-electron reversible reduction at moderate potentials. These couples are delineated below.

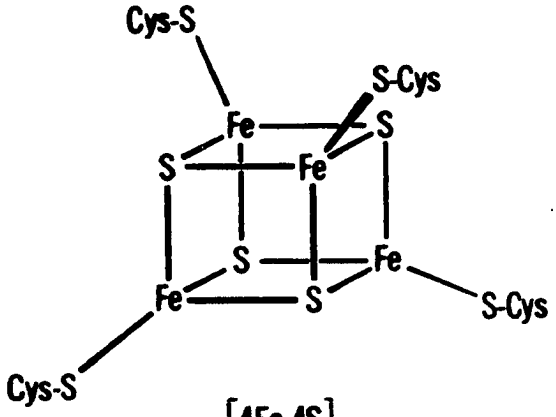

[4Fe-4S]

1

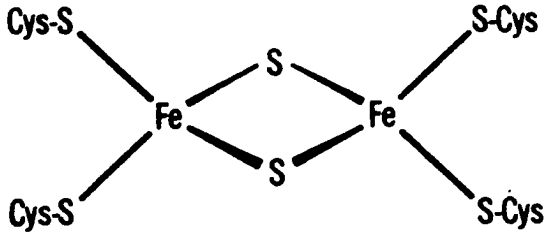

[2Fe-2S]

2

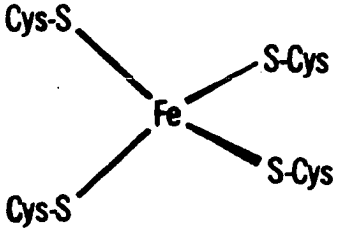

3

Figure 1. Active sites of iron-sulfur proteins

$$\underset{\substack{Rd_{ox}\\Fe(III)}}{Fe(S\text{-}cys)_4^-} \quad \overset{E^{o'} = -0.04 \text{ to } -0.06V}{\rightleftharpoons} \quad \underset{\substack{Rd_{red}\\Fe(II)}}{Fe(S\text{-}cys)_4^{2-}}$$

$$\underset{\substack{Fd_{ox}\\2Fe(III)\\[2Fe\text{-}2S]^{3+}}}{Fe_2S_2(S\text{-}cys)_4^{2-}} \quad \overset{E^{o'} = -0.24 \text{ to } -0.43V}{\rightleftharpoons} \quad \underset{\substack{Fd_{red}\\Fe(II),Fe(III)\\[2Fe\text{-}2S]^{+}}}{Fe_2S_2(S\text{-}cys)_4^{3-}}$$

$$\underset{\substack{HiPIP_{ox}\\3Fe(III),Fe(II)\\[4Fe\text{-}4S]^{3+}}}{Fe_4S_4(S\text{-}cys)_4^-} \quad \overset{E^{o'} \approx +0.35V}{\rightleftharpoons} \quad \underset{\substack{HiPIP_{red},Fd_{ox}\\2Fe(III),2Fe(II)\\[4Fe\text{-}4S]^{2+}}}{Fe_4S_4(S\text{-}cys)_4^{2-}} \quad \overset{E^{o'} = -0.28 \text{ to } -0.49V}{\rightleftharpoons} \quad \underset{\substack{Fd_{red}\\3Fe(II),Fe(III)\\[4Fe\text{-}4S]^{+}}}{Fe_4S_4(S\text{-}cys)_4^{3-}}$$

It is well-established that these iron-sulfur centers are responsible for the catalytic activity of these proteins. The active sites of these proteins can be removed by a variety of methods. Lovenberg, Buchanan and Rabinowitz[10] obtained an apoferredoxin by treating clostridial ferredoxin with a mercurial. Isolated in 1966,[11] the apoprotein exhibits no visible absorption spectrum and no catalytic activity. Apoproteins can also be generated by treatment with α,α'-bipyridyl.[12] Later methods[13-17] involve denaturing the protein with DMSO and extruding the iron-sulfur core intact with thiophenol. Extensions of these intact core extrusion methods in aqueous surfactant solutions will be discussed in a later section.

All of these apoproteins can be reconstituted to exhibit characteristics and activities identical to those of the native proteins by treatment with Fe^{2+} or Fe^{3+} and sulfide with mercaptoethanol, the latter apparently being necessary to reduce any disulfide bonds formed during oxidation of the apoprotein.[18-20]

Because all these iron-sulfur proteins entail roughly tetrahedral coordination by four cysteine residues, and because the amino acid sequences among them are often strikingly similar,[21-23] one could expect that apoproteins could accept, upon reconstitution, a core different from its original. This is indeed the case, as Christou, Ridge, and Rydon[24] have accomplished the conversion of C.p. rubredoxin to a metastable [4Fe-4S] metalloprotein. Sugiura et al.[25] have accomplished the conversion of apoadrenodoxin to a rubredoxin-like derivative, then to the native [2Fe-2S] protein.

SYNTHETIC ANALOGS: HISTORICAL PERSPECTIVE

Synthetic analogs for the active sites of these iron-sulfur proteins were a particularly attractive goal because detailed physical and chemical characterizations are often rendered difficult by the surrounding matrix of proteins. When these model compounds could be established as faithful representations of their biological analogs by correlating their structures and various spectral characteristics, they might allow insight into how the protein environment influences the chemistry at the active site. In addition, by delineating the pathways of assembly of the synthetic analogs, one might gain insight into the mechanisms of assembly of iron-sulfur sites in vivo.

The first successful reconstitution of an apoferredoxin (i.e., a protein from which the Fe-S cluster had been removed) was announced by Hong and Rabinowitz in 1967.[26] They found that they could restore the apoprotein to full activity by combining it with an aqueous solution of mercaptoethanol, sodium sulfide, and Fe^{2+} or Fe^{3+}. Within the next few years, many other ferredoxins were found to be amenable to the same process. In like fashion, came the first attempt at a synthetic analog from Yang and Huennekens in 1970.[27] From the same reagents, but without the apoprotein, they obtained in solution a complex whose absorption spectrum strongly resembled those of plant ferredoxins. They also established that complex formation was maximized when iron and sulfur were present in equimolar quantities, drawing the analogy to the equimolar iron-sulfur constitution of the proteins, but they proposed

unfortunate octahedral models which invoked coordination of the hydroxylic groups of the mercaptoethanol ligands and they could not isolate their product.

Since that time, the great majority of advances in this area have occurred in the laboratories of Richard Holm who has worked in tandem with crystallographer James Ibers. In 1972, Herskovitz et al. reported the preparation, structure, and properties of $(Et_4N)_2$ $[Fe_4S_4(SCH_2Ph)_4]$ thereby "clearly demonstrating that a structure closely related to that of the active site of four- and eight-iron bacterial proteins can be stabilized in discrete synthetic complexes...."[28] The active site of Chromatium high-potential iron protein had recently been studied crystallographically at 2.25 Å resolution by Carter et al.[29] and the geometry and dimensions of the [4Fe-4S] core were in agreement. Furthermore, magnetic susceptibilities, Mössbauer parameters and electronic spectra of an oxidized ferredoxin, reduced high-potential iron-protein, and the model compound were comparable.

Synthetic details were presented some months later for a number of these four-iron, four-sulfur clusters with various thiolate ligands.[30] Performing all operations under an atmosphere of pure dinitrogen, these clusters were assembled from methanolic solutions of ferric chloride, thiol, sodium hydrosulfide, and sodium methoxide in reactions with the stoichiometry:

$$4FeCl_3 + 6NaSR + 4NaHS + 4NaOMe \xrightarrow{MeOH} Na_2[Fe_4S_4(SR)]_4 + RSSR + 12NaCl + 4MeOH \quad (1)$$

Yields of pure products varied from 30 to 77% (depending on the nature of the thiolate) after isolation of the clusters as air-sensitive salts of various quaternary ammonium cations.

An active site analog for the two-iron, two-sulfur ferredoxins was first prepared in 1973 by employing the chelating ligand o-xylyl-α,α'-dithiolate (S_2-o-xylyl).[31] The compound, $[Fe_2S_2(S_2\text{-o-xylyl})_2]^{2-}$, was later found to undergo ligand substitution by other thiols (vide infra) to afford a variety of anionic clusters of composition $[Fe_2S_2(SR)_4]^{2-}$.[32] These results were the culmination of synthetic efforts based on some good guesswork which was directed by careful analysis of physico-chemical data for spinach ferredoxin and related proteins. Earlier studies[33,34] had already suggested the bitetrahedral $Fe_2S_2(S\text{-cys})_4$ formulation for the active site. Noting the structural similarity between this unit and the faces of [4Fe-4S] cores, Mayerle and coworkers may have discovered the chemical relationship which prompted them to select a chelating dithiolate which could not span the thiolate coordination sites within a tetrameric cluster.

Isolated as salts of quaternary ammonium and phosphonium cations, $[Fe_2S_2(S_2\text{-o-xylyl})_2]^{2-}$ was prepared by the general reaction:

$$2FeCl_3 + 4NaSR + 2NaHS + 2NaOMe \xrightarrow{MeOH} Na_2[Fe_2S_2(SR)_4] + 6NaCl + 4MeOH \quad (2)$$

This preparation succeeds only when $2RS^- = C_6H_4(CH_2S)_2^{2-}$. If a monodentate thiol is employed, the only iron-sulfur product isolated is the tetrameric $[Fe_4S_4(SR)_4]^{2-}$.

Though x-ray crystallographic studies were not to confirm the structure of the [2Fe-2S] active sites in proteins until 1980, the validity of the analog was well-established by the strong similarities of electronic spectra, Mössbauer parameters, and magnetic susceptibilities.[31,32]

The simplest of these active site analogs was actually the last to be prepared. The rubredoxins, the only iron-sulfur proteins lacking acid-labile sulfide, were well characterized by the early 1970s. First detected in 1963 by Buchanan et al.[35] and Mortenson,[36] the $Fe(S\text{-}cys)_4$ active site with nearly tetrahedral geometry was firmly established on the basis of chemical and spectroscopic properties[37] before the x-ray diffraction studies[38,39] confirmed the formulation.

Coucouvanis and coworkers had previously prepared tetrakis (benzene-thiolate) iron (II)[40] from a dithiosquarate complex,[41] with both of these latter compounds serving as crude approximations of the rubredoxin site, when efforts using aliphatic thiols began to bear fruit in 1975.[42,43]

Again, using o-xylyldithiol (a benzylic rather than strictly aliphatic, thiol), tetrahedral, thiolate - ligated complexes were prepared of both iron (II) and iron (III) from the following reaction:

$$(Et_4N)_2[FeCl_4] + 2Na_2[(SCH_2)_2C_6H_4] \xrightarrow{EtOH} (Et_4N)_2[Fe(S_2\text{-}o\text{-}xylyl)_2] + 4NaCl \quad (3)$$

Solutions of the product produce the iron (III) species upon exposure to air. The iron(II) and iron(III) compounds are analogs for rubredoxins in the reduced and oxidized state.

While electronic absorption and Mossbauer spectra did establish the correlation, the strongest confirmation came from x-ray diffraction work. Lane et al.[42,43] determined the structures of both $(Et_4N)[Fe(S_2\text{-}o\text{-}xylyl)_2]$ and an acetonitrile adduct of $Na(Ph_4P)[Fe(S_2\text{-}o\text{-}xylyl)_2]$. These anions are very nearly tetrahedral with iron-sulfur distances practically invariant within each species. The iron (III) anion has those distances in the range of 2.267 ± 0.009 Å with S-Fe-S angles averaging 109.46 ± 2.17 degrees.

In a 1.2 Å refinement of the x-ray structure of C.p. rubredoxin,[44,45] the four iron-sulfur distances are nearly equivalent, their mean value of 2.29 Å in good agreement with the oxidized form of the analog. Thus, it appears now that most known one-iron, two-iron, and four-iron active sites are represented by synthetic analogs of nearly identical geometries with similar spectroscopic properties.

There remains, at the time of this writing, the question of the nature and existence in vivo of three-iron centers in some ferredoxins. Azotobacter vinelandii Fd I was first isolated in 1970.[46,47] The protein was originally thought to contain two [4Fe-4S] centers in the HiPIP oxidation level on the basis of EPR results and core extrusion studies.[14,48,49] However, analyses persistently indicated that only

seven irons and seven sulfurs were present.[50] Refinement of the x-ray data to 2 Å resolution finally permitted identification of a [3Fe-3S] moiety.[51]

Subsequent to the work on A.v. Fd I, Desulfovibrio gigas Fd II, which consists of four subunits, was found to contain a [3Fe-3S] center in each one.[52] It should be noted, however, that most of these studies -- especially the x-ray work of Stout and coworkers -- have been performed on proteins which have been subjected to aerobic isolation and purification. A very recent study has found that apoferredoxin I from A. vinelandii can be reconstituted anaerobically to give an eight-iron instead of a seven-iron protein. Furthermore, the eight iron-protein so constituted decomposes in air to give the 7-Fe Fd I in low yield.[53]

Several lines of evidence also point to the existence of a [3Fe-4S] center in certain proteins. It is similar to the [3Fe-3S] center except that another bridging sulfide has replaced an aquo and a cysteine ligand.

Anaerobic addition of Fe^{2+} results in conversion to a [4Fe-4S] center.[54] Thus, the [3Fe-3S] and [3Fe-4S] centers may be artifacts of oxidation arising during purification of some iron-sulfur proteins. These centers are also the only two which have not yet been modeled synthetically.

Since their original preparations, the syntheses of these active site analogs have undergone some modifications. In 1974, Schrauzer et al.[55] found that $[Fe_4S_4(SR)_4]^{2-}$ could be prepared using Li_2S, thereby eliminating the need for prior preparation of the hydrosulfide salts.

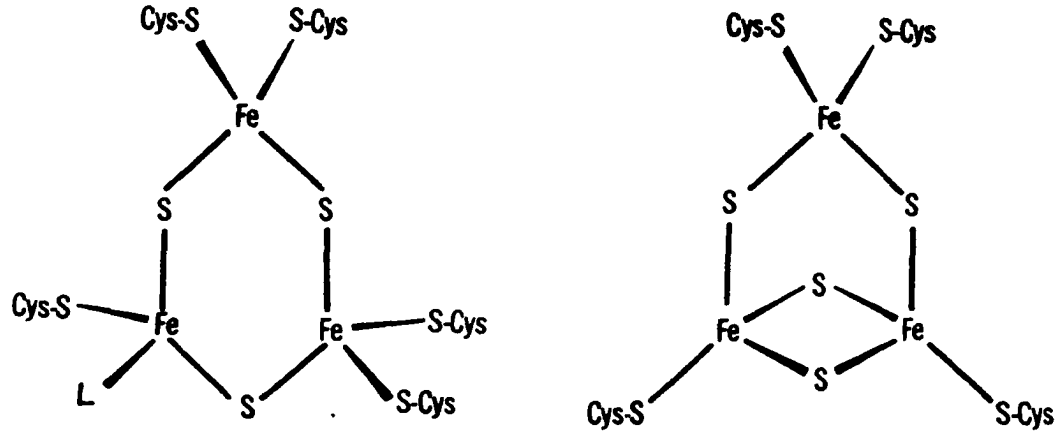

Figure 2. [3Fe-3S] and [3Fe-4S] centers

In 1978, Christou, Ridge and Rydon[56] found that selenium could be incorporated as the core chalcogen in tetramers starting with elemental selenium and reducing it with excess thiolate. In 1979, Christou and Garner[57] extended this approach using elemental sulfur in place of NaHS. This simplest of all methods is undoubtedly in most common use today.

In 1980, Reynolds and Holm[58] incorporated into the dimer synthesis the ideas of Christou and Garner. Where the latter preparation involved combining methanolic solutions of iron (II or III) chloride with thiolate and sulfur followed by introduction of a quaternary ammonium salt, Reynolds and Holm found that if the ammonium cation were present throughout, $(R_4N)_2[Fe_2S_2(SR)_4]$ would precipitate upon its formation before it could proceed on to tetramer.

$$4FeCl_3 + 14LiSR + 4S \xrightarrow{MeOH} Li_2[Fe_4S_4(SR)_4] + 5RSSR + 12LiCl \quad (4)$$

$$2FeCl_3 + 8\ NaSR + 4S + 2R_4NX \xrightarrow{MeOH} (R_4N)_2[Fe_2S_2(SR)_4] + 2RSSR + 6NaCl + 2NaX \quad (5)$$

This method generalized the dimer synthesis to a variety of ligands without requiring the original use of o-xylyl-α,α'-dithiol.

The best representation of the rubredoxin active site was probably achieved with o-xylyl-α,α'-dithiol, but the preparation of $[Fe(SPh)_4]^{2-}$ was improved in 1981.[59] It was found that attempts to prepare the oxidized species resulted in internal redox chemistry which led to production of disulfide. An iron (III) analog was subsequently prepared[60] using 2,3,5,6-tetramethylbenzenethiolate as ligand. Presumably, steric hindrance would not permit formation of a disulfide in this case, thereby preserving the iron (III) oxidation state.

Properties

As noted earlier, metrical and spectroscopic data have confirmed that the one-iron, two-iron and four-iron synthetic analogs are faithful representations of their counterpart moieties contained within iron-sulfur proteins. Since the properties of iron-sulfur clusters have been the subject of several recent reviews,[1,61-63] only the properties most relevant to the present work are discussed in detail below.

Structures

In all of these clusters, iron is coordinated in an essentially tetrahedral manner to thiolate sulfur or both thiolate sulfur and bridging sulfide. A cursory inspection suggests some structural relationships: that a dimer is composed of two monomer fragments which have substituted two bridging S^{2-} for four RS^-, and that a tetramer is the result of joining two dimers which have each lost two cis vicinal thiolates. In the cases of dimer and tetramer, metal-metal distances indicate metal-metal bonding of approximately single order.

Except for the monomeric compounds, it is common to view these systems as iron-sulfide "cores" to which are attached terminal ligands in synthetic analogs or cysteinate residues in proteins. From the abridged sets of data presented in Tables 1-3, one may draw the following conclusions: (1) The aryl- and alkylthiolate-ligated monomers have identical average Fe-S distances which appear close to those for rubredoxins in their respective oxidation states. (2) In dimers and tetramers, core dimensions do not vary appreciably upon changing terminal ligands, even when that ligand is chloride instead of thiolate. Moreover, any slight changes which occur do not seem to correlate with the electron-donating ability of the ligand.

The monomeric complexes exhibit significant distortion from tetrahedral symmetry, presumably arising both from Jahn-Teller distortion and crystal packing effects. For the two-iron species are observed minor deviations from idealized D_{2h} symmetry which appear to be random and so

Table 1. Structural data for rubredoxins and synthetic analogs[a]

Fe^{2+}/Fe^{3+} Site	Fe-S,(Å) Range	Fe-S,(Å) Mean[b]	S-Fe-S(deg) Range	S-Fe-S(deg) Mean[b]	Refs.
$[Fe(S_2\text{-}o\text{-}xylyl)_2]^{1-}$	2.252-2.279	2.267(9)	105.8-112.6	109.5(2.3)	42,43
C. pasteurianum Rd_{ox}	2.24-2.33	2.29(4)	103.7-114.3	109.5(4.8)	44,45
$[Fe(S_2\text{-}o\text{-}xylyl)_2]^{2-}$	2.324-2.378	2.356(26)	103.5-114.9	109.5(4.3)	43
$[Fe(SPh)_4]^{2-}$	2.338-2.372	2.356(14)	97.6-119.5	109.5(8.4)	64
P. aerogenes Rd_{red}[c]	(EXAFS)	2.32(2)	----	----	65

[a]From X-ray crystallography unless otherwise noted.

[b]Numbers in parentheses are estimated standard deviations from mean.

[c]From EXAFS.

Table 2. Structural data for $Fe_2S_2X_4^{2-}$ (X = terminal ligand)

Cluster anion	Distances, Å[a]			Angles, Deg				Refs.
	Fe-Fe	Fe-S	Fe-X	Fe-S-Fe	S-Fe-S	X-Fe-X	X-Fe-S	
$[Fe_2S_2(S_2\text{-}o\text{-xylyl})_2]^{2-}$	2.698(1)	2.185(2) 2.232(1)	2.305(2)	75.3	104.7	106.4	112.2 110.7	32
$[Fe_2S_2(S\text{-}p\text{-}C_6H_4CH_3)_4]^{2-}$	2.691(1)	2.200(1) 2.202(1)	2.312(1)	75.4	104.6	111.2	115.1 105.4	32
$[Fe_2S_2Cl_4]^{2-}$	2.716(1)	2.199(1) 2.202(1)	2.252(9)	76.2	103.8	106.4	112.0	66

[a]Numbers in parentheses are estimated standard deviations from mean.

Table 3. Structural data for $Fe_4S_4X_4^{n-}$ (X = terminal ligand)

Cluster Anion	Distances, Å[a]			Angles, deg		Refs.
	Fe-Fe	Fe-S	Fe-X	S-Fe-S	Fe-S-Fe	
$[Fe_4S_4(SPh)_4]^{2-}$	2.730(2) 2.736(4)	2.267(4) 2.296(8)	2.263	104.3	73.5	67
$[Fe_4S_4(SPh)_4]^{3-}$	2.730(2) 2.750(4)	2.351(4) 2.288(8)	2.295	104.8	72.9	68
$[Fe_4S_4(SCH_2Ph)_4]^{2-}$	2.776(2) 2.732(4)	2.239(4) 2.310(8)	2.251	104.1	73.8	30
$[Fe_4S_4(SCH_2CH_2CO_2)_4]^{6-}$	2.778(2) 2.743(4)	2.261(4) 2.300(8)	2.250	103.4	74.1	69
$[Fe_4S_4Cl_4]^{2-}$	2.755(2) 2.771(4)	2.260(4) 2.295(8)	2.216	103.5	74.6	66

[a]Standard deviations do not appear in this table. The numbers enclosed in parentheses are the number of distances averaged. Unspecified, the mean of all distances is given.

are probably due solely to solid-state effects. The $[2Fe\text{-}2S]^{2+}$ cores are exactly planar for all species listed.

For the four-iron, four-sulfur clusters the highest idealized symmetry is T_d. The clusters in fact closely approach D_{2d} symmetry as a result of compression along the $\bar{4}$ axis leaving the $[4Fe\text{-}4S]^{2+}$ cores with four short and eight long Fe-S distances. In the examples listed in Table 3, all species but one have the same core oxidation level. The exception is $[Fe_4S_4(SPh)_4]^{3-}$ which is reduced by one electron and is included for a brief comparison: It has been observed that these cubane-like clusters elongate along the $\bar{4}$ axis upon reduction and that these longer bonds seem to be more susceptible to distortion.

An iron-thiolate compound not thus far mentioned is the deca(benzenethiolato)tetraferrate(II)dianion, $[Fe_4(SPh)_{10}]^{2-}$. This compound, crystallized as its tetramethylammonium salt,[70] contains an adamantane-like M_4S_6 core consisting of an approximate tetrahedron of iron atoms within an octahedron of bridging sulfur atoms. The mean iron-iron distance of 3.93 Å indicates that no metal-metal bonding is present and so this may be considered an oligomerization product of the mononuclear $[Fe(SPh)_4]^{2-}$.

^1H NMR spectra

The proton resonances of ligands bound to iron-sulfur clusters are often both unique for each cluster and in chemical shift regions relatively unoccupied by other signals. These properties are due to

the paramagnetism of the iron or iron-sulfide center to which the ligands are bound. With alkyl-thiolate ligands, we find that the methylene and methyl resonances are broadened and shifted downfield, both effects being attenuated with increasing distance from the metal.[71]

In the cases of aryl-thiolates, used exclusively in this study, the chemical shift behavior is more intricate and unique for each cluster. As a result, the NMR spectra of clusters or mixtures of clusters containing these ligands are aptly diagnostic.

With bound thiolate, "contact" (through bond) magnetic interactions arise from ligand-to-metal anti-parallel spin transfer which gives the ligand the character of a π-radical:

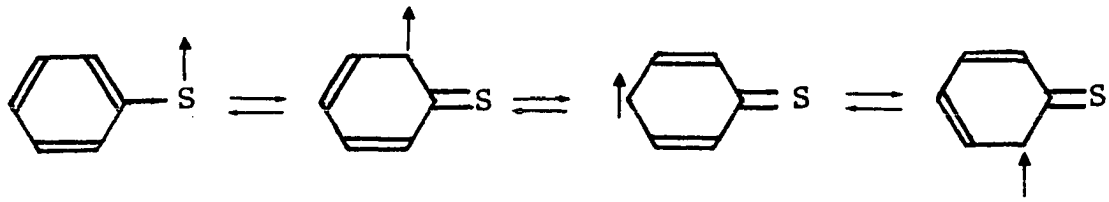

This mechanism accounts for net positive spin in the HOMO of the phenyl ring, negative spin arising at the meta positions through spin correlation effects. That the interaction is essentially contact in nature is verified by the parallel temperature dependencies of solid-state magnetic susceptibilities and magnitudes of isotropic chemical shifts.[71]

The pattern of proton resonances observed is that protons in the ortho and para ring positions are always shifted to higher field,

whereas those residing at the meta positions always appear downfield from the free ligand signal (i.e., from the diamagnetic shift). The isotropic contact shift is defined as the difference between the observed signal and that for the free thiol:

$$(\Delta H/H_o)^{iso} = (\Delta H/H_o)^{obs} - (\Delta H/H_o)^{dia}$$

As stated earlier, the magnitude of the isotropic shift varies considerably with the magnitude of the paramagnetism, allowing easy identification of mixtures of iron-sulfur species. The isotropic shifts for various benzenethiolate species are shown in Table 4.[59] Because several NMR spectra will be presented, the chemical shifts in CD_3CN vs. TMS are given in Table 5.

Table 4. Isotropic shifts in CD_3CN at ~27°C[a]

	$(\Delta H/H_o)^{iso}$, ppm		
Complex	o-H	m-H	p-H
$[Fe(SPh)_4]^{2-}$	+9.60	-15.1	+16.8
$[Fe_2S_2(SPh)]_4^{2-}$	+2.30	-2.11	+3.82
$[Fe_4(SPh)_{10}]^{2-}$	+10.4(t) +16.2(b)	-9.00(t) -9.00(b)	+16.2(t) +19.2(b)
$[Fe_4S_4(SPh)_4]^{2-}$	+1.34	-1.03	+1.91

[a]Negative and positive values denote, respectively, downfield and upfield shifts.

Table 5. Chemical shifts in CD_3CN at ~27°C (vs. TMS)[a]

Complex	o-H	m-H	p-H
$[Fe(SPh)_4]^{2-}$	+2.4	-22.3	+9.6
$[Fe_2S_2(SPh)_4]^{2-}$	-4.9	- 9.3	-3.4
$[Fe_4(SPh)_{10}]^{2-}$	+3.2(t) +9.0(b)	-16.2(t) -16.2(b)	+9.0(t) +12.0(b)
$[Fe_4S_4(SPh)_4]^{2-}$	-5.9	-8.2	-5.3

[a]Upfield and downfield shifts are denoted by positive and negative values, respectively.

Electronic absorption spectra and electrochemical reduction potentials

The visible absorption spectra of $[Fe(SPh)_4]^{2-}$ and $[Fe_4(SPh)_{10}]^{2-}$ in acetonitrile are nearly featureless and consequently rather useless as an indication of sample composition. The monomeric dianion exhibits only a shoulder at ~390 nm which is nearly indistinguishable from the ~430 nm shoulder of the tetranuclear compound.[59] While both compounds absorb intensely at higher energy wavelengths, colors of their solutions appear quite different to the eye. Fairly concentrated solutions of $[Fe(SPh)_4]^{2-}$ are nearly colorless but perceptibly pale green, while concentrated samples of $[Fe_4(SPh)_{10}]^{2-}$ appear brownish-yellow.

In contrast, the absorption spectra of sulfide-containing compounds are rather interesting and are often suitably diagnostic of sample composition. It should be remarked, though, that the visible appearance

and electronic spectra of samples containing both $[Fe_2S_2(SPh)_4]^{2-}$ and $[Fe_4S_4(SPh)_4]^{2-}$ are often deceptive and that NMR gives the only reliable evaluation of the relative abundance of each.

From the data in Table 6, it is observed that among both dimers and tetramers ligated by aryl-thiolates, one of the visible absorption maxima and the 2-/3- reduction potential vary according to the electron-donating ability of the ligand. The absorption bands in the 330-360 nm

Table 6. Absorption maxima and 2-/3-reduction potentials[a,b]

Dianion	$\lambda_{max}(\varepsilon)$ nm($M^{-1}cm^{-1}$)	$E_{1/2}$(V)[c]
$Fe_2S_2(S_2$-o-xylyl$)_2^{2-}$	294(14500), 338(16200), 414(11000) ~ 455(sh,9200), 590(4800)	-1.49V
$Fe_2S_2(S$-p-$C_6H_4CH_3)_4^{2-}$	268(42400), 336(18600), 502(11200)	-1.15V
$Fe_2S_2(SPh)_4^{2-}$	270(39000), 333(19500), 490(11200)	-1.09V
$Fe_2S_2(S$-p-$C_6H_4Cl)_4^{2-}$	277(42800), ~330(sh,22100), 483(12800)	-0.97V
$Fe_4S_4(S$-p-$C_6H_4CH_3)_4^{2-}$	262(46800), ~350(sh,22000), 461(18600)	-1.09V
$Fe_4S_4(SPh)_4^{2-}$	260(45000), ~350(sh,22000), 457(17700)	-1.04V
$Fe_4S_4(S$-p-$C_6H_4Cl)_4^{2-}$	267(44800), ~360(sh,19400), 449(15300)	-0.95V

[a]From ref. 32.

[b]All measurements in DMF.

[c]vs. S.C.E.

region are not observed to vary in this way and so are assigned to a charge transfer from core sulfide to iron. But with the higher wavelength absorptions, we see that as the ligand becomes less electron-donating, the transitions move to higher energy. Hence, they have been assigned to charge transfer from thiolate sulfur to iron. One should also note that the voltage required to reduce a dianion to a trianion diminishes appropriately as the thiolate becomes less electron-donating. As noted earlier, however, these electronic effects do not seem to be reflected by variations in core structural dimensions.

Reaction chemistry

It was first reported in 1984 that the tetranuclear clusters $[Fe_4S_4(SR)_4]^{2-}$ would undergo stepwise substitutions of their terminal thiolate ligands according to equation 6.[67,72]

$$[Fe_4S_4(SR)_4]^{2-} + nR'SH \rightarrow [Fe_4S_4(SR)_{4-n}(SR')_n]^{2-} + nRSH \qquad (6)$$

It was first noted that the equilibrium position lies far to the right when R'SH is an aryl thiol and later established that the substitution tendencies of R'SH show a correlation with aqueous acidities in the range $6.5 \leq pK_a \leq 10.6$. Bound t-butylthiolate (pK_a for t-BuSH is 11.1 to 11.2)[67] is replaced by any more acidic thiol and, consequently, aromatic thiols substitute more effectively than do aliphatic thiols. Taken from the most extensive study,[67] Table 7 describes the ligand replacement series in acetonitrile solution according to equation 6.

Table 7. Ligand replacement series for $[Fe_4S_4(S\text{-}t\text{-}Bu)_4]^{2-}$

$pK_a(R'SH)$[a]	R'SH[b]	Fraction replaced[c]
3.20	CH_3COSH	0.98
4.50	$p\text{-}O_2NC_6H_4SH$	0.97
6.43	C_6H_5SH	0.96
6.52	$p\text{-}CH_3C_6H_4SH$	0.98
7.41	$p\text{-}Me_2NC_6H_4SH$	0.90
9.4	$PhCH_2SH$	0.85
9.61	$HOCH_2CH_2SH$	0.78
10.61	CH_3CH_2SH	0.59
10.70	$p\text{-}CH_3C_6H_4OH$	0.17

[a]See ref. 67.

[b]The first and last listings are not thiols but are included here for comparison.

[c]Equiv. t-BuSH released for each equiv. R'SH added.

These ligand substitution reactions have enjoyed frequent use in the synthesis and isolation of new tetrameric iron-sulfur clusters.

As noted earlier, early synthesis of dimers, $[Fe_2S_2(SR)_4]^{2-}$, was only possible when 2RS = $\underline{o}\text{-}C_6H_4(CH_2S)_2$. Until development of the current synthetic approach,[58] dimers containing monodentate thiolates could only be obtained by the ligand substitution reaction 7.[32]

$$[Fe_2S_2((SCH_2)_2C_6H_4)_2]^{2-} + 4\ R'SH \rightarrow [Fe_2S_2(SR')_4]^{2-} + 2\ o\text{-}C_6H_4(CH_2SH)_2 \qquad (7)$$

Although some questions remain, insight into the mechanism of ligand substitutions of these types was provided by a kinetic study performed in 1974 by Dukes and Holm.[73] They found that the rate dependence for the first substitution step was second-order overall, first-order each in tetramer and added thiol. They also found support for the acidity correlation, noting that pseudo-first-order rate constants increased with the increasing acidity of incoming thiol, and proposed protonation of cluster-bound thiolate as the rate-determining step which gives rise to the following mechanism:

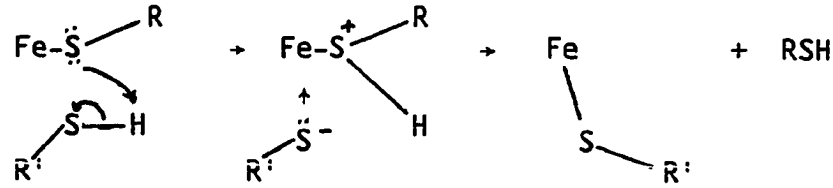

(8)

It appears, however, that ligand substitution does not always proceed using a protonation step. An acetonitrile solution of two different tetramers spontaneously scrambles ligands according to equation 9 to provide a roughly statistically-distributed product,[67] and acetonitrile is aprotic.

$$[Fe_4S_4(S\text{-}\underline{t}\text{-}Bu)_4]^{2-} + [Fe_4S_4(S\text{-}\underline{p}\text{-}tol)_4]^{2-} \rightarrow [Fe_4S_4(S\text{-}\underline{t}\text{-}Bu)_{4-n}(S\text{-}\underline{p}\text{-}tol)_n]^{2-} \quad (9)$$

Also, sodium benzenethiolate is every bit as effective as benzenethiol in substituting for cluster-bound t-butylthiolate.[67] Reaction 9 suggests that facile terminal ligand dissociation plays a significant role in the chemistry of these clusters, a point which should become clearer when one considers their reactions with electrophiles, which are discussed below.

Ligand substitutions of the first sort were also employed in attempts to simulate cluster coordination by cysteine-containing proteins. In 1974, DePamphilis et al. prepared an N-acetyl amide of cysteine, a monodentate aliphatic thiol whose structure suggests a cysteine residue within a protein:[74]

"Ac-L-Cys-NHMe"

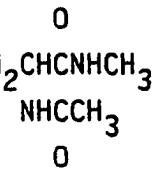

They also succeeded in preparing in situ $[Fe_4S_4(Ac\text{-}\underline{L}\text{-}Cys\text{-}NHMe)_4]^{2-}$ which, at that time, was declared the closest representation of oxidized ferredoxin sites on the basis of spectral and redox characteristics. Later that year, Que et al.[75] reported the preparations of oligopeptide complexes of $[Fe_4S_4]^{2+}$ cores. They prepared two "protein fragments", one containing three cysteines (9-peptide) and the other, four (12-peptide). Noting that amino acid sequences[21-23] of iron-sulfur proteins

invariably find cysteine amino acids spaced by two others, these peptides were constructed likewise with two glycines between each cysteine. Reactions of these peptides with $[Fe_4S_4(S\text{-}\underline{t}\text{-}Bu)_4]^{2-}$ in 4 DMSO/1 H_2O produced, respectively, $[Fe_4S_4(9\text{-peptide})(S\text{-}\underline{t}\text{-}Bu)]^{2-}$ and $[Fe_4S_4(12\text{-peptide})]^{2-}$ which were isolated as their tetraphenylphosphonium salts. The parallels between the properties of these compounds and unfolded ferredoxins are striking.[76]

Substitution of core atoms is also known. In 1970, Hong and Rabinowitz[77] reported that a [4Fe-4S] ferredoxin constituted with either ^{59}Fe or ^{35}S would undergo exchange of either with nonradioactive Fe(II) or S^{2-} salts while retaining full enzymatic activity. In 1981, Reynolds and Holm[78] undertook the study of core chalcogenide exchange in synthetic analogs. They did not, however, need to use radioisotopes, for by this time the selenium-containing compounds $[Fe_4Se_4(SR)_4]^{2-}$,[79] $[Fe_2Se_2(SR)_4]^{2-}$,[80] and $[Fe_4Se_4(SR)_4]^{3-}$,[81] were known and easily obtained. With p-tolyl thiol as the terminal ligand, core chalcogenide exchange could be easily followed by ^1H NMR. Solutions in CD_3CN of any of the above with its sulfide-containing congener present in equimolar amounts would, after several days, be transformed to an equilibrium mixture of statistically-distributed mixed-chalcogen clusters. These reactions have no clear precedent in metal cluster chemistry.

In 1978, Wong, Bobrik and Holm[82] announced the preparation of the halide-ligated complexes $[Fe_nS_nX_4]^{2-}$ (n = 2,4), which heralded yet another chapter in the reactivity of iron-sulfur clusters. These syntheses were achieved by reacting thiolate-containing clusters with

either benzoyl chloride or benzoyl bromide according to equations 10 and 11.

$$[Fe_2S_2(S_2\text{-}\underline{o}\text{-xyl})_2]^{2-} + 4\ PhCOX \xrightarrow{CH_3CN}$$

$$[Fe_2S_2X_4]^{2-} + 2 \quad \text{ 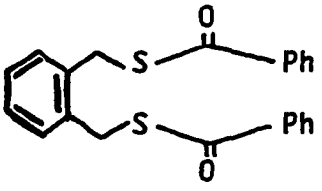 } \quad (10)$$

$$[Fe_4S_4(SR)_4]^{2-} + 4\ PhCOX \xrightarrow{CH_3CN} [Fe_4S_4X_4]^{2-} + 4\ PhCOSR\ (R = \underline{t}\text{-Bu, Ph}) \quad (11)$$

The original thiolate tetramers could be re-obtained by treating the halide-ligated clusters with thiol and equimolar tetramethylammonium hydroxide as shown in equation 12. No reaction was observed without the presence of the deprotonating agent.

$$[Fe_nS_nX_4]^{2-} + 4\ RSH + 4\ Me_4NOH \xrightarrow{CH_3CN} [Fe_nS_n(SR)_4]^{2-} + 4\ H_2O + 4\ Me_4NX \quad (12)$$

The iodide-ligated clusters were obtained via general reaction 13 and consideration of the general features of reactions 12 and 13

$$[Fe_nS_nX_4]^{2-} + 4\ NaI \xrightarrow{CH_3CN} [Fe_nS_nI_4]^{2-} + 4\ NaX. \quad (13)$$

prompted at least one attempt at preparing a synthetic compound intended as a representation for an iron-sulfur cluster coordinated by tyrosine residues.[83] Shown here in equation 14, this attempt met with some success. Inspection of reactions 12-14

$$[Fe_4S_4Cl_4]^{2-} + 4\ ArO^- \rightarrow [Fe_4S_4(OAr)_4]^{2-} + 4\ Cl^- \qquad (14)$$

suggests them all to be simple nucleophilic substitutions. They conform to an established scale of nucleophilicity[84,85] which predicts the anionic-ligand replacement series $CH_3CO_2^-$ < Cl^- < PhO^- < Br^- < I^- < PhS^- < $PhSe^-$.[86]

Reactions of iron-sulfur clusters with electrophiles were shown to be more general by Johnson and Holm.[87] They demonstrated that the general reaction 15 is a stepwise one where the electrophile can be an

$$[Fe_4S_4(SR)_4]^{2-} + nYX \rightarrow [Fe_4S_4(SR)_{4-n}X_n]^{2-} + nYSR \qquad (15)$$

acid anhydride or a sulfonate ester as well as an acid halide. In each of these cases, there can be little doubt that the thermodynamic driving force for these reactions is provided by nucleophilic attack upon a carbonyl or other positive carbon atom. Though facile terminal-ligand dissociation from iron-sulfur clusters does not seem to be widely recognized in the literature, it seems likely that such nucleophilic attack comes from free thiolate.

Possible pathways of cluster assembly

In a 1981 paper[59] entitled "Definition of Reaction Sequences Resulting in Self-Assembly of $[Fe_4S_4(SR)_4]^{2-}$ Clusters from Simple Reactants", Hagen, Reynolds and Holm presented the cluster assembly scheme shown in Figure 3. Since that time, the discovery of three new iron-thiolate compounds suggests that the possible pathways of synthetic cluster assembly are considerably more elaborate.

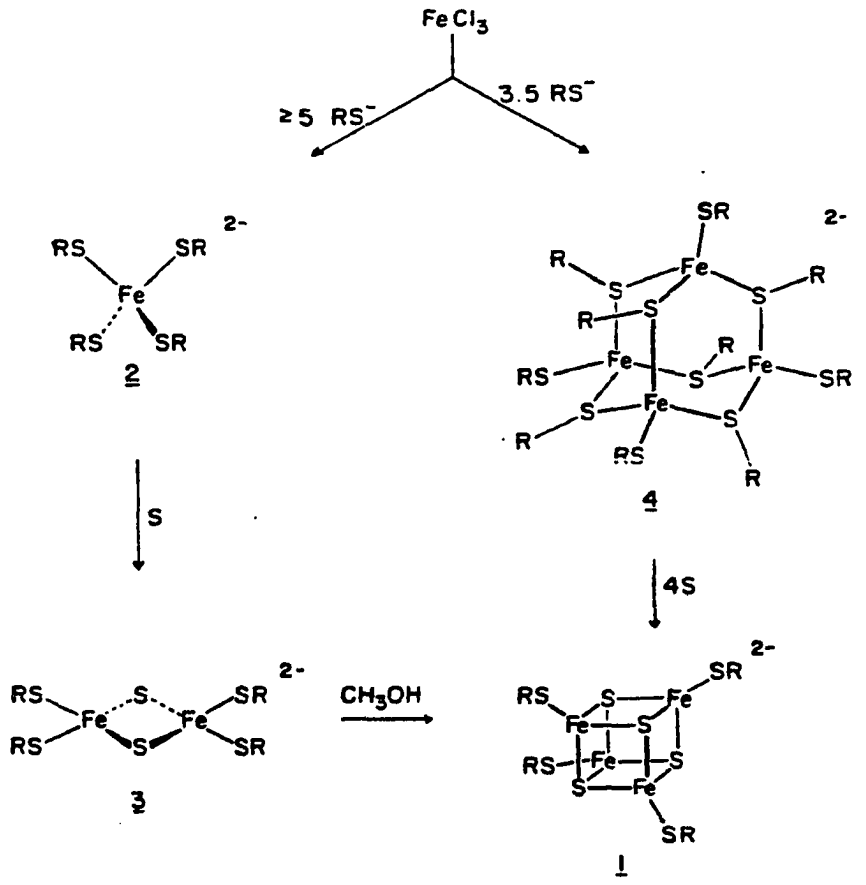

Figure 3. Cluster assembly scheme proposed by Hagen, Reynolds and Holm[59]

In addition to the 2.5:1 and 4:1 thiolate:iron stoichiometries found, respectively, in $[Fe_4(SR)_{10}]^{2-}$ and $[Fe(SR)_4]^{2-}$, Coucouvanis et al.[88] have prepared $[Fe_4(SPh)_6Cl_4]^{2-}$ which has 1.5 PhS^-/Fe(II). This molecule has the adamantane-like framework of $[Fe_4(SPh)_{10}]^{2-}$ but bears four chlorides in place of the terminal thiolate ligands. A 1:1 RS^-/Fe(II) stoichiometry was achieved with the preparation of the trinuclear $[Fe_3(SPh)_3Cl_6]^{3-}$ which is a planar trianion consisting of a triangular array of $FeCl_2$ units edge-bridged by thiolates.[89] Finally, a 3:1 RS^-/Fe(II) has been realized with the isolation and characterization[89] of the bitetrahedral $[Fe_2(SEt)_6]^{2-}$ which resembles $[Fe_2S_2(SR)_4]^{2-}$ but has thiolates in the bridging positions instead of sulfides.

The question of whether these species can be made one from another by successive additions of thiolate has not been thoroughly addressed, but work in our laboratories has shown that reaction of $[Fe_4(SPh)_{10}]^{2-}$ with excess PhSH and NEt_3 produces $[Fe(SPh)_4]^{2-}$ and the equilibrium $3[Fe_2(SEt)_6]^{2-} \neq 2[Fe(SEt)_4]^{2-} + [Fe_4(SEt)_{10}]^{2-}$ has been postulated by Hagen and Holm.[90] A more unified and comprehensive possible cluster assembly scheme is presented in Figure 4 below. Although some of the steps are entirely speculative, all of the species shown are known to exist with R = Et or Ph. Addition of sulfur to $[Fe(SPh)_4]^{2-}$ produces, as the initial identifiable product, $[Fe_2S_2(SPh)_4]^{2-}$ which in protic solvents spontaneously and quantitatively converts to $[Fe_4S_4(SPh)_4]^{2-}$.[91] In acetonitrile, the ethylthiolate species have been shown to follow the same pathway.[92] On the opposite side of the scheme, however, it is observed that $[Fe_4(SPh)_{10}]^{2-}$ reacts with 1-4 equivalents

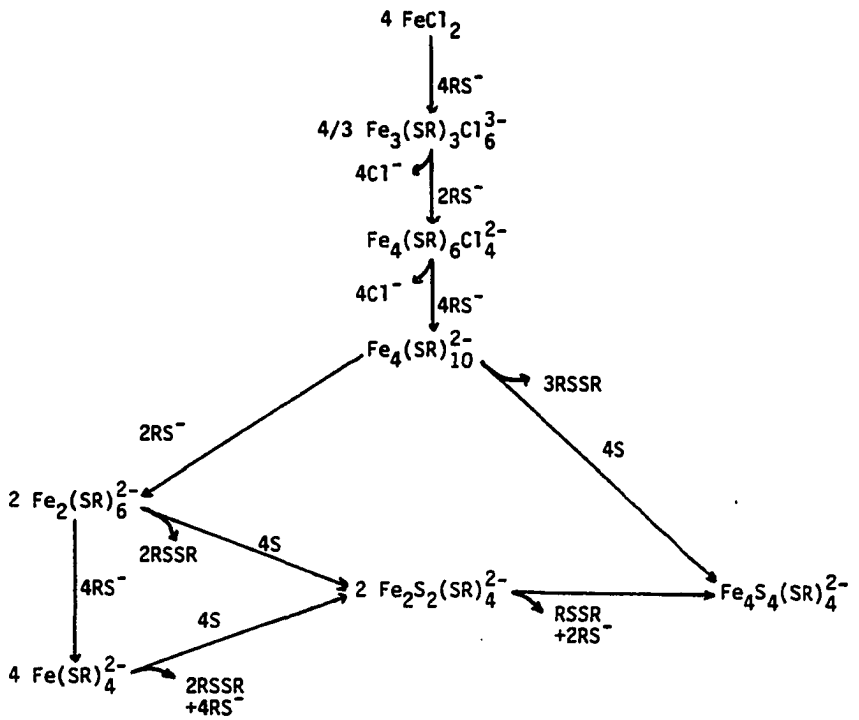

Figure 4. A more comprehensive possible cluster assembly scheme

of sulfur to produce, without detectable intermediates, $[Fe_4S_4(SPh)_4]^{2-}$ in an apparent all-or-nothing stoichiometry.[59]

Micellar solutions

Biomimetic chemistry is an attempt to study or perform chemical reactions under artificial conditions contrived to resemble those of biological situations. In this study, nonionic surfactants and their

utility to this end are of primary focus. Their properties[93-95] and effectiveness in mimicking *in vivo* milieu[96-100] have been extensively reviewed.

In living systems, biological membranes spatially organize cell components, providing microenvironments which allow for the controlled transport of solutes. Membranes are composed of a bilayer of lipids, which are amphiphilic biological molecules. Lipids contain hydrophobic aliphatic chains and hydrophilic phosphate or carboxylate ester groups which induce them to aggregate in an aqueous environment such that their hydrophobic regions surround one another. In the vicinity of membranes, the biochemistry which occurs is of a "microheterogeneous" or interfacial nature.

Attempts to mimic biological reaction conditions were chiefly prompted by the desire to understand and simulate photosynthesis. As Calvin[100] remarked in 1978, "Our work in biomimetic chemistry began with the relatively limited knowledge we had of how the green plant converts the sunshine into chemical energy." While that knowledge seems still rather limited, tenable photosynthetic schemes have been proposed for electron excitation and transport. While foregoing a detailed discussion here, it should be noted that these schemes involve at some point a membrane-bound ferredoxin as an agent for electron transport.

Resembling lipids for their amphiphilic character are surfactants (a contraction of "surface-active agent"), otherwise known as detergents, which also form aggregates called micelles. These micelles seem to be able to provide microenvironments that resemble those of the

biological world, rendering possible a variety of interfacial chemistry and accommodating light-induced charge separation in artificial photosynthesis.[98,99] Indeed, so similar are nonionic surfactant molecules and biological lipids that they form mixed micelles with one another.[97]

Among the most popular nonionic surfactants is poly(oxyethylene) p-tert-octylphenyl ether, commonly known as Triton X-100, which was used in this study. Shown in Figure 5, it consists of a nonpolar aliphatic and aromatic end with a long oxyethylene chain.

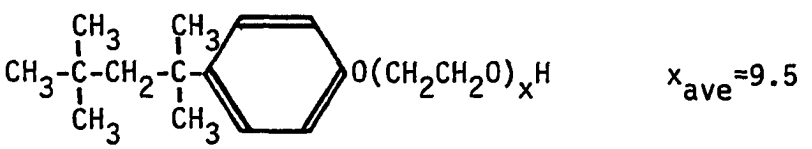

Figure 5. Triton X-100

Triton dissolves as monomeric units up to the critical micelle concentration (cmc) which varies in the range 0.1 mM to 0.8 mM. Temperature[101] and salt concentration[102] have little effect on the cmc. (0.5 M salt affects the cmc by less than a factor of two.) Once the cmc is exceeded, Triton aggregates into micelles with molecular weights near 90,000. Since the monomers have an average molecular weight of 646, each micelle must contain approximately 150 Triton molecules.

The exact fashion in which these molecules are arranged is not known with certainty, but there is no doubt that micelles in aqueous solution consist of a hydrophobic interior, out from which project the hydrophilic chains. Calculations assuming particular chain conformations for the Triton monomers indicate that a spherical micellar shape should be unattainable and suggest instead an oblate ellipsoid with half-axis dimensions 27 x 52 Å.[103] In support, small angle x-ray scattering experiments also find an oblate ellipsoid 32 x 50 Å[104] and coupling conductance with intrinsic viscosity data leads to a 20 x 54 Å ellipsoid.[105]

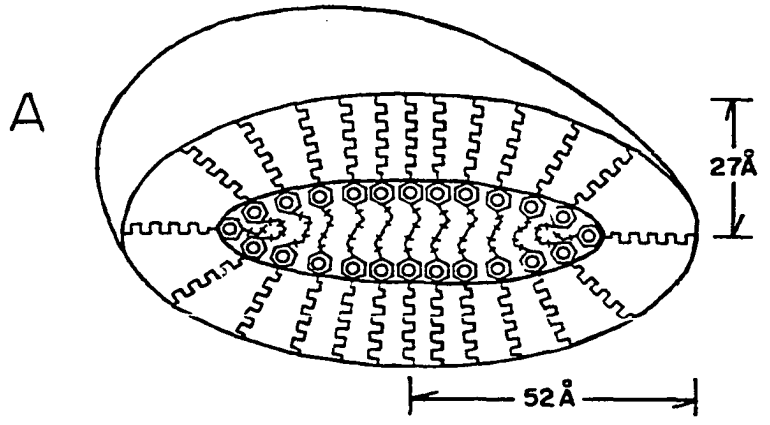

Figure 6. A Triton micelle (from Ref. 97)

In the hydrophobic cores of these micelles can reside "solubilized" nonpolar molecules otherwise insoluble in aqueous media. Solubilization, however, seems to be a dynamic phenomenon and residence

times on the microsecond scale have been determined by flash photolysis and relaxation techniques.[96] Dynamic processes notwithstanding, water penetration into the hydrophobic core seems minimal, as suggested by NMR chemical shifts and spin-lattice relaxation time measurements.[106-108] The ethylene oxide units on the other hand, are highly hydrated. These are important considerations. In the work which follows, it is necessary to envision certain processes taking place in micellar solutions, protected to various degrees from the protic nature of an otherwise aqueous environment.

Iron-sulfur clusters in micellar media

As it was mentioned in the early part of the introduction, iron-sulfur cores may be extruded intact from their proteins in the manner of reaction 16 by diluting an aqueous solution of the protein with

$$\text{holoprotein} + \text{PhSH} \rightarrow [Fe_nS_n(SPh)_4]^{2-}\ (n = 2,4) + \text{apoprotein} \qquad (16)$$

four parts hexamethylphosphoramide and treating with benzenethiol.[13-17] The HMPA acts both to unfold the protein and to solubilize the aromatic thiol, which performs ligand substitution for protein crysteinate.

In 1982, Kurtz[109] reported an alternative method of iron-sulfur core extrusion from proteins, the kinetics and equilibria of which are discussed by Bonomi and Kurtz.[110] The original work, dealing with the $[2Fe\text{-}2S]^{2+}$ core of spinach ferredoxin, was later found to generalize to $[4Fe\text{-}4S]^{2+}$ cores as well.[111] Core extrusions are still accomplished in

this method via ligand substitution by benzenethiol, but the solvent system is > 80% aqueous and contains 5% Triton X-100 detergent which serves to solubilize the benzenethiol and the extruded cores. Et_4N^+ salts of $[Fe_2S_2(SPh)_4]^{2-}$ and $[Fe_4S_4(SPh)_4]^{2-}$, which are insoluble in water, are soluble and stable for at least several hours in aqueous Triton, although benzenethiol must be present in excess to inhibit the conversion of dimer to tetramer. Under these conditions, the absorption spectra of both salts have been reported.[109] The relevant spectral parameters for $(Et_4N)_2[Fe_2S_2(SPh)_4]$ in 90% aqueous buffer/5% DMF/5% Triton are: λ_{max} = 474 nm (sh, ~425 nm), $\varepsilon = 1.00 \times 10^3\ M^{-1}cm^{-1}$; $A_{474}/A_{550} = 1.24 \pm 0.02$; $A_{454}/A_{550} = 1.20 \pm 0.01$; $A_{474}/A_{600} = 1.84 \pm 0.04$. For $(Et_4N)_2[Fe_4S_4(SPh)_4]$, the relevant parameters are: λ_{max} = 454 nm, $\varepsilon = 17{,}400\ M^{-1}cm^{-1}$; $A_{454}/A_{550} = 2.05 \pm 0.03$. These parameters are useful for determining whether or not cluster decomposition has occurred either during or after extrusion and whether the solution contains both dimer and tetramer.

Inasmuch as this type of solvent system works well for iron-sulfur core extrusions -- offering decreased extrusion time in some cases, increased sensitivity, and the avoidance of toxic HMPA -- it also seems to be a good candidate for a biomimetic environment in which to do synthetic reaction chemistry.

Certain synthetic clusters containing the [2Fe-2S] and [4Fe-4S] core geometries, when preassembled in organic solvents, have been shown to be stable in either aqueous or aqueous/organic media.[13,15,91,112-114] However, the implicit attitude towards aqueous solvents during

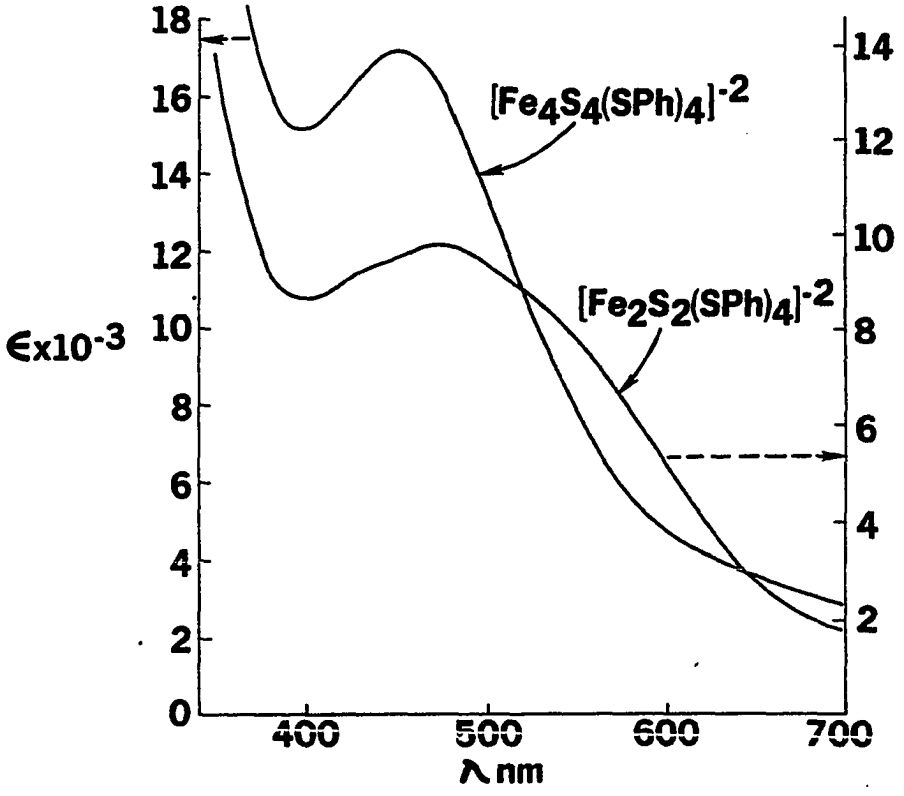

Figure 7. Visible absorption spectra of $[Fe_2S_2(SPH)_4]^{2-}$ $[Fe_4S_4(SPh)_4]^{2-}$ in 90/5/5 vol % buffer/DMF/Triton X-100 containing excess benzenethiol

assembly of such synthetic clusters at times seems to fulfill one dictionary definition of hydrophobia. Nevertheless, it is quite likely that, at least during some stages of FeS and MoFeS cluster assembly in vivo, appreciable concentrations of water are present. An aqueous detergent medium such as ours may be closer to that in vivo with respect to cluster assembly, especially if such assembly occurs at the surface of a membrane.

Inorganic chemistry in aqueous micellar media has been limited mainly to ligand substitition reactions,[115,116] and electron transfer reactions, both thermal[117] and photochemical.[118,119] Except for this work, we are unaware of published studies of transition metal cluster assembly reactions in aqueous detergent media. Therfore for the reaction system 4 PhSH/$FeCl_3$/S in aqueous Triton, we have sought to define (i) unique features compared to organic solvents, and (ii) simple techniques which can be used to work up, analyze, anad monitor these reactions.

EXPERIMENTAL

General Procedures

All reactions were performed at room temperature under an atmosphere of argon which had been further purified by passage over BASF catalyst R3-11 unless otherwise specified. Standard-taper round-bottom flasks equipped with stopcock sidearms and other Schlenk-type ware were used for anaerobic manipulations employing standard inert-atmosphere techniques.[120] Stainless steel cannulas of diameter 18 gauge were often used for the transfer of solutions and solvents. Gas-tight syringes were used otherwise and disposable syringes were also found to perform satisfactorily.

The vacuum/argon apparatus employed involved two manifolds, each approximately 1m by 28mm diameter, interfaced by five 3-way high-vacuum stopcocks. Two liquid nitrogen-cooled traps were placed in sequence between the vacuum pump and manifold to protect the pump oil from dilution by highly volatile solvents such as ether. Both the argon and vacuum manifolds terminated in 80cm mercury manometers to prevent air flow into the system. Performance of the system was considered satisfactory if the pressure inside the vacuum manifold did not exceed 0.050 torr. Solvents and solutions were usually purged of air by four or five cycles of vacuum and argon. Highly volatile solvents were often degassed by bubbling argon through them for several minutes.

Preparation of compounds

$(Et_4N)_2[Fe_2S_2(SPh)_4]$,[80] $(Et_4N)_2[Fe_4S_4(SPh)_4]$,[121] $(Et_4N)_2[Fe_4(SPh)_{10}]$[59] and $(n\text{-}Bu_4N)_2[Fe_4(SPh)_{10}]$[59] were prepared by published procedures and used as starting materials for reactions of pre-isolated compounds. Bis(p-fluorobenzene)disulfide was prepared by oxidation of p-fluorobenzenethiol with either $K_3Fe(CN)_6$ or I_2 according to the procedure used for preparation of bis(p-trifluoromethylbenzene)disulfide.[15] The product was dried over $CaSO_4$ yielding a yellow oil. This compound has also been prepared by oxidation of the thiol with H_2O_2.[122] Diphenyldisulfide was prepared by oxidation of benzenethiol with iodine in methanol. Concomitant with the disappearance of the iodine color was the appearance of a white precipitate which was collected, washed with methanol and air-dried. Its melting point and NMR spectrum were identical with those of the white crystalline material isolated from reactions in aqueous media, thereby identifying the latter as diphenyldisulfide. Concentrations of stock solutions of $(Et_4N)_2[Fe_2S_2(SPh)_4]$ in DMF (distilled from BaO) were determined from absorption spectra using published extinction coefficients.[80]

Reactions in aqueous media

The following general procedure was used for reactions of $FeCl_3$, PhSH and S and subsequent workup. To a slurry of 1.01g (3.75 mmol) $FeCl_3 \cdot 6H_2O$ in 8 mL of acetonitrile was added 1.6 mL (15 mmol) PhSH. To the resulting dark green solution was added 8 mL of Triton X-100 (Triton). (For reactions without Triton, 8 mL additional buffer were

used instead.) This latter solution was transferred to a stirred mixture of 144 mL of buffer (unless otherwise specified, 0.20M sodium N-[tris-(hydroxymethyl)methyl]-3-aminopropanesulfonate (NaTAPS, pH 9.0) containing 0.120g (3.75 mmol) of solid sulfur and 0.10M R_4NBr (R = Me, Et, n-Pr, n-Bu or n-pentyl (n-Pe)). The final solvent composition is ~90/5/5 vol.% aqueous buffer/CH_3CN/Triton.[123] After stirring for 8-9 h at room temperature, the mixture was allowed to sit unstirred for 2-10 days at room temperature, while a precipitate gradually formed. The resulting solid was collected by filtration and washed alternately with diethylether (to remove diphenyldisulfide, thiophenol, Triton and other nonpolar contaminants) and water (to remove excess quaternary ammonium salts, other inorganic salts and buffers). After final ether washes, the solid was dried in vacuo for several hours.

$(Et_4N)_2[Fe_4S_4(SPh)_4]$ This compound was prepared by the general procedure except that the quaternary ammonium salt was withheld until after ~ 7h of reaction. The solid obtained in 82% yield was analytically pure without recrystallization. Anal. Calc'd for $C_{40}H_{60}N_2S_8Fe_4$: C, 45.80; H, 5.78; N, 2.67. Found: C, 45.61; H, 5.77; N, 2.64. UV-vis (in DMF) and NMR (in CD_3CN Figure 8) were also in full agreement with those spectra published for the pure compound.[59,32]

$(n\text{-}Pe_4N)_2[Fe_2S_2(SPh)_4]$ The general procedure was used with $R_4N^+ = n\text{-}Pe_4N^+$ and the experiment was performed thrice. A solid obtained in > 92% yield was determined to be analytically pure without recrystallization. Calc'd for $C_{64}H_{108}N_2S_6Fe_4$: C, 63.55; H, 9.00; N,

2.32; Fe, 9.23; S, 15.90. Found: C, 63.27; H, 9.13; N, 2.27; Fe, 9.11; S, 15.75. A second time, the solid was harvested early (while color remained in the mother liquor) and was obtained in only 87% yield. Anal. Found: C, 63.28; H, 8.82; N, 2.49; Fe, 16.08; S, 9.16. When buffer was replaced by 0.10M LiOH the solid was obtained in (nominally) 94% yield but its NMR spectrum (Figure 9) showed it to contain trace amounts of $(n\text{-}Pe_4N)_2[Fe(SPh)_4]$ and $(n\text{-}Pe_4N)_2[Fe_4S_4(SPh)_4]$. In the two previous cases, the NMR spectra of the solids showed no signals for iron-thiolate species except those attributable to $(n\text{-}Pe_4N)_2[Fe_2S_2[SPh)_4]$.

$(n\text{-}Bu_4N)_2[Fe(SPh)_4]$ The general procedure ($R_4N^+ = n\text{-}Bu_4N^+$) was modified by omission of S, substitution of 1.89g (45 mmol) $LiOH\cdot H_2O$ for NaTAPS in 144 mL water and 4.8 mL (45 mmol) PhSH giving a $PhSH/Fe^{3+}$ ratio of 12. The reaction was concluded when a black oil was found at the bottom of the flask under a clear, colorless liquor which had a final pH of 8.7. The liquor was removed by cannula and the oil was washed repeatedly with ether in like fashion. When vacuum was applied, the oil bubbled up into a filmy light green solid which was dried *in vacuo* and obtained in > 92% yield. Its identify and purity were confirmed by integration of the *m*-H ^1H NMR resonance at -22.3 ppm[59] in CD_3CN *vs.* the methylene and methyl resonances of *n*-Bu_4N^+. No trace of the *m*-H resonance of $[Fe_4(SPh)_{10}]^{2-}$ at -16.2 ppm[59] was detected (Figure 10). Satisfactory elemental analyses of this compound were never obtained from Galbraith Laboratories and it was later learned that they are unable to maintain complete exclusion of atmospheric oxygen

Figure 8. ^1H NMR spectrum in CD_3CN of solid isolated from a reaction performed according to the general procedure except that Et_4NBr was withheld for 7 h. No additional signals were detected in the range -60 to +60 ppm

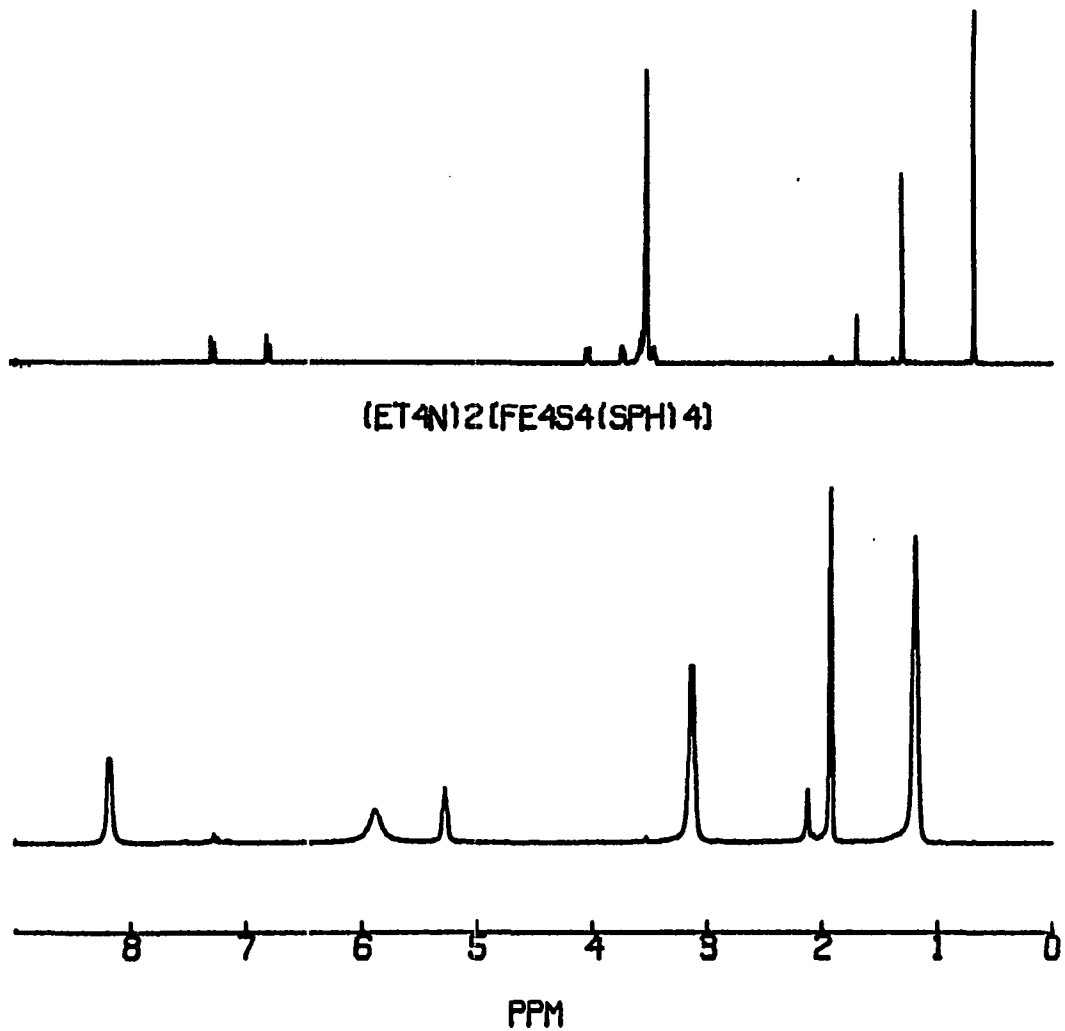
TRITON X-100
(ET4N)2[FE4S4(SPH)4]
8
7
6
5
4
3
2
1
0
PPM

Figure 9. ^{1}H NMR spectrum at 300 MHz in CD_3CN of solid isolated from a reaction performed according to the general procedure with R_4NBr = $\underline{n}$-Pe_4NBr. No other signals were observed in the -60 to +60 ppm range

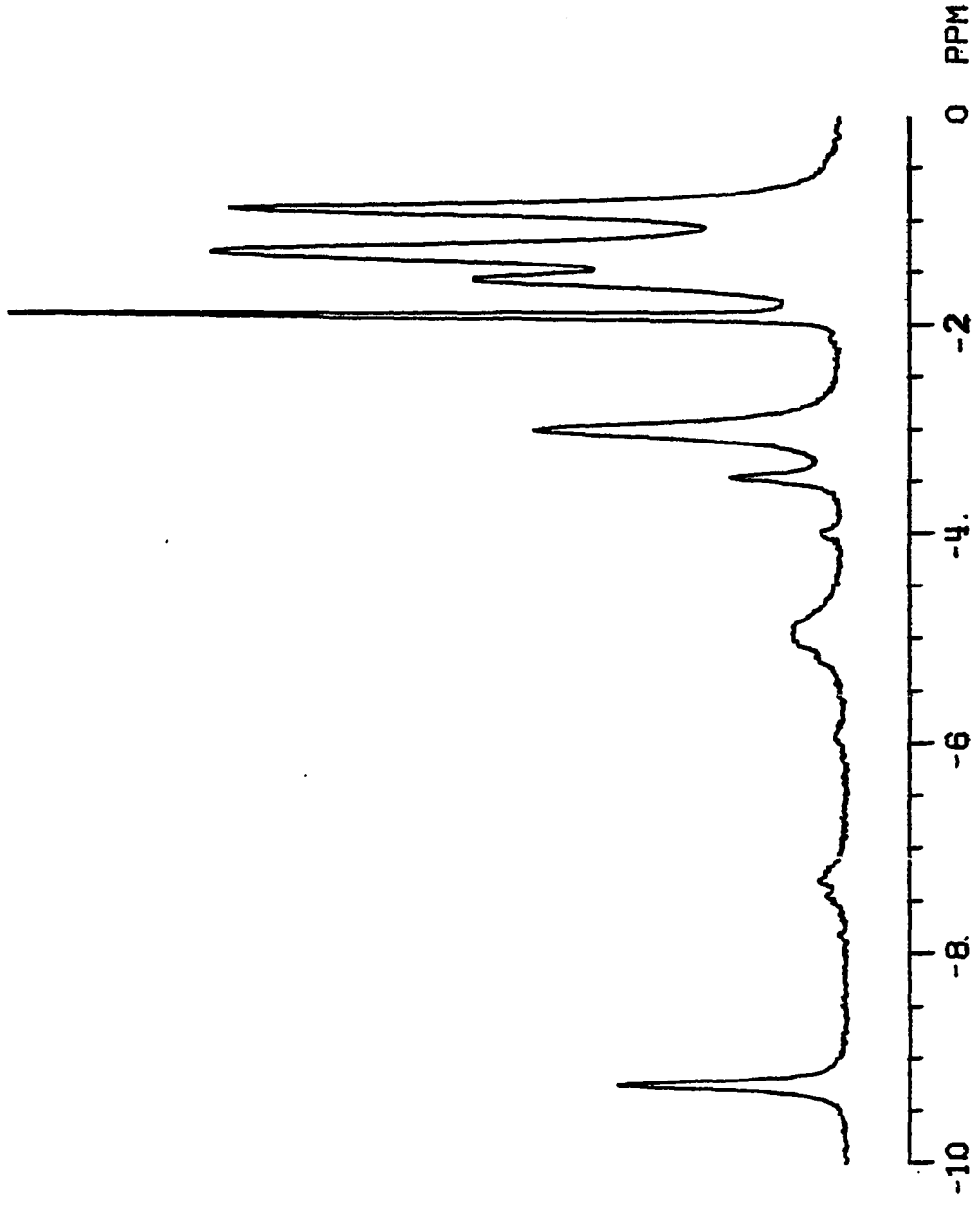
0 PPM
-2
-4.
-6
-8.
-10

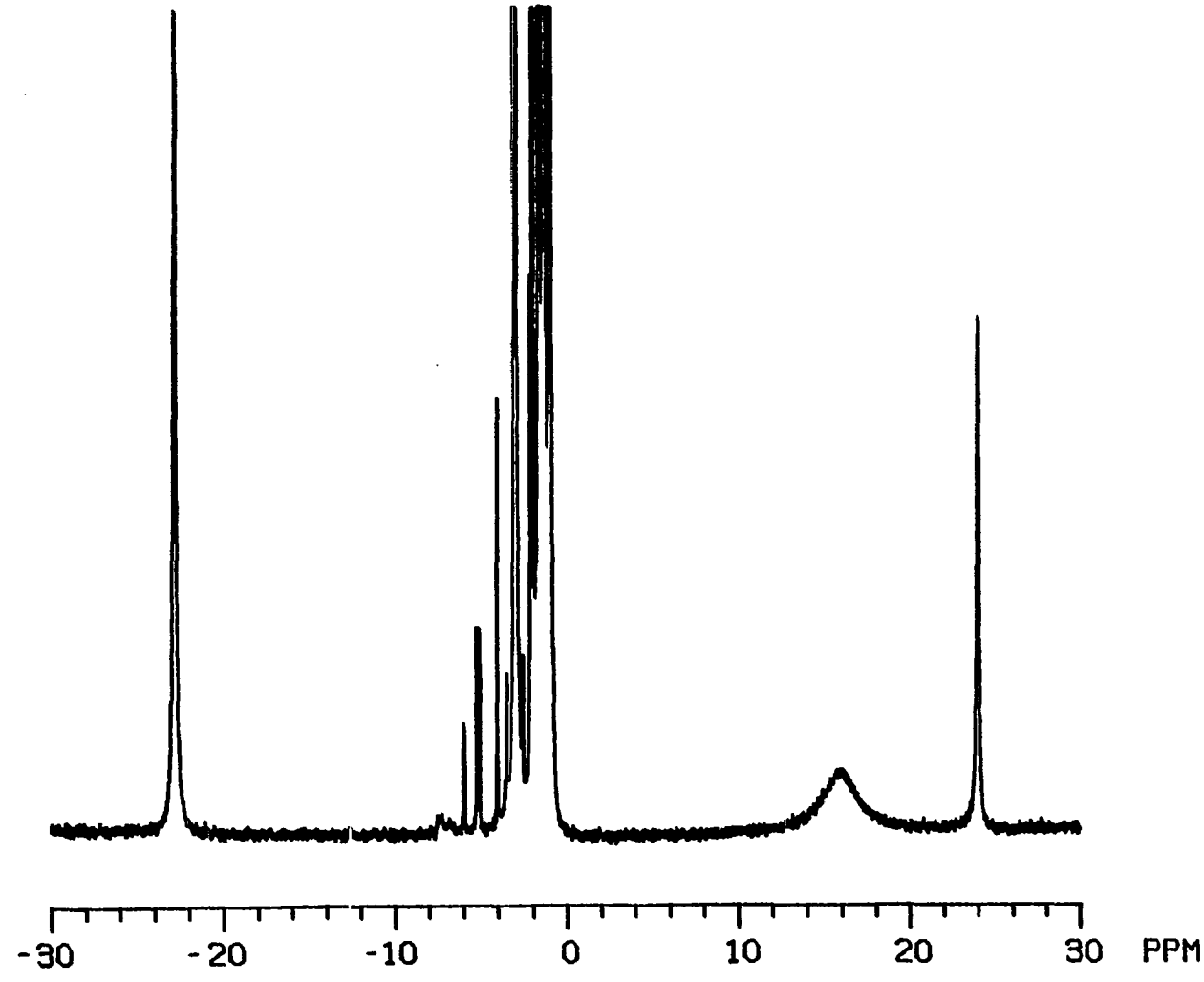

Figure 10. ^{1}H NMR spectrum at 300 MHz in CD_3CN of solid isolated from a reaction which had 12PhSH/Fe^{3+}, omitted S, used LiOH in place of buffer and had R_4NBr = $\underline{n}$-Bu_4NBr

throughout elemental analysis. However, an analysis performed by Schwarzkopf Microanalytical Labs, Inc. confirms the purity of $(\underline{n}\text{-}Bu_4N)_2]Fe(SPh)_4]$. Calc'd for $C_{56}H_{92}N_2FeS_4$: C, 68.81; H, 9.49; N, 2.87; Fe, 5.71; S. 13.12. Found: C, 68.61; H, 9.66; N, 2.77; Fe, 5.41; S, 13.02.

In solid form, quaternary ammonium salts of $[Fe_2S_2(SPh)_4]^{2-}$ (dimer) and $[Fe_4S_4(SPh)_4]^{2-}$ (tetramer) are sensitive to dioxygen. However, these solids can be handled in air for very short periods of time (i.e., weighing, transferring, etc.) without experiencing noticeable decomposition. In contrast, solid salts of $[Fe(SPh)_4]^{2-}$ and $[Fe_4(SPh)_{10}]^{2-}$ begin rapid decomposition immediately upon exposure to air and must be handled using strict anaerobic procedures[120] (glove bags, etc.). Elemental analyses on dimer and tetramer were performed by Galbraith Laboratories, Inc. which weighed the samples under a dinitrogen atmosphere. Schwarzkopf Microanalytical Labs, Inc. was able to maintain anaerobic conditions throughout analysis and was used for the elemental analysis of $(\underline{n}\text{-}Bu_4N)[Fe(SPh)_4]$.

Reactions and workup in aqueous media of pre-isolated salts of $[Fe(SPh)_4]^{2-}$, $[Fe_4(SPh)_{10}]^{2-}$, $[Fe_2S_2(SPh)_4]^{2-}$ and $[Fe_4S_4(SPh)_4]^{2-}$ were carried out according to the general procedure except that stock solutions of the above in CH_3CN were used in place of the $FeCl_3$ + PhSH solution. Additional variations are given in the text and figure legends.

Physical Measurements

UV/Visible spectrophotometry

Optical absorbance spectra were typically recorded from 900 to 200 nm on a Perkin Elmer 554 spectrophotometer. Cylindrical quartz cells of 0.50 mm pathlength were employed and measurements were performed against a background pre-recorded using the spectral solvent system (whether CH_3CN, DMF, or 90/5/5 vol. % aqueous buffer/CH_3CN/-Triton X-100) in both the sample and reference beams. The cells were equipped with septa and evacuated several times prior to filling to permit exclusion of atmospheric oxygen.

^1H NMR in deuterated solvents

Proton magnetic resonance spectra of isolated solids were recorded at 300 MHz in d^3-acetonitrile on either a Nicolet NT-300 or Bruker WM-300 spectrometer. All variable temperature measurements were performed on the Bruker. Highest quality (Wilmad Glass Co., 527PP) 5mm tubes were used and samples were usually quite concentrated. The use of a lower-field (90 MHz) instrument was attempted but abandoned when the machine was found impossible to tune. Presumably, the paramagnetic nature of the samples broadened the deuterium lock signal so much as to render the instrument immune to attempts to optimize it. This problem is substantially diminished when using a higher field magnet but highly paramagnetic samples (i.e., those giving rise to signals downfield of -10 ppm) still required adjustment of the coarse shimming controls.

Sweep width was generally set at ±20,000 Hz which provided a spectral window extending from roughly 70 ppm downfield of TMS to 60 ppm upfield. No signals were ever observed outside of -35 ppm to +35 ppm range but, because the resonances of interest were broad, the superior resolution obtainable from a smaller spectral window was deemed unnecessary. CD_2HCN (-1.93 ppm) was used as internal reference and upfield and downfield chemical shifts are designated as positive and negative, respectively.

Integrations of resonances to determine the relative distribution of products were performed using the spectrometer's computer software.

^1H NMR in aqueous solution

Proton NMR spectra of solutes in predominantly aqueous solutions can be obtained by a variety of methods. Sophisticated multiple-pulse techniques, usually requiring meticulous control and refinement of pulse angles and delays, are probably best for observing species whose protons are exchangeable with water. We have had some success using a two 45° pulse sequence for examining proteins on the Nicolet spectrometer. Superior software now exists which sequences the pulses according to binomial expansions.

In this work, we have used other techniques which utilize the spectrometer's spin decoupler unit in suppressing the water signal. The Nicolet program PRESAT appears roughly equivalent to homonuclear decoupling in the HG mode on the Bruker spectrometer. These experiments involve activating the decoupler to irradiate the water resonance

position until the upper spin state is saturated (in our case, a 3s duration was used), turning off the decoupler, applying a 90° pulse and observing the F.I.D. If the water resonance is not suppressed in this way, its signal will so dominate interaction with the receiver that most solute species will be impossible to detect. Another method that has given us satisfactory results is decoupling on the WM-300 in the HD mode. Here, the receiver and decoupler are gated synchronously with dwell -- which means that the decoupler is on during the spectrum acquisition period, but only between the times when data points are being taken.

Since we were interested only in observing in an *in situ* manner the *meta*-^{1}H resonances of thiophenolate ligands (which are not exchangeable with water) bound to cluster precursors, we were able to make our reaction solutions with the aqueous component 20% D_2O for purposes of lock and field refinement. (This percentage is not feasible when the protons of interest are exchangeable with D_2O. Also, in some cases of exchangeable protons, using the decoupler to saturate solvent water will effect saturation of the signals of interest as well.) Our experiments, with and without the presence of quaternary ammonium salts, were assembled to detect species present prior to reaction with sulfur under conditions as nearly identical to those of preparative reactions as possible. Except for the absence of granular sulfur in suspension, the only difference was that the probe temperature was lowered to 278 K to slow possible exchange processes and preserve greater sample homogeneity. All samples

were measured in 5 mm tubes and became somewhat heterogeneous with time. Relative areas of signals were determined by planimetric integration.

^{19}F NMR in aqueous solution

Using a fluorinated ligand, 4-fluorothiophenol, we were also able to follow reaction progress with ^{19}F NMR. The Bruker WM-300 multinuclear instrument was used for these measurements at 282.4 MHz and, using an auxiliary frequency synthesizer, was locked on $^{1}H_2O$ so that the presence of deuterium was unnecessary. As in the case with aqueous proton NMR, the highly paramagnetic nature of the precursor solutes and significant sample heterogeneity caused attempts to shim the magnet to have little effect.

For adequate signal to noise under these conditions, ^{19}F samples should be measured in 10 mm NMR tubes. These tubes, however, are unsuitable for strictly anaerobic manipulations as their thin walls render them susceptible to implosion during evacuation. This problem was remedied using special sample tubes available from Wilmad Glass Co. (cat. no. 529-E-10) which have a cylindrical sample cup designed to fit just within a 10 mm NMR tube. They can be obtained equipped with a 5 mm stem which protrudes through the cap of the outer 10 mm tube and can easily withstand evacuation through a tight-fitting silicon rubber septum.

It is necessary to have a liquid which will interfere neither with lock or signal in the outer tube above and below the sample for field homogeneity. We used CCl_4 and also dissolved therein 2-3 μL of

α,α,α-trifluorotoluene as external reference. The relative areas of ^{19}F signals were also determined by planimetric integration. α,α,α-Trifluorotoluene was added as internal reference for spectra in CD_3CN.

Solvents

Except where Triton was omitted, the solvent compositions were, by volume, 5% organic solvent/5% Triton X-100/90% aqueous buffer. Acetonitrile was used chiefly for the organic solvent but some experiments were conducted using methanol, N,N-dimethylformamide or N-methylpyrollidone. These solvents were used without purification, their chief purposes being the provision of a medium for combination of iron salts and thiols and rendering the viscous Triton detergent more readily soluble in water. Triton X-100 was purchased from Aldrich Chemical Co. and used without further purification.

Buffers were generally prepared to a concentration of 0.20 M. While NaTAPS, sodium[tris(hydroxymethyl)methylamino]-3-propanesulfonate, at pH 9.0 enjoyed widest use, we also used the chloride and sulfate salts of TRIS (or THAM), tris(hydroxymethylamino)methane, at pH 8.5 and the sodium salt of 4-morpholine ethanesulfonic acid (MES) at pH 6.0. Two earlier experiments used an acetate buffer at pH 4.85 and in some cases lithium hydroxide was employed in place of buffer.

Deuterated acetonitrile was often trap-to-trap distilled from P_2O_5 but quite often was simply degassed and used without further treatment. We regarded this solvent (99.6 atom-% enriched) as sufficiently dry when the water signal at -2.15 ppm was absent or substantially smaller than

the residual solvent peak at -1.93 ppm. Acetonitrile-d^3 obtained from Cambridge Isotope Laboratories contained impurities which appear in many of our spectra and are so designated.

Reagents

Ferric chloride hexahydrate was obtained in lump form and pulverized before use. Anhydrous ferric chloride powder was used in early experiments but it was thought that the hydrate would permit greater control of stoichiometry especially when weighings were performed under humid conditions. Even so, the hexahydrate does deliquesce. Sulfur used was in granular form.

All thiols used were obtained from Aldrich Chemical Co. and were used without further purification. While benzenethiol was used for most of the work described herein, other thiols were occasionally used whose properties are tabulated below.

Table 8. Relevant properties of thiols

Thiol	F.W.(g/mol)	d(g/mL)	M(mol/L)	pK_a[124]
t-Butylthiol	90.19	0.8	8.9	11.1
Benzyl mercaptan, 99%	124.21	1.058	8.50	9.4
Benzenethiol, 97%	110.18	1.073	9.45	6.4
4-Fluorobenzenethiol, 97%	128.17	1.28	9.69	--

The quaternary ammonium salts used were: tetramethylammonium-bromide (Me_4NBr), tetraethylammonium bromide and chloride (Et_4NBr and $Et_4NCl \cdot H_2O$), tetra-n-propylammonium bromide (n-Pr_4NBr), tetra-n-butylammonium bromide (n-Bu_4NBr), and tetra-n-pentylammonium bromide (n-Pe_4NBr). They were all obtained from Aldrich Chemical Co. and used without further purification.

Cloud Points

In order to examine the effects of various solutes on the micellar solution properties, the lower consolute temperatures (cloud points) of the following mixtures were measured according to a literature method.[125] The components were combined in 2-dram vials which were sealed and placed in a water bath. For most samples, the temperatures for both the onset and disappearance of inhomogeneity (manifested as a cloudy opalescence) were determined by respectively warming and cooling the sample and were either identical or within one degree. Except where noted, solutions were 95% (3.8 mL) buffer and 5% (0.2 mL) Triton. The buffer used in all cases was TRIS-Cl pH 8.3 (50 mM).

The general features observed are: (1) R_4NBr raises the cloud point in the order Et < Pr < Bu (behavior like saturated hydrocarbons rather than electrolytes), (2) benzenethiol lowers the cloud point, and (3) acetonitrile raises the cloud point.

Table 9. Effects of R_4NBr, PhSH and CH_3CN on cloud points of Triton solutions

Solute	Cloud Point, °C
none	63.0
20 μL (50 mM) PhSH	45.0
40 μL (100 mM) PhSH	20.5
84 mg (0.10 M) Et_4NBr	64.0
Et_4NBr + 50 mM PhSH	47.0
Et_4NBr + 100 mM PhSH	22.5
129 mg (0.10 M) n-Bu_4NBr	83.5
n-Bu_4NBr + 50 mM PhSH	64.0
n-Bu_4NBr + 100 mM PhSH	36.5
106 mg (0.10 M)n-Pr_4NBr + 100 mM PhSH	25.8
n-Pr_4NBr + 100 mM PhSH + 0.2 mL CH_3CN	28.0

RESULTS AND DISCUSSION

The scheme in Figure 11 summarizes the cluster assembly pathways found to occur for the reaction system 4PhSH/$FeCl_3$/S in 90/5/5 and the effects of various additives. Although the pathways illustrated in Figure 11 leading to assembly of $[Fe_4S_4(SPh)_4]^{2-}$ are identical to those shown to occur in organic solvents by Hagen et al.,[59] several effects on the reaction system appear to be unique to 90/5/5. We have chosen this solvent composition mostly as a matter of convenience. Similar compositions would likely lead to similar results. We have found that below ~ 3.5 vol % Triton on our preparative scale, reagent and product solubilities decrease significantly. However, as discussed below, these decreases do not prevent cluster assembly. The two most prominent unique features of reactions performed in these aqueous media are (i) the ability of detergent aggregates with relatively hydrophobic R_4N^+ to shield $[Fe_2S_2(SPh)_4]^{2-}$ from water, thereby inhibiting its conversion to $[Fe_4S_4(SPh_4]^{2-}$, and (ii) the facility with which the equilibrium between precursors $[Fe_4(SPh)_{10}]^{2-}$ and $[Fe(SPh)_4]^{2-}$ can be shifted.

General Features of the Cluster Assembly Reactions in Aqueous Media

Preparation of $(Et_4N)_2[Fe_4S_4(SPh)_4]$ is accomplished by following the general procedure but withholding Et_4NBr during ~7 h of reaction. At the reagent concentrations used,the 90/5/5 reaction mixture is probably best characterized as an emulsion. Portions of the reaction mixture diluted fivefold with the same solvent are, however, homogeneous

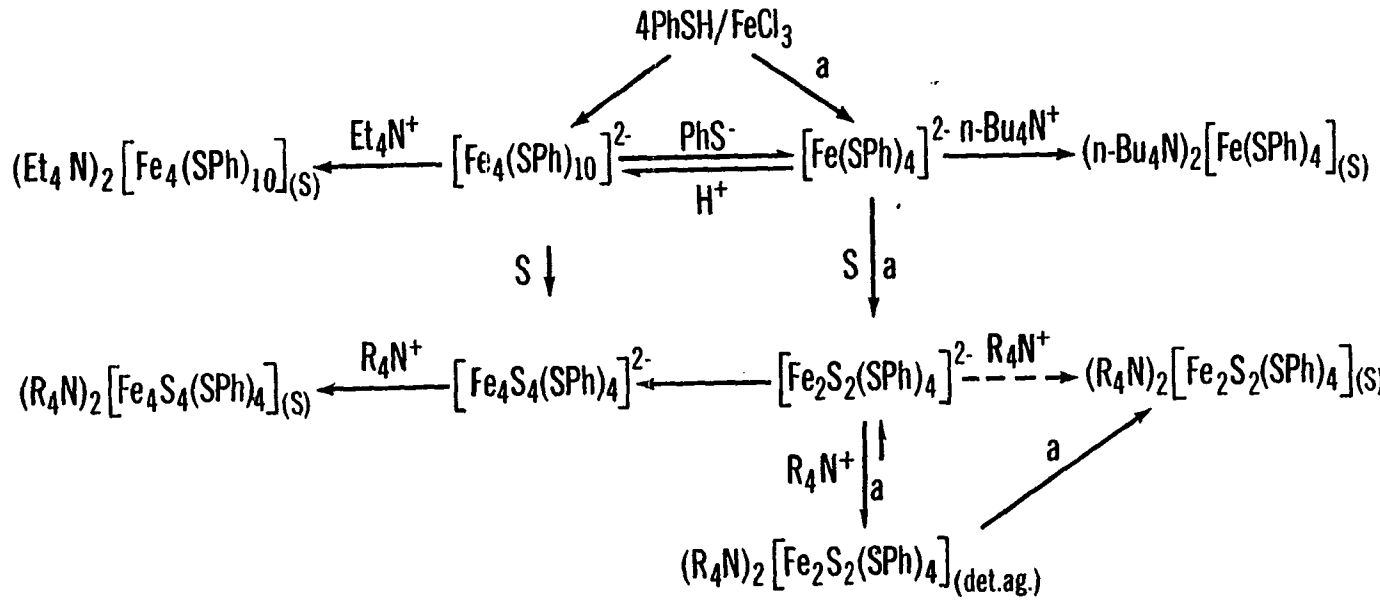

Figure 11. Schematic diagram of cluster assembly pathways and effects thereon for 4/1/1 $PhSH/FeCl_3/S$ in aqueous media. Relative lengths of arrows upon reaction with S are meant to show qualitatively that pathways containing $[Fe(SPh)_4]^{2-}$ to $[Fe_2S_2(SPh)_4]^{2-}$ are favored. The dashed arrow refers to a pathway followed mainly in nondetergent media. det. ag. = detergent aggregate. The pathway marked "a" appears to be followed exclusively in 90/5/5 when R_4N^+ = n-Pe_4N^+

and transparent such that absorption spectra are readily obtained during the course of the reaction.

Shown in Figure 12, the fairly featureless spectrum obtained before addition of sulfur contains shoulders at ~ 335 and 390 nm, both of which are characteristic of the spectrum of $[Fe(SPh)_4]^{2-}$ measured in acetonitrile. The spectrum obtained 6 h after addition of sulfur has λ_{max} = 454 nm and A_{454}/A_{550} = 2.05. These values are both characteristic of the spectrum of $[Fe_4S_4(SPh)_4]^{2-}$ (t^{2-}) measured in the same solvent.[107] Using ε_{454} = 17,400 M^{-1} cm^{-1}, the spectrophotometric yield is calculated to be 96%. This corresponds to $[t^{2-}]$ = 5.6 m$\underline{M}$, about ten times the calculated micelle concentration in 5 vol % (84 m$\underline{M}$) Triton, assuming 140-150 Triton molecules/micelle.[95] The solubilization of t^{2-} in the 5-fold diluted solutions cited above gives a t^{2-}/micelle ratio of ~ 2. This ratio is not unreasonable considering the estimated micellar radius of 43 Å or even the radius of the hydrophobic core of the micelle at 28 Å.[95]

When 0.1 $\underline{M}$ R_4NBr is included in the aqueous buffer at the outset of the reaction, a bluish-black opalescent emulsion forms upon mixing with the $FeCl_3$ + PhSH solution in CH_3CN/Triton. When solid sulfur is present, a purple color emanates from the particles which disappears within two hours. In contrast to those without cation, dilutions of these latter reaction mixtures remain cloudy. With the exception of $R_4N^+ = Me_4N^+$, these emulsions gradually break down over the course of several days at room temperature to give dark solids plus faintly colored solutions. When R = $\underline{n}$-Pe the solid consists of analytically

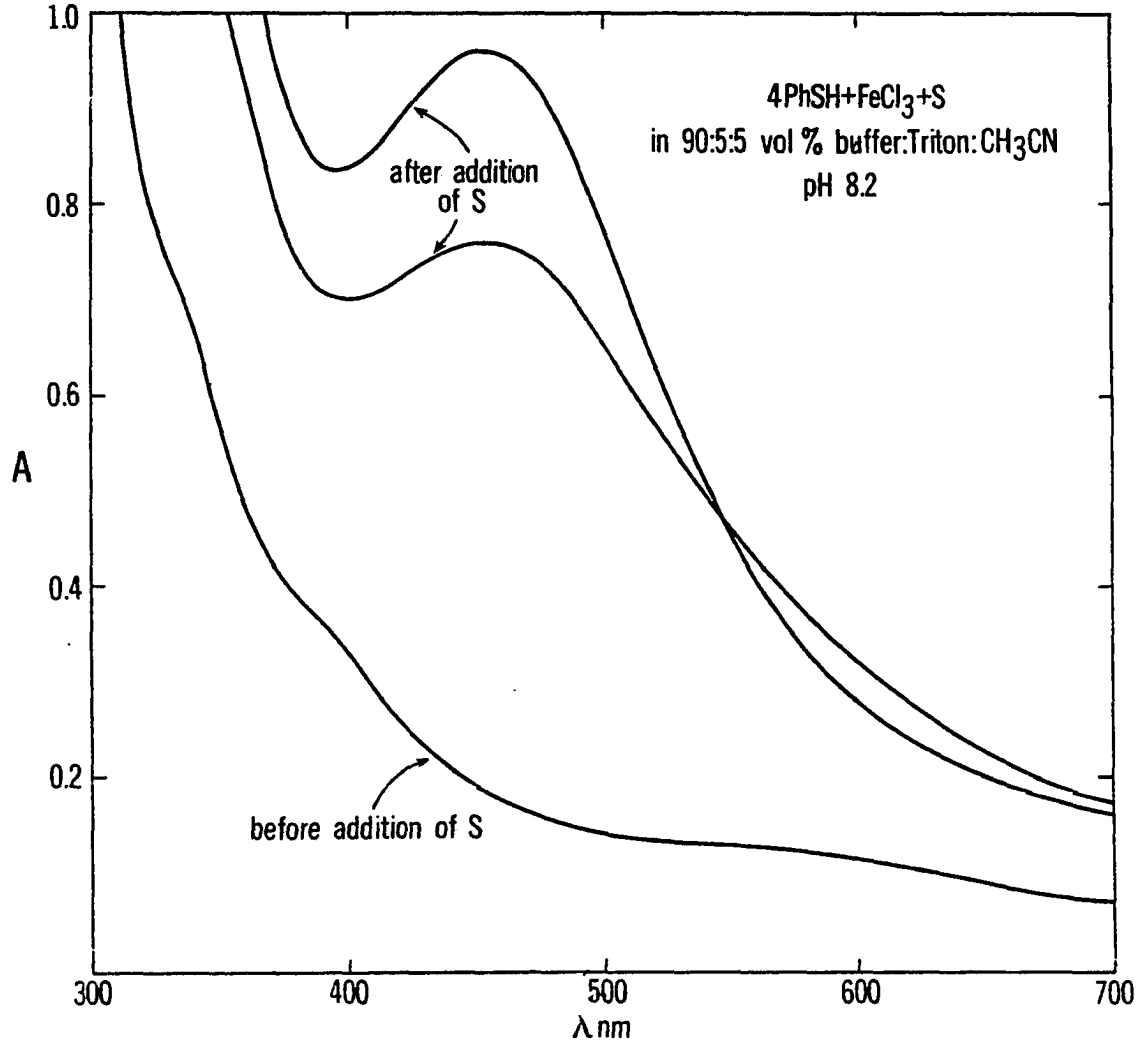

Figure 12. Visible absorption spectra of fivefold dilutions of reaction performed according to the general procedure except that R_4NBr has been withheld. Cell path length was 0.5 mm. Spectra were obtained ~ 30 min (lower A_{454} and higher A_{600}) and ~ 6h after addition of sulfur

pure $(\underline{n}\text{-}Pe_4N)_2[Fe_2S_2(SPh)_4]$. Product distributions in other cases are discussed below.

The turbidity of these solutions is most likely due to an increase in micellar weight related to the "cloud point" phenomenon of Triton.[126] We have confirmed that 100 m$\underline{M}$ PhSH in 5 vol % Triton in aqueous Tris-Cl pH 8.3 lowers the cloud point from 63.0°C to 20.5°C. Storage of the reaction mixtures at 4°C significantly reduces their turbidities and prevents the precipitation referred to above.

$(Et_4N)_2[Fe_4S_4(SPh)_4]$ can also be prepared in 71% yield when Triton is omitted from the reaction mixture. Solid materials are present throughout the course of the reaction as the liquor gradually assumes the color of $[Fe_4S_4(SPh)_4]^{2-}$. Here also, 4.0 g Et_4NBr is added after 7 h and results in almost immediate precipitation of a brown-black solid. Collection of the crude solid and recrystallization from CH_3CN/H_2O gives the analytically pure product. Anal. Calc'd for $C_{40}H_{60}N_2S_8Fe_4$: C, 45.80; H, 5.78; N, 2.67. Found: C, 45.92; H, 5.79; N, 2.66. Similarly, reactions omitting Triton but containing at the outset 0.1 $\underline{M}$ R_4NBr and S are inhomogeneous, resulting in essentially complete precipitation within 2 h. Product distributions in these cases are discussed below.

The importance of premixing $FeCl_3$ + 4PhSH in CH_3CN (which leads to reduction of Fe^{3+} to Fe^{2+} with production of PhSSPh) in the absence of Triton was demonstrated by showing that omission of premixing leads to decreased yields and purity. The reaction system of Christou and Garner,[57] which was used to prepare $[Fe_4S_4(SPh)_4]^{2-}$ in 76% yield, was

used but water was substituted for methanol. Thus, addition of 1.01 g (3.75 mmol) of $FeCl_3 \cdot 6H_2O$ in 8 mL H_2O to 152 mL of water containing 0.67 g (16 mmol) $LiOH \cdot H_2O$, 1.6 mL (15 mmol) PhSH resulted in a heterogeneous mixture which persisted after 0.120 g (3.75 mmol) S were added. After stirring overnight, the mixture was filtered, yielding a red-brown solution with pH 7.4. After addition of 4.2 g (20 mmol) Et_4NBr to the filtrate, a low yield of $(Et_4N)_2[Fe_4S_4(SPh)_4]$ contaminated by $(Et_4N)_2[Fe_4(SPh)_{10}]$ was isolated according to the general procedure. These products were identified by their m-H resonances in a ^1H NMR spectrum of the solid dissolved in CD_3CN, shown in Figure 13.

While we claim no general advantages for our methods on a preparative basis, our yields in 90/5/5 of R_4N^+ salts of $[Fe_4S_4(SPh)_4]^{2-}$ (82%), $[Fe_2S_2(SPh)_4]^{2-}$ (87%,96%), $[Fe(SPh)_4]^{2-}$ (> 90%) compare favorably with those obtained in methanol.[57,59,80] In the case of $[Fe_2S_2(SPh)_4]^{2-}$, yields of 50-55% in methanol after recrystallization as R_4N^+ salts are obtained compared to the ~90% analytically pure yield obtained without recrystallization for the n-Pe_4N^+ salt using our method. Therefore, if $(n\text{-}Pe_4N)_2[Fe_2S_2(SPh)_4]$ is desired (which, unlike the Et_4N^+ salt, is soluble in relatively nonpolar solvents such as dichloromethane), ours is currently the preparative method of choice. These high yields also suggest that this chemistry may be similar to that which occurs in vivo.

Effects of R_4N^+ on product distribution

Our initial attempts to trap $[Fe_2S_2(SPh)_4]^{2-}$ in 90/5/5 using the general procedure and $R_4N^+ = Et_4N^+$ gave a solid consisting of a mixture

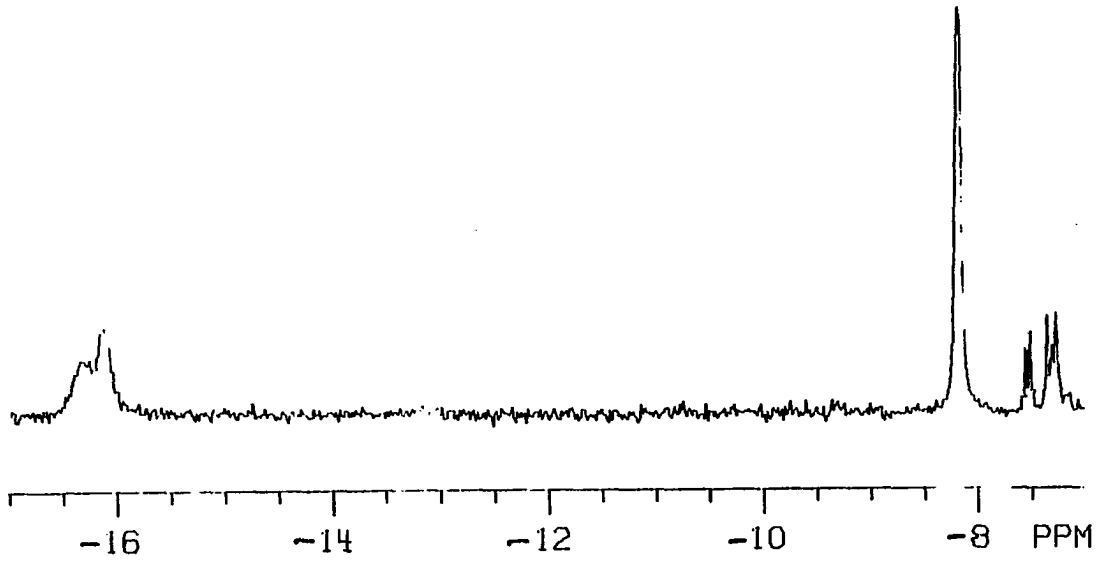

Figure 13. ^{1}H NMR in CD_3CN of solid isolated from a reaction designed to be an aqueous analog to the synthetic method of Christou and Garner[57] (i.e., H_2O and LiOH are used in place of MeOH and LiOMe). Details are given in the text

of $(Et_4N)_2[Fe_2S_2(SPh)_4]$ and $(Et_4N)_2[Fe_4S_4(SPh)_4]$ based on their isotropically shifted m-H NMR resonances in CD_3CN at -9.3 and -8.2 ppm, respectively.[59] This result prompted us to vary R_4N^+ systematically and led to the interesting correlation illustrated in Figure 14. (Individual spectra are shown in Figures 15-20.) Increasing the chain length of the R group leads to a monotonic increase in the proportion of $[Fe_2S_2(SPh)_4]^{2-}$ in the solid reaction product until with R = n-Pe no $[Fe_4S_4(SPh)_4]^{2-}$ is detectable. As discussed above, the latter solid consists of analytically pure $(n\text{-}Pe_4N)_2[Fe_2S_2(SPh)_4]$. The selectivity of $n\text{-}Pe_4N^+$ for $[Fe_2S_2(SPh)_4]^{2-}$ is apparently confined to aqueous media. A reaction conducted according to the general procedure with $R_4N^+ = n\text{-}Pe_4N^+$, but substituting NaOMe in MeOH for aqueous buffer, gave a 77% yield of $(n\text{-}Pe_4N)_2[Fe_4S_4(SPh)_4]$ whose ^1H NMR spectrum in CD_3CN showed only a trace of $[Fe_2S_2(SPh)_4]^{2-}$. The Fe analysis (10.84%) from the solid isolated from the reaction mixture containing $n\text{-}Bu_4N^+$ is consistent with a mixture of $(n\text{-}Bu_4N)_2[Fe_2S_2(SPh)_4]$ and $(n\text{-}Bu_4N)_2[Fe_4S_4(SPh)_4]$ in which the mole fraction of $(n\text{-}Bu_4N)_2[Fe_2S_2(SPh)_4]$ is 0.91. The ratio of areas of the m-H resonances in the corresponding spectrum of Figure 19 gives a mole fraction of 0.89. From the weight of solid recovered from the $n\text{-}Bu_4N^+$ reaction mixture and its Fe analysis, a 96% recovery of Fe is calculated. Anal. Calculated for a mixture which is 90.9% dimer and 9.1% tetramer: C, 60.52; H, 8.34; N, 2.52; Fe, 10.84. Found: C. 59.84; H, 8.02; N, 2.57; Fe, 10.84. These results indicate that using the general procedure, the reaction system of $4PhSH/FeCl_3/S$ in 90/5/5

Figure 14. ^1H NMR spectra in CD_3CN at ~22°C of unrecrystallized solids isolated from the reaction system of 4/1/1 PhSH/$FeCl_3$/S in 90/5/5 containing the R_4N^+ ion listed nearest each spectrum. Reactions were conducted according to the general procedure described in the experimental section. m-H resonances of $[Fe_2S_2(SPh)_4]^{2-}(d^{2-})$ at -9.3 ppm and $[Fe_4S_4(SPh)_4]^{2-}(t^{2-})$ at -8.2 ppm are labeled on the top spectrum. d^{2-}/t^{2-} mole ratios determined from the integrated areas of the m-H resonances are listed near each spectrum. Numbers in parentheses are ratios obtained for reactions conducted in the absence of Triton. No resonances other than those shown were observed in any of the spectra from -60 to +60 ppm. The multiplet near -7.5 ppm is due to PhSSPh. Peaks upfield of -3.4 ppm are due to cation, CD_2HCN (-1.93 ppm) or water (-2.1 ppm). x denotes solvent impurity

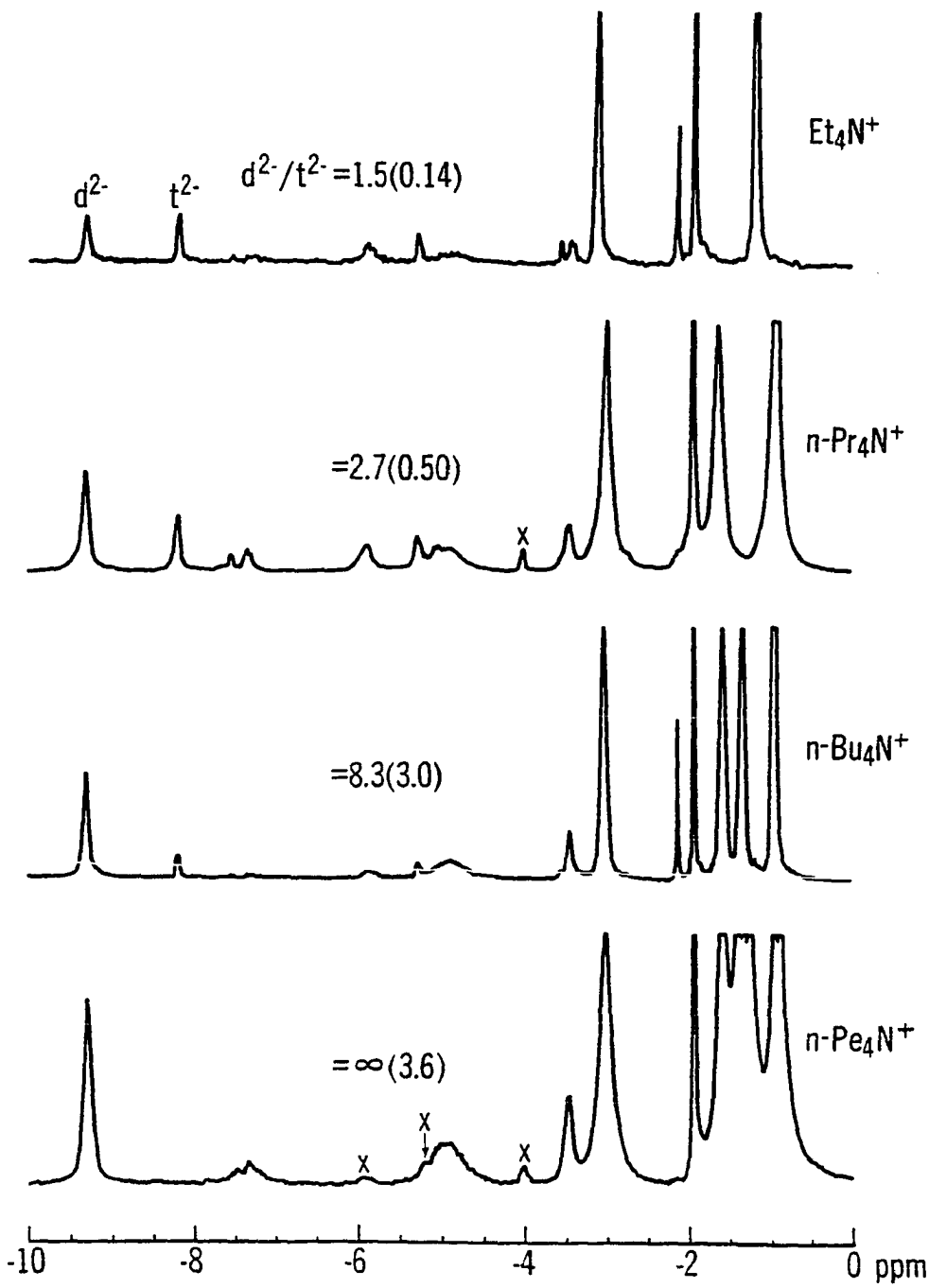
d2-
t2-
d2-/t2-=1.5(0.14)
Et4N+
=2.7(0.50)
n-Pr4N+
=8.3(3.0)
n-Bu4N+
=∞(3.6)
n-Pe4N+
X
-10
-8
-6
-4
-2
0 ppm

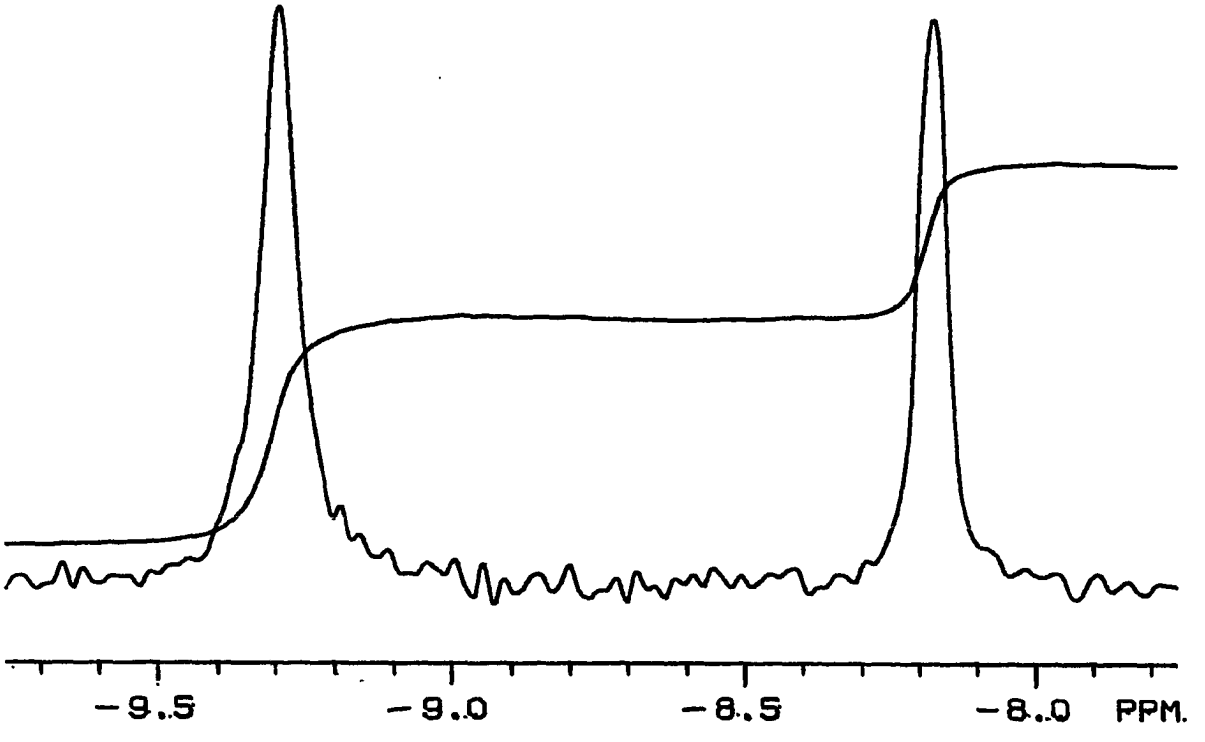

Figure 15. ^{1}H NMR spectrum in CD_3CN of solid isolated from the reaction performed using the general procedure with R_4NBr = Et_4NBr

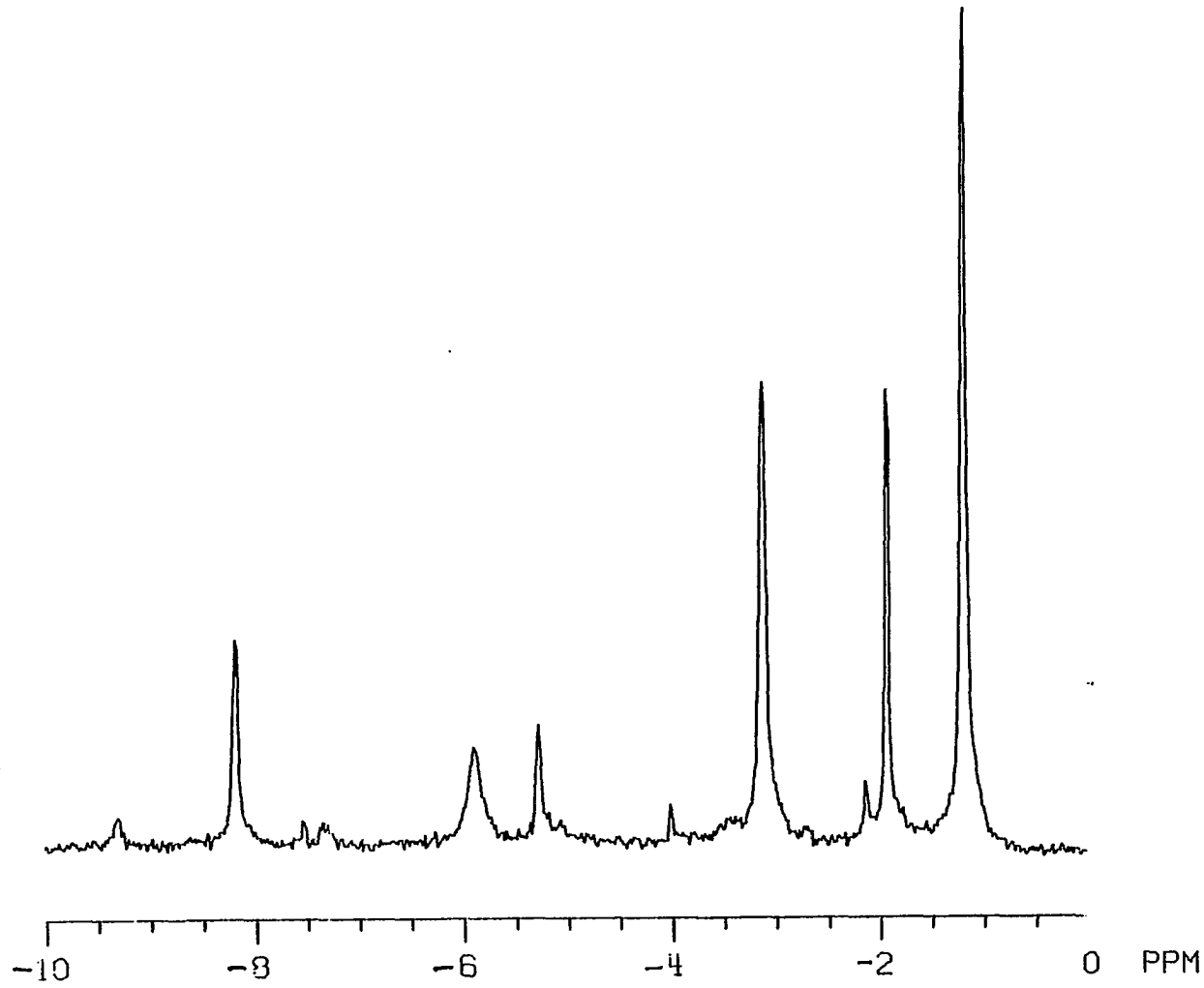

Figure 16. ^{1}H NMR spectrum in CD_3CN of solid isolated from the reaction performed in the absence of Triton with R_4NBr = Et_4NBr

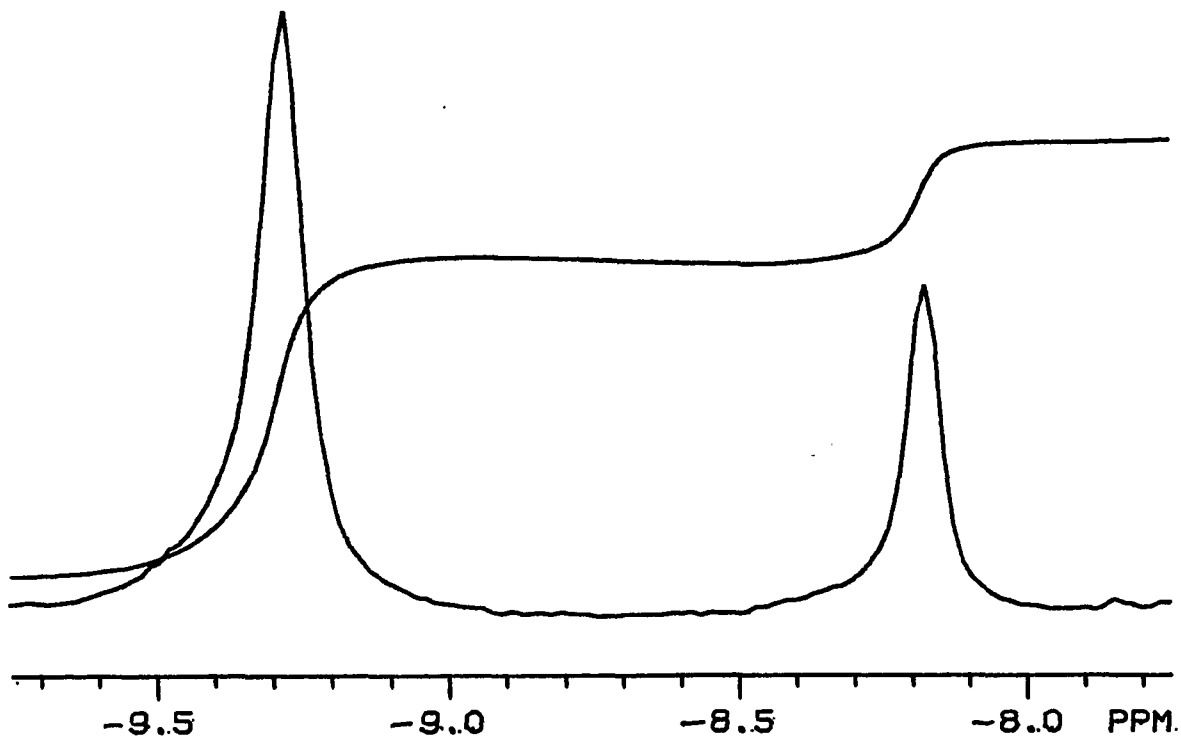

Figure 17. ^{1}H NMR spectrum in CD_3CN of solid isolated from the reaction performed using the general procedure with R_4NBr = $\underline{n}$-Pr_4NBr

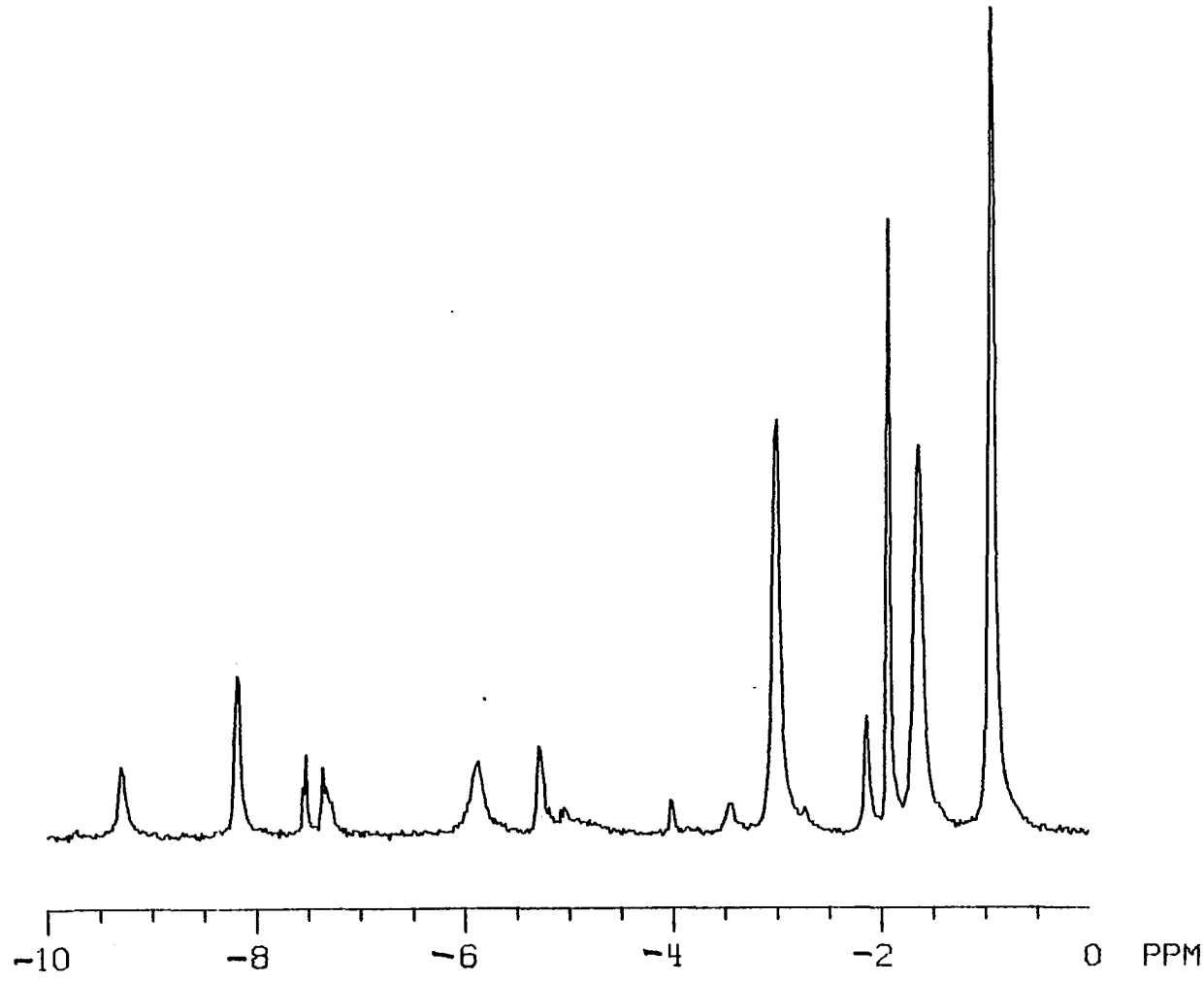

Figure 18. ^{1}H NMR spectrum in CD_3CN of solid isolated from the reaction performed in the absence of Triton with R_4NBr = $\underline{n}$-Pr_4NBr

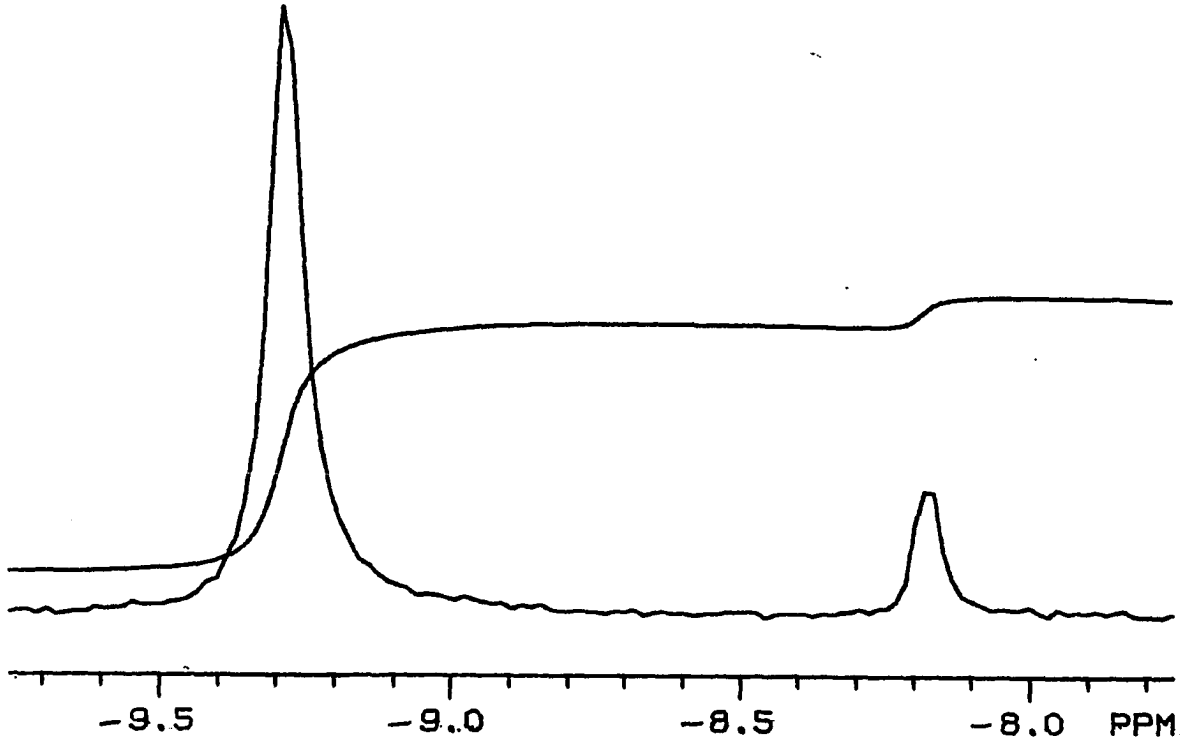

Figure 19. ^{1}H NMR spectrum in CD_3CN of solid isolated from the reaction performed using the general procedure with R_4NBr = $\underline{n}$-Bu_4NBr

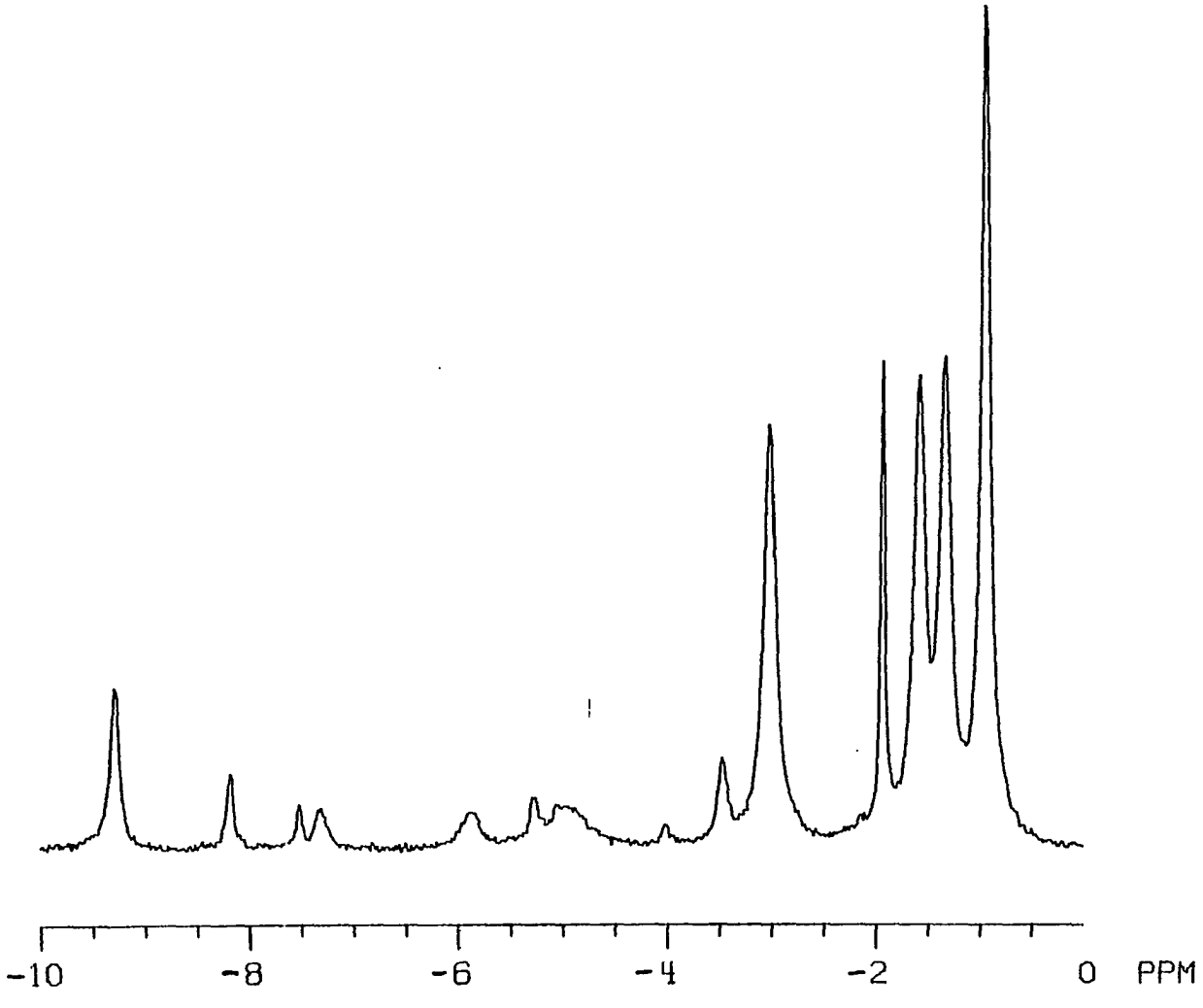

Figure 20. ^{1}H NMR spectrum in CD_3CN of solid isolated from the reaction performed in the absence of Triton with R_4NBr=$\underline{n}$-Bu_4NBr

yields essentially only R_4N^+ salts of $[Fe_2S_2(SPh)_4]^{2-}$ and $[Fe_4S_4(SPh)_4]^{2-}$. Further evidence for this conclusion is that no $[Fe(SPh)_4]^{2-}$ (m-H at -22.3 ppm) or $[Fe_4(SPh)_{10}]^{2-}$ (m-H at -16.2 ppm) was detected in any of the spectra of Figure 14. No significant differences or trends were detected in the rates of precipitation of these solids.

The preceding results suggest that the cation influences the rate of $[Fe_2S_2(SPh)_4]^{2-}$ to $[Fe_4S_4(SPh)_4]^{2-}$ conversion and/or the distribution of precursors, presumably $[Fe(SPh)_4]^{2-}$ and $[Fe_4(SPh)_{10}]^{2-}$. That the former influence is operative can be seen from Figure 21. Shown are absorption spectra of a stock solution of a predetermined concentration of $(Et_4N)_2[Fe_2S_2(SPh)_4]$ in DMF diluted with equal volumes of Triton followed by dilutions with aqueous buffer containing either Et_4NBr or n-Bu_4NBr such that the final solvent composition is ~ 90/5/5 vol % buffer/DMF/Triton. The $[R_4N^+]/[Fe]$ ratio used for these spectra is the same as used in the general procedure, but the concentrations are diluted ~ 11-fold. With excess Et_4NBr, the spectrum obtained 5 min after mixing in 90/5/5 is nearly identical with that of $[Fe_4S_4(SPh)_4]^{2-}$ in the same medium having λ_{max} at 452 nm and A_{452}/A_{550} = 2.04.[107] Only minor changes occur thereafter and the spectrum stops changing significantly ~ 40 min after mixing. Using the final absorbance and ε_{454} = 17,400 M^{-1} cm^{-1} gives a 100% yield of $[Fe_4S_4(SPh)_4]^{2-}$ assuming transformation according to reaction 17, which under our conditions appears to be irreversible.[91,107] In contrast, a solution prepared

$$2[Fe_2S_2(SPh)_4]^{2-} \rightarrow [Fe_4S_4(SPh)_4]^{2-} + PhSSPh + 2PhS^- \qquad (17)$$

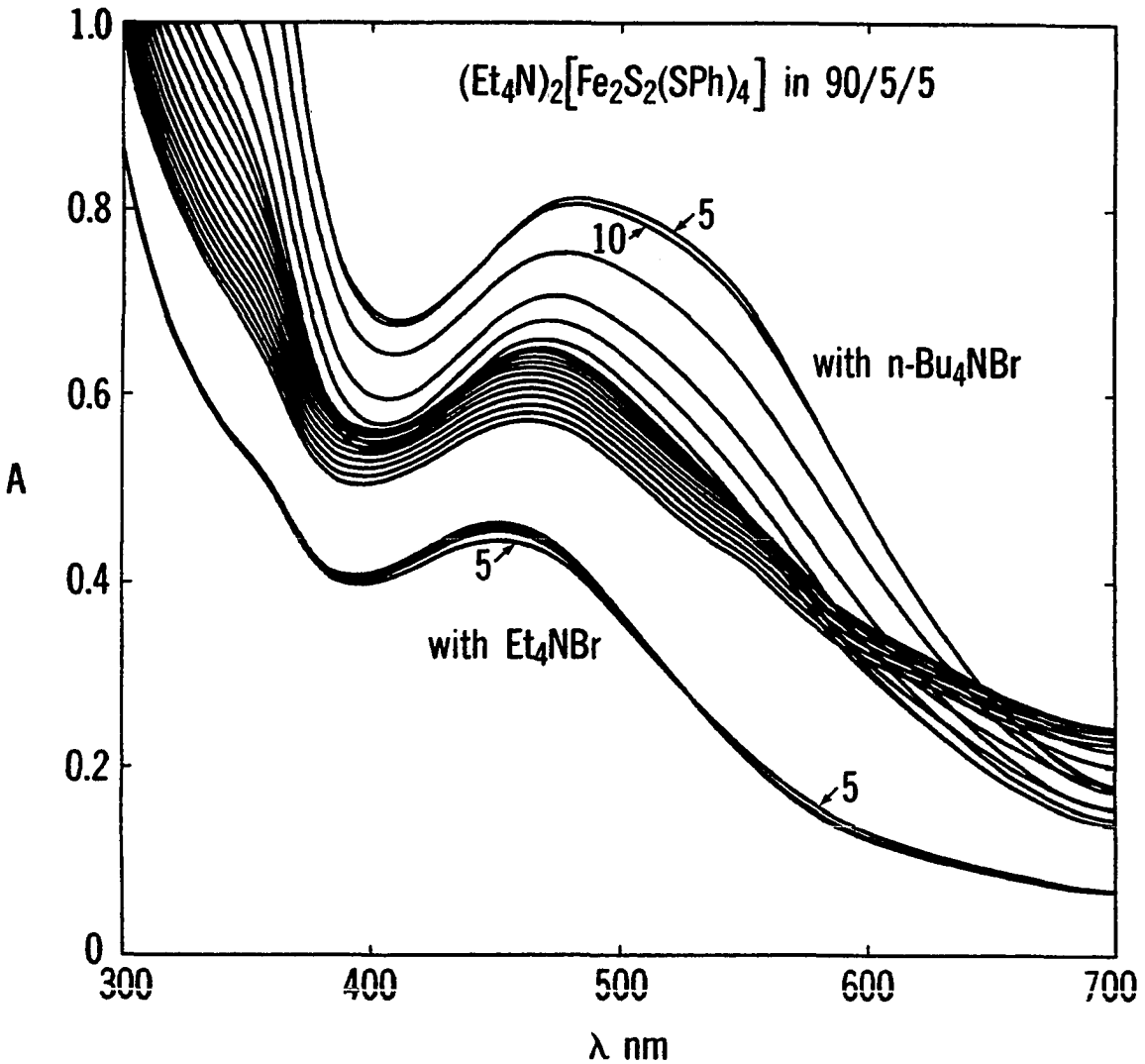

Figure 21. Absorption spectra resulting from dilutions of a 20.9 mM stock solution of $(Et_4N)_2[Fe_2S_2(SPh)_4]$ in DMF with Triton followed by aqueous 0.20 M Tris-sulfate at pH 8.5 containing (upper spectra) 8.9 mM n-Bu_4NBr or (lower spectra) 8.9 mM Et_4NBr. Final solvent composition is ~ 90/5/5 vol % aqueous buffer/DMF/Triton. Numbers near spectra refer to minutes after mixing. Unlabeled spectra were recorded thereafter every 30 min for the upper (n-Bu_4NBr) set and every 20 min for the lower (Et_4NBr) set. Cell path length = 0.50 mm

identically but containing n-Bu_4NBr in place of Et_4NBr gives a spectrum 5 min after mixing (λ_{max}, 484 nm, sh ~ 540 nm) closely resembling that of $[Fe_2S_2(SPh)_4]^{2-}$ in DMF (λ_{max}, 490, sh ~ 540 nm).[32] Over the course of ~ 9 h, the spectra gradually approach that of $[Fe_4S_4(SPh)_4]^{2-}$. After several hours the absorbance starts to increase with time at longer wavelengths due to gradual precipitation of $(n\text{-}Bu_4N)_2[Fe_nS_n(SPh)_4]$ (n = 2,4). When reaction 17 proceeds to completion in the absence of excess R_4N^+, addition of n-Pe_4NBr to a concentration of 0.10 M does not reverse the reaction.

If the effect illustrated in Figure 21 is the only influence of R_4N^+ in the 90/5/5 reaction mixture, the correlation of cation size with proportion of $[Fe_2S_2(SPh)_4]^{2-}$ illustrated in Figure 14 could be explained as an influence of R_4N^+ on the partitioning of $[Fe_2S_2(SPh)_4]^{2-}$ between water-rich and water-poor regions of the solvent. The increasing hydrophobicity of R_4N^+ with increasing alkyl chain length would, by ion pairing, increase the solubility of $[Fe_2S_2(SPh)_4]^{2-}$ in hydrophobic regions of the Triton micelles or aggregates which are also likely to contain higher concentrations of PhSH. Lack of exposure to water and high PhSH concentrations are both known to inhibit $[Fe_2S_2(SPh)_4]^{2-} \rightarrow [Fe_4S_4(SPh)_4]^{2-}$ conversion.[91,107] This interpretation is consistent with the increased solubility of $(n\text{-}Pe_4N)_2[Fe_2S_2(SPh)_4]$ compared to $(Et_4N)_2[Fe_2S_2(SPh)_4]$ in less polar solvents such as THF and CH_2Cl_2.

The mole ratios $[Fe_2S_2(SPh)_4]^{2-}/[Fe_4S_4(SPh)_4]^{2-}$ obtained using the general procedure but omitting Triton are listed in parentheses in

Figure 14 for each R_4N^+. Although the same trend is observed, the R_4N^+ are not nearly so effective at increasing the proportion of $[Fe_2S_2(SPh)_4]^{2-}$ in the absence of Triton. These results support the above conclusions concerning inhibition of reaction 17. In the absence of Triton, the trend of increasing proportion of $[Fe_2S_2(SPh)_4]^{2-}$ with increasing alkyl chain length of R_4N^+ is probably due to the effect discussed below.

Influence of R_4N^+ on distribution of Fe-SPh precursors

We have also gathered evidence that R_4N^+ influences the distribution of the nonsulfide containing precursors to $[Fe_2S_2(SPh)_4]^{2-}$ and $[Fe_4S_4(SPh)_4]^{2-}$ in 90/5/5. Stirring of preassembled $(Et_4N)_2[Fe_4(SPh)_{10}]$ or $(\underline{n}\text{-}Bu_4N)_2[Fe_4(SPh)_{10}]$ in 90/5/5 containing 0.1 M Et_4NBr or 0.1 M $\underline{n}\text{-}Bu_4NBr$, respectively, yields solids which, when dissolved in CD_3CN give the ^1H NMR spectra shown in Figure 22 in the $\underline{m}$-H region. The doublet at -16.2 ppm is due to the bridging and terminal thiolates of $[Fe_4(SPh)_{10}]^{2-}$ and is the only major resonance observed in the case of the solid isolated from the Et_4N^+ containing mixture. This solid contains essentially only the starting material and was recovered in 85% yield. On the other hand, the solid isolated from the $\underline{n}\text{-}Bu_4N^+$ containing mixture yields several resonances in the $\underline{m}$-H region, only some of which have previously been identified. Although the doublet at -16.2 ppm due to the starting $[Fe_4(SPh)_{10}]^{2-}$ remains, the majority of the intensity occurs at -22.8 ppm and is due to $[Fe(SPh)_4]^{2-}$. Additional resonances occur at -25.2, -14.7 and -10.6 ppm. As shown in

Figure 23, essentially the same distribution of species in the solid product is obtained using the general procedure (R_4N^+ = $\underline{n}$-Bu_4N^+) but omitting S, except that the -10.6 and -25.2 ppm resonances are extremely weak. Coucouvanis *et al.*[88] have reported that $[Fe_4(SPh)_6Cl_4]^{2-}$, with an adamantane-like Fe-S framework and terminal Cl's has $\underline{m}$-H at -14.4, $\underline{p}$-H at +17.3 and $\underline{o}$-H at +20.3 ppm in CD_3CN at ~27°C. We have verified these peak positions by the titration shown in Figure 24 of $(\underline{n}\text{-}Bu_4N)_2[Fe_4(SPh)_{10}]$ with PhCOCl in CD_3CN, which effects substitution of terminal PhS^- by Cl^-. With 4 equivalents of PhCOCl we find the major isotropically shifted ^1H resonances at -14.6, +17.6 and +20.6 ppm at ~22°C. However, we do not observe resonances at or near 17.6 and 20.6 ppm in upfield regions of the spectra of either Figures 22 or 23. A clue to the assignment of the -14.7 ppm resonance lies in the temperature dependent spectra shown in Figure 23. Hagen and Holm[90] have shown that equilibrium 18 occurs in acetonitrile. ^1H NMR of the species of equilibrium 18 shows that, as the temperature is lowered the CH_2

$$3[Fe_2(SEt)_6]^{2-} \rightleftarrows 2[Fe(SEt)_4]^{2-} + [Fe_4(SEt)_{10}]^{2-} \qquad (18)$$

resonances shift downfield for $[Fe(SEt)_4]^{2-}$ and $[Fe_4(SEt)_{10}]^{2-}$ and upfield for $[Fe_2(SEt)_6]^{2-}$. As can be seen from Figure 23, an upfield shift with lower temperature is observed only for the -14.8 ppm resonance, suggesting its assignment to $[Fe_2(SPh)_6]^{2-}$. This assignment also places the shifts of Figure 23 in the order corresponding to those of the CH_2 resonances of $[Fe(SEt)_4]^{2-}$ (-196 ppm), $[Fe_4(SEt)_{10}]^{2-}$ (-133, -113 ppm) and $[Fe_2(SEt)_6]^{2-}$ (-69 ppm) at 297K.[90] Titrations of

$[Fe_4(SPh)_{10}]^{2-}$ with PhCOCl in CD_3CN reveal a terminally substituted intermediate $[Fe_4(SPh)_6(SPh)_{4-x}Cl_x]^{2-}$ (x = 1-3) with m-H at -15.5 ppm at -22°C. Thus, the weak resonances between -16.2 and -14.7 ppm in Figure 22 (from a mixture with no Cl^-) are likely due to terminally substituted species of the type $[Fe_4(SPh)_6(SPh)_{4-x}(OH)_x]^{2-}$. The -25.0 ppm resonance in the 297K spectrum of Figure 23 (-25.2 in Figure 22) has a nearly parallel temperature dependence to that due to $[Fe(SPh)_4]^{2-}$ at -22.6 ppm, suggesting assignment of the former to a mononuclear Fe(II)SPh species. The much greater intensity of the -10.6 ppm resonance in Figure 22 than in Figure 23 suggests its derivation from $[Fe_4(SPh)_{10}]^{2-}$, and its doublet structure suggests bridging and terminal thiolates. $[Fe_3(SPh)_3Cl_6]^{3-}$ with a six-membered Fe-S ring contains only bridging thiolates with m-H at -12.3 ppm at -30°C.[89] One reasonable interpretation of Figure 22 is that $[Fe_4(SPh)_{10}]^{2-}$ fragments by loss of $Fe(SPh)_2L_2^{2-}$ units (-25.2 ppm) generating in turn $[Fe_3(SPh)_8]^{2-}$ (-10.6 ppm), $[Fe_2(SPh)_6]^{2-}$ (-14.7 ppm) and $[Fe(SPh)_4]^{2-}$ (-22.8 ppm).[127] Since Figure 23 shows less of the intermediate fragmentation species and was generated from a mixture containing free PhS^-, an appropriate formulation for 4PhSH/$FeCl_3$ in 90/5/5 is probably equilibrium 19 with $[Fe_2(SPh)_6]^{2-}$ as a metastable intermediate. In this case, the transformations in equilibrium 19 would occur via equilibria 20 and 21.

$$[Fe_4(SPh)_{10}]^{2-} + 6PhS^- \rightleftarrows 4[Fe(SPh)_4]^{2-} \quad (19)$$

$$[Fe_4(SPh)_{10}]^{2-} + 2PhS^- \rightleftarrows 2[Fe_2(SPh)_6]^{2-} \quad (20)$$

$$[Fe_2(SPh)_6]^{2-} + 2PhS^- \rightleftarrows 2[Fe(SPh)_4]^{2-} \quad (21)$$

Equilibrium 19 was previously suggested but not observed by Hagen et

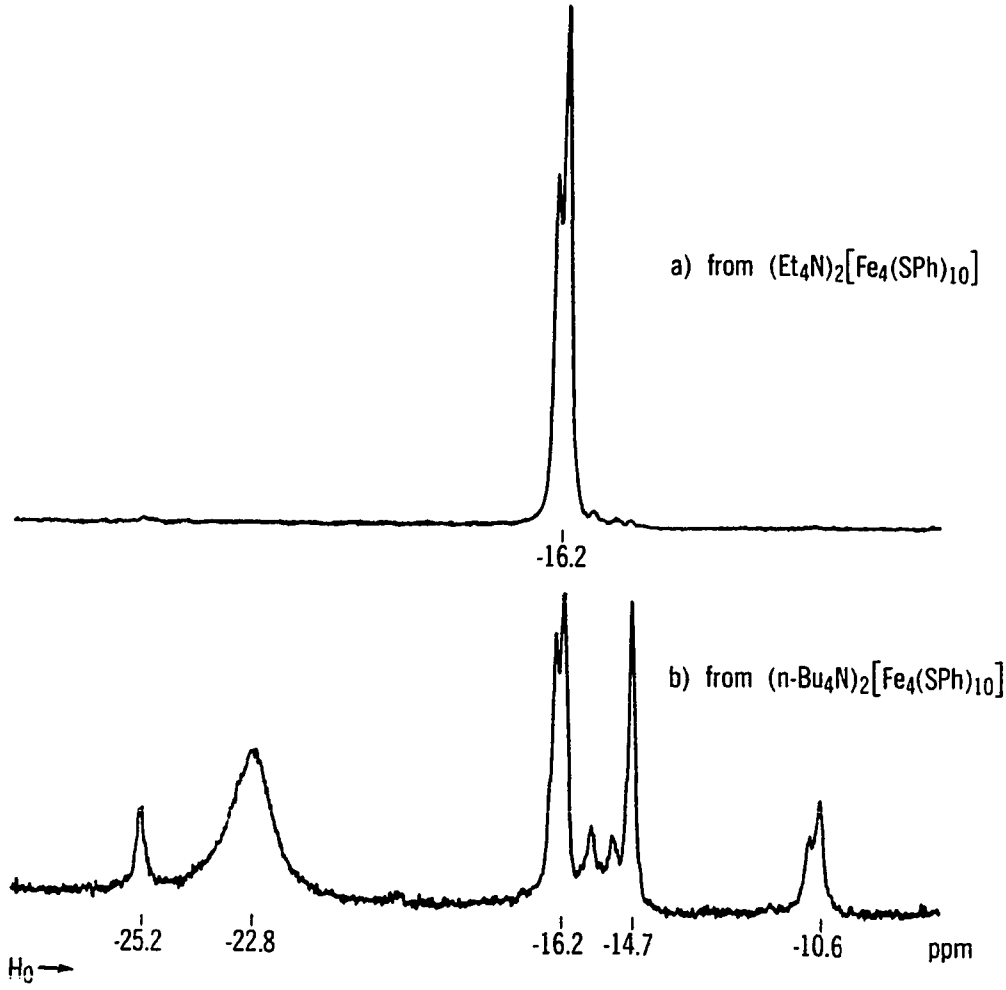

Figure 22. ^1H NMR spectra in CD_3CN at ~22°C of solids isolated from the following procedure: 1.38 g $(R_4N)_2[Fe_4(SPh)_{10}]$ were dissolved in 8 mL CH_3CN and transferred to 8 mL Triton. This mixture was then transferred to 144 mL 0.20 M Tris-sulfate (pH 8.5) which contained 0.10 M R_4NBr, the quaternary ammonium salt having the same cation as the cluster anion above. This mixture emulsified and was stirred for 20 hrs, after which stirring was stopped. Workup was identical to that of the general procedure after solids precipitated

Figure 23a. ^1H NMR spectra in CD_3CN at the indicated temperatures of solids isolated from the 90/5/5 reaction mixture containing 4PhSH/$FeCl_3$ and 0.1 M $\underline{n}$-Bu_4NBr. Doublet near -7.5 ppm is due to PhSSPh. Peaks marked with x are due to solvent impurities

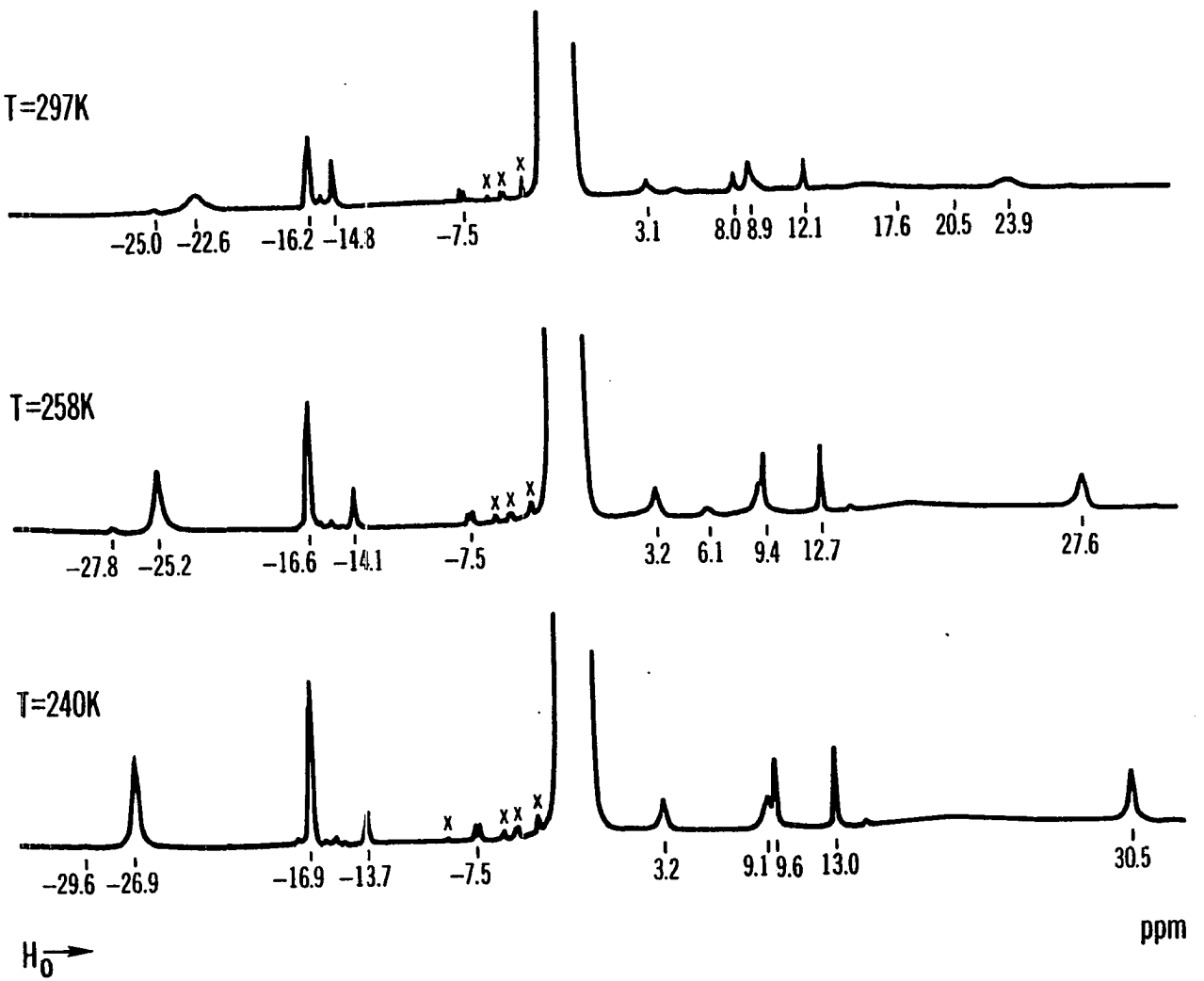
^1H NMR in CD_3CN from 4PhSH/$FeCl_3$ in 90/5/5
T=297K
-25.0 -22.6 -16.2 -14.8 -7.5
3.1 8.0 8.9 12.1 17.6 20.5 23.9
T=258K
-27.8 -25.2 -16.6 -14.1 -7.5
3.2 6.1 9.4 12.7 27.6
T=240K
-29.6 -26.9 -16.9 -13.7 -7.5
3.2 9.1 9.6 13.0 30.5
ppm
H_0

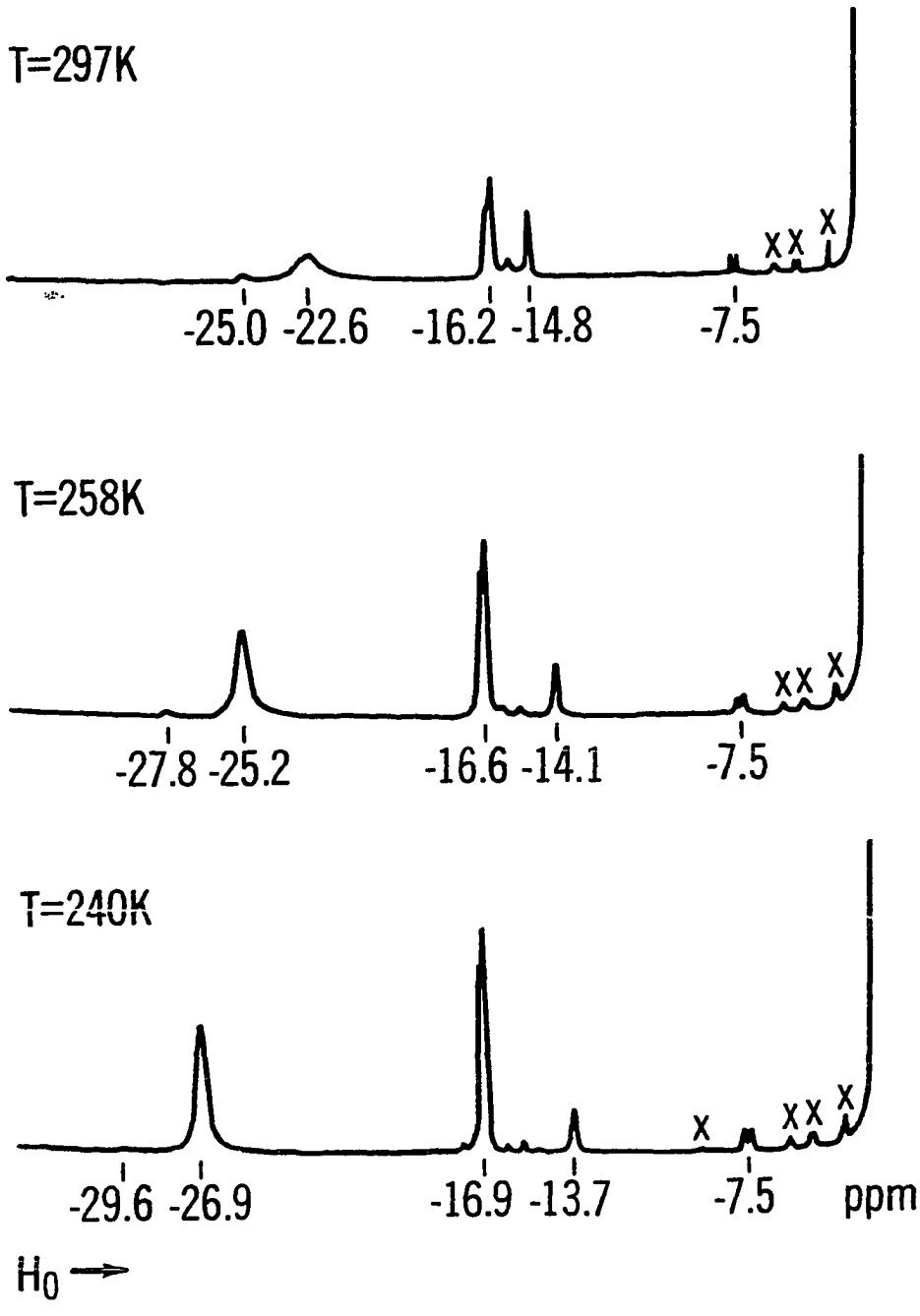

Figure 23b. The m-H region of Figure 23a

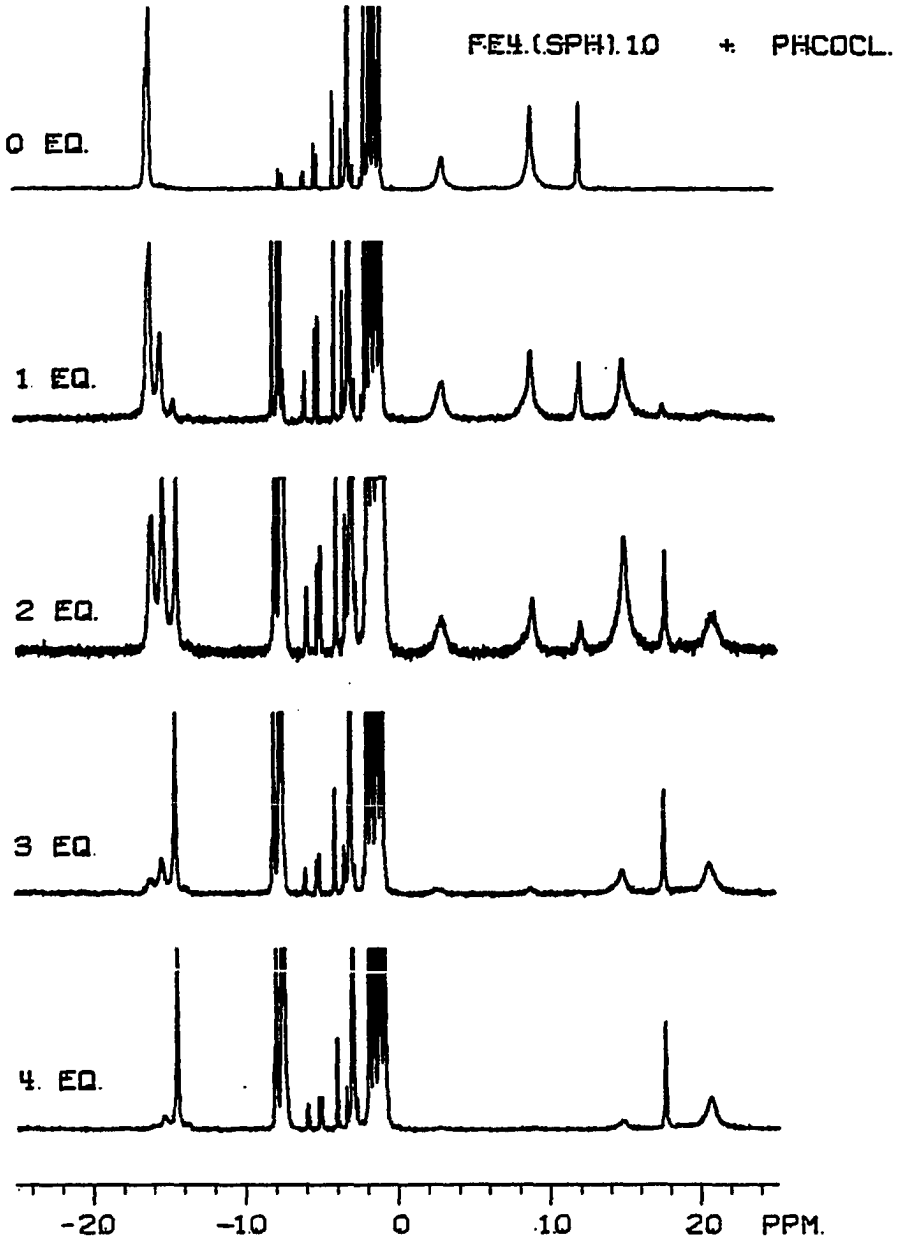

Figure 24. ^1H NMR spectra in CD_3CN at ~22°C resulting from the reaction of 0.0154 g (8.56 μmol) $(Bu_4N)_2[Fe_4(SPh)_{10}]$ with 1-4 eq benzoyl chloride (0.992 μL = 1 eq) in ~0.7 mL CD_3CN

al.[59] for organic solvents. In support of this suggestion, equimolar quantities of Et_3N and PhSH added in excess to the CD_3CN solution in Figure 22b convert all m-H resonances to a single resonance at -22.3 ppm due to $[Fe(SPh)_4]^{2-}$.

An even more striking effect of R_4N^+ is seen in 90/5/5 containing 12PhSH/$FeCl_3$ and LiOH equimolar to PhSH in place of buffer. At this PhS^-/Fe^{3+} ratio in acetonitrile or methanol, $[Fe(SPh)_4]^{2-}$ is essentially the only iron-thiolate species. Analogously in 90/5/5, $(n\text{-}Bu_4N)_2[Fe(SPh)_4]$ can be isolated in nearly quantitative yield in the presence of excess n-Bu_4NBr as described in the Experimental Section. However, under identical conditions in 90/5/5 only $(Et_4N)_2[Fe_4(SPh)_{10}]$ (see Figure 25) can be isolated in ~76% yield when Et_4NBr is substituted for n-Bu_4NBr. These results demonstrate that equilibria 19-21 are quite facile in 90/5/5 and readily shifted by the nature of R_4N^+. The effect of n-Bu_4N^+ on the 4PhSH/$FeCl_3$ system in 90/5/5 cannot be explained solely by preferential solubilization of $[Fe(SPh)_4]^{2-}$ in the interior of a micelle. Nearly the same distribution of species illustrated in Figure 23 is obtained from a reaction mixture identical to that used for Figure 23 but omitting Triton. In this case, a lower solubility of $(n\text{-}Bu_4N)_2[Fe(SPh)_4]$ vs. $(n\text{-}Bu_4N)_2[Fe_4(SPh)_{10}]$ may produce the observed effect.

In acetonitrile, salts of $[Fe_4(SPh)_{10}]^{2-}$ upon reaction with S yield only $[Fe_4S_4(SPh)_4]^{2-}$.[59] However, Figure 26 shows that in 90/5/5 both Et_4N^+ and n-Bu_4N^+ salts of $[Fe_4(SPh)_{10}]^{2-}$ upon reaction with S yield substantial proportions of $[Fe_2S_2(SPh)_4]^{2-}$ as well. The result with

Figure 25. ^1H NMR spectra in CD_3CN at ~22°C of solids isolated from the 90/5/5 reaction mixture containing 12PhSH/$FeCl_3$ and 0.1 M R_4NBr. Doublet near -7.5 ppm is due to PhSSPh. Peaks marked with x are due to solvent impurities.

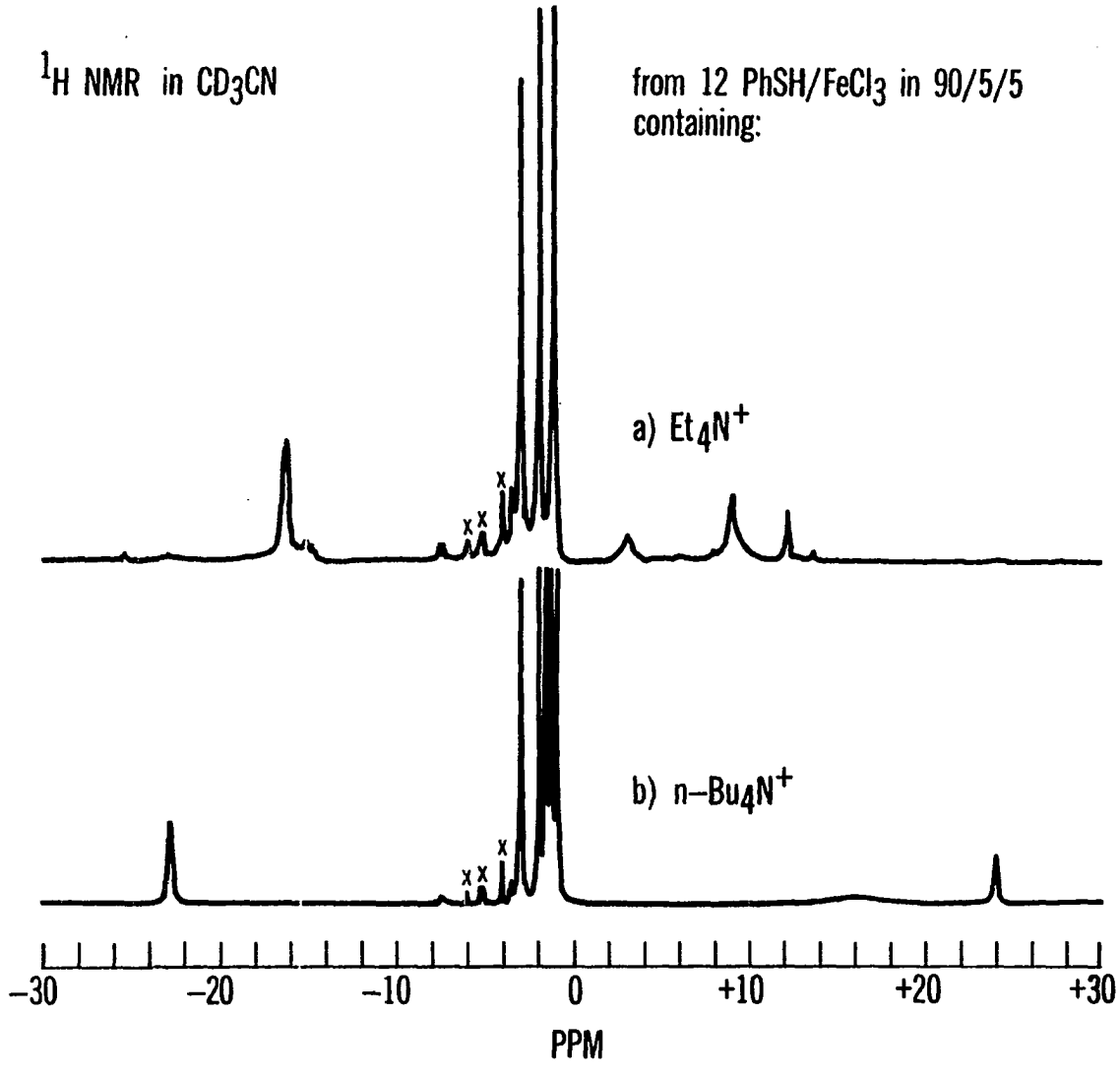
^{1}H NMR in CD_3CN
from 12 PhSH/$FeCl_3$ in 90/5/5 containing:
a) Et_4N^+
b) n–Bu_4N^+
x
x
x
x
x
x
−30
−20
−10
0
+10
+20
+30
PPM

Figure 26. ^1H NMR spectra in CD_3CN at ~22°C of solids isolated from the reaction of $(R_4N)_2[Fe_4(SPh)_{10}]$ with 4 eq S. Reactions were assembled to match the stoichiometry and concentration of the general procedure (i.e., 3.75 mmol Fe, 15 mmol S). Buffer component of 90/5/5 was 0.20 m Tris-sulfate pH 8.5 and contained 0.1 M Et_4NBr or 0.1 M n-Bu_4NBr, respectively. Positions of the m-H resonances of $[Fe_2S_2(SPh)_4]^{2-}$ (d^{2-}) and $[Fe_4S_4(SPh)_4]^{2-}$ (t^{2-}) are indicated. Multiplet near -7.5 ppm is due to PhSSPh. The feature near -7 ppm is due to residual Triton. No other signals were observed in the range -30 to +30 ppm

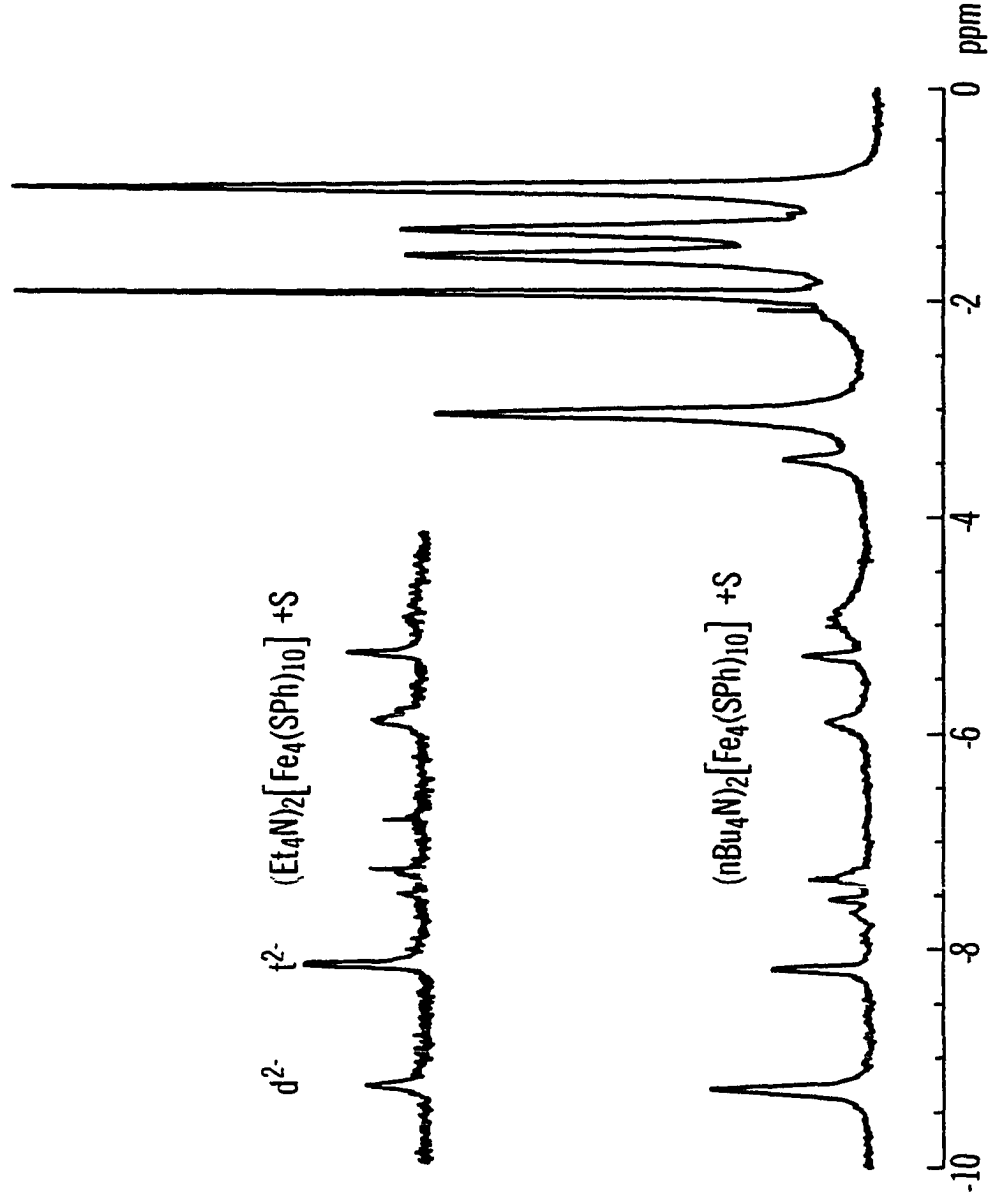
d2-
t2-
(Et4N)2[Fe4(SPh)10] +S
(nBu4N)2[Fe4(SPh)10] +S
0
-2
-4
-6
-8
-10
ppm

$(\underline{n}\text{-}Bu_4N)_2[Fe_4(SPh)_{10}]$ is consistent with the fragmentation discussed above and illustrated in Figure 22b. Consistent with the effects of R_4N^+ discussed above, the proportion of $[Fe_4S_4(SPh)_4]^{2-}$ is larger in the mixture containing Et_4N^+. However, the fact that any $[Fe_2S_2(SPh)_4]^{2-}$ is obtained from this latter mixture is further evidence that in 90/5/5 an equilibrium such as 19 occurs and that both the $[Fe(SPh)_4]^{2-} \rightarrow [Fe_2S_2(SPh)_4]^{2-} \rightarrow [Fe_4S_4(SPh)_4]^{2-}$ and $[Fe_4(SPh)_{10}]^{2-} \rightarrow [Fe_4S_4(SPh)_4]^{2-}$ pathways are operative. In addition, the latter result suggests that reaction with S shifts equilibrium 19 to the right in 90/5/5. This shift could derive from faster reaction of $[Fe(SPh)_4]^{2-}$ than $[Fe_4(SPh)_{10}]^{2-}$ with S and/or from release of PhS^- according to reaction 22, as opposed to reaction 23, which releases no PhS^-.[59] These results show that,

$$2[Fe(SPh)_4]^{2-} + 2S \rightarrow [Fe_2S_2(SPh)_4]^{2-} + PhSSPh + 2PhS^- \quad (22)$$

$$[Fe_4(SPh)_{10}]^{2-} + 4S \rightarrow [Fe_4S_4(SPh)_4]^{2-} + 3PhSSPh \quad (23)$$

unlike the case in organic solvents, the extents of reactions 17 and 19-23 in 90/5/5 are influenced by the nature of R_4N^+. Furthermore, for the $4PhSH/FeCl_3/S$ reaction system in 90/5/5 with $\underline{n}\text{-}Pe_4N^+$, products result only via reaction 22, subsequent to establishment of equilibria 19-21.

Effects of $PhSH/Fe^{3+}$ ratio on product distributions

For the case where $R_4N^+ = \underline{n}\text{-}Bu_4N^+$ several $PhSH/Fe^{3+}$ ratios were used in the experiments described above. These results plus additional data in Table 10 show that the higher $PhSH/Fe^{3+}$ ratios favor $[Fe(SPh)_4]^{2-}$ and $[Fe_2S_2(SPh)_4]^{2-}$ as is the case in acetonitrile or methanol. However, with $[Fe_4(SPh)_{10}]^{2-}$, which arises from an effective $PhSH/Fe^{3+}$ ratio of 3.5 (accounting for the initial redox chemistry),

substantial proportions of $[Fe(SPh)_4]^{2-}$ and $[Fe_2S_2(SPh)_4]^{2-}$ are observed in 90/5/5 unlike the case in organic solvents.[59] The entry in Table 10 at 5PhSH/Fe^{3+}/S was actually a reaction of S with preformed $(\underline{n}\text{-}Bu_4N)_2[Fe(SPh)_4]$. The product of this reaction was $(\underline{n}\text{-}Bu_4N)_2[Fe_2S_2(SPh)_4]$ (> 90% yield) with only a trace of $[Fe_4S_4(SPh)_4]^{2-}$ detectable in the ^1H NMR spectrum of the isolated solid dissolved in CD_3CN (Figure 27). This result shows that $\underline{n}\text{-}Bu_4N^+$ is quite

Table 10. Product distributions from 90/5/5 with 0.1 M n-Bu_4NBr at various PhSH/Fe^{3+} mole ratios

mol PhSH/mol Fe^{3+}	Product distribution[a]
12	$[Fe(SPh)_4]^{2-}$
4 3.5[b]	$[Fe(SPh)_4]^{2-}$ > $[Fe_4(SPh)_{10}]^{2-}$ > "$[Fe_2(SPh)_6]^{2-}$"[c]
6 + S	$[Fe(SPh)_4]^{2-}/[Fe_2S_2(SPh)_4]^{2-}/[Fe_4S_4(SPh)_4]^{2-}$ ~ 4/1/0.08
5[d] + S	$[Fe_2S_2(SPh)_4]^{2-}/[Fe_4S_4(SPh)_4]^{2-}$ ~ 50
4 + S	$[Fe_2S_2(SPh)_4]^{2-}/[Fe_4S_4(SPh)_4]^{2-}$ = 8.3[e]
3.5[b] + S	$[Fe_2S_2(SPh)_4]^{2-}/[Fe_4S_4(SPh)_4]^{2-}$ ~ 3[f]

[a]Based on relative areas of m-H ^1H NMR resonances of isolated solids dissolved in CD_3CN.

[b]Using $[Fe_4(SPh)_{10}]^{2-}$, which is equivalent to PhSH/Fe^{3+} = 3.5.

[c]See text and Figures 4 and 5.

[d]Using $[Fe(SPh)_4]^{2-}$, which is equivalent to PhSH/Fe^{3+} = 5.

[e]Figure 2.

[f]Figure 6.

Figure 27. ^1H NMR spectrum in CD_3CN at ~22°C of solid isolated from the reaction of 3.4 mmol pre-isolated ($\underline{n}$-$Bu_4N)_2[Fe(SPh)_4]$ with 15 mmol sulfur in 90/5/5. Buffer was 0.20 $\underline{M}$ Tris-sulfate pH 8.5 which contained 0.10 $\underline{M}$ $\underline{n}$-Bu_4NBr. With the exception of a very small signal due to $[Fe_4S_4(SPh)_4]^{2-}$, signals are due to ($\underline{n}$-$Bu_4N)_2[Fe_2S_2(SPh)_4]$, CD_2HCN, PhSSPh and solvent impurities

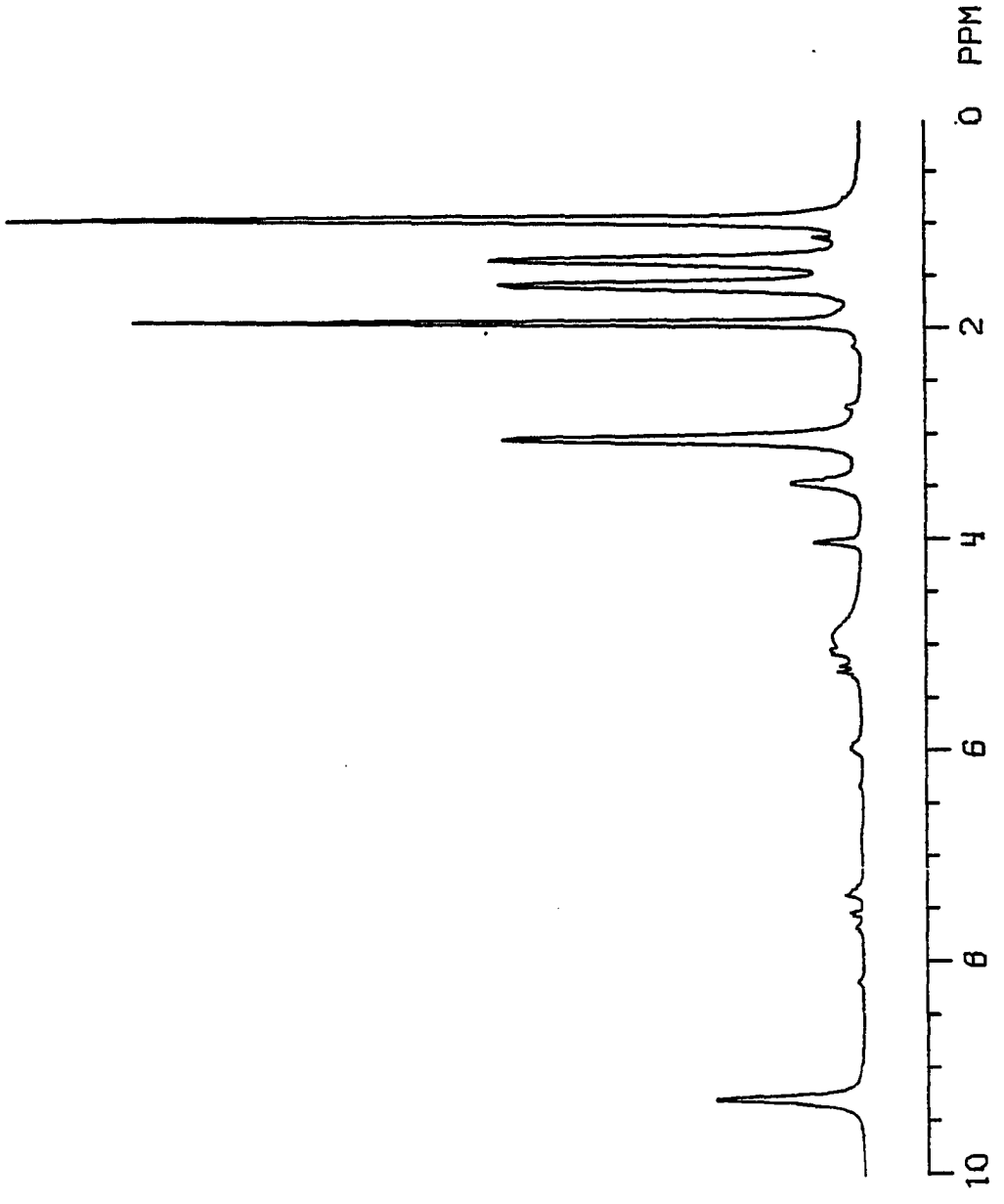
0
2
4
6
8
10
PPM

effective at suppressing reaction 17 in 90/5/5. The results at 3.5 and 4PhSH/Fe^{3+}/S thus show that although both pathways of Figure 3 occur in 90/5/5, that involving $[Fe(SPh)_4]^{2-} \rightarrow [Fe_2S_2(SPh)_4]^{2-}$ is clearly favored in the presence of $\underline{n}$-Bu_4N^+.

Effects of pH on product distributions and yields

Table 11 lists proportions of $[Fe_2S_2(SPh)_4]^{2-}$ and $[Fe_4S_4(SPh)_4]^{2-}$ and combined yields obtained for the reaction system 4PhSH/$FeCl_3$/S in 90/5/5 at various pHs. As can be seen, the optimal combination of yield and selectivity occurs in the region near pH 8 for both $[Fe_2S_2(SPh)_4]^{2-}$ and $[Fe_4S_4(SPh)_4]^{2-}$. The decreased yields at low pH are not unexpected in light of previous studies demonstrating decreased stability of the Fe_4S_4 core below pH 6.5.[112,113] Apparently, precipitation and/or solubilization in hydrophobic regions of Triton aggregates sufficiently stabilize these clusters at low pH so that yields in the range of 50% are obtainable. In fact, the yields at low pH are surprisingly high, both from the point of view of core instability and the fact that PhSH, with a pK_a of 6.4-6.8,[115] would not be substantially deprotonated, even at the initial pH of 6.0. No $[Fe(SPh)_4]^{2-}$ or $[Fe_4(SPh)_{10}]^{2-}$ were detected in the reaction products at these lower pHs. Table 11 also shows that a smaller proportion of $[Fe_2S_2(SPh)_4]^{2-}$ is obtained at these lower pHs. This latter result can be explained by protonation of PhS^- which would tend to shift equilibrium 3 to the left, thereby favoring the $[Fe_4(SPh)_{10}]^{2-} \rightarrow [Fe_4S_4(SPh)_4]^{2-}$ pathway.

Table 11. Distributions and yields of $[Fe_4S_4(SPh)_4]^{2-}$ (t^{2-}) and $[Fe_2S_2(SPh)_4]^{2-}$ (d^{2-}) at various pHs for the reaction system 4PhSH/$FeCl_3$/S in 90/5/5[a]

Final pH[b]	R_4N^+[c]	Product[d]	Combined Yield, %[e]
~ 10.5	none	t^{2-}	(73)
~ 10.5	n-Pe_4N^+	d^{2-}/t^{2-} ~ 20	n.d.[f]
8.2	none	t^{2-}	82(96)
7.9	Et_4N^+	d^{2-}/t^{2-} = 1.5	n.d.[f]
7.9	n-Pe_4N^+	d^{2-}	87
4.8	none	t^{2-}	48
4.8	Et_4N^+	t^{2-}	52
4.5	n-Pe_4N^+	d^{2-}/t^{2-} = 7.1	57

[a]Reactions were conducted and products isolated using the general procedure described in the Experimental Section.

[b]Initially the "buffers" were: pH ~ 10.5, 0.1 M LiOH; pH 8.2, 0.5 M Na-TAPS pH 8.5; pH 7.9, 0.2 M Na-TAPS pH 9.0; pH 4.5 or 4.8, 0.2 M Na-MES pH 6.0.

[c]Where "none" is entered, the product was isolated as the Et_4N^+ salt, the cation being added at 7-9 h reaction time.

[d]Where both d^{2-} and t^{2-} were obtained, the mole ratio determined by NMR is given.

[e]Yields in parentheses were determined spectrophotometrically. Others are by weight based on the starting amount of Fe and the d^{2-}/t^{2-} ratio.

[f]Not determined.

R_4N^+ metathesis

The larger proportion of $[Fe_4S_4(SPh)_4]^{2-}$ at low pH is probably not due to an increase in the rate of reaction 17. Solid $(Et_4N)_2[Fe_2S_2(SPh)_4]$ was added to 90/5/5 whose aqueous component was 0.10 M n-Pe_4NBr and 0.20 M Na-MES (sodium 4-morpholineethanesulfonate) pH 5.0. After 4 days, the mixture was filtered, yielding a faint pink filtrate pH 4.9 and a red-purple solid, which was washed with ether, water and ether, then dried in vacuo. The ^1H NMR spectrum of this solid dissolved in CD_3CN was essentially identical to that of analytically pure $(n\text{-}Pe_4N)_2[Fe_2S_2(SPH)_4]$. Thus, a metathesis reaction between excess n-Pe_4NBr and $(Et_4N)_2[Fe_2S_2(SPh)_4]$ can occur in 90/5/5 without reaction 17 even at low pH. Similarly, solid isolated after 6 days from a mixture of $(Et_4N)_2[Fe_4S_4(SPh)_4]$ in 90/5/5 containing 0.1 M n-Pe_4NBr (aqueous component 0.20 M Na-TAPS pH 9.0) gave a ^1H NMR spectrum in CD_3CN showing resonances (in addition to solvent) due only to $[Fe_4S_4(SPh)_4]^{2-}$ and n-Pe_4N^+. This latter result constitutes further evidence that under our conditions reaction 17 is irreversible.

Species present in the reaction mixture

In order to substantiate our conclusions based on the distribution of species in the isolated solids, we turned our attention to the reaction mixture itself. Figure 28 shows the ^1H NMR spectrum in the m-H region of the reaction system 4PhSH/$FeCl_3$ in 90/5/5. The reaction was assembled according to the general procedure omitting S and R_4NBr and contained 20% D_2O. Two major peaks are present at -21.4 and -15.9 ppm

relative to the HDO resonance which was assigned to -4.80 ppm. On the basis of their similar chemical shifts to those in CD_3CN we assign the -21.4 ppm resonance to $[Fe(SPh)_4]^{2-}$ (-22.5 in CD_3CN) and the -15.9 resonance to $[Fe_4(SPh)_{10}]^{2-}$ (-16.2 in CD_3CN). Although we see no direct evidence for the resonance assigned to the putative $[Fe_2(SPh)_6]^{2-}$ at -14.7 ppm in CD_3CN, the relative broadness of the -15.9 ppm resonance could represent an overlap of two resonances. The ratio of integrated intensity of the -21.4 ppm to that of the -15.9 resonance in Figure 28 is 0.61. Assuming the -15.9 ppm resonance is due entirely to $[Fe_4(SPh)_{10}]^{2-}$ and taking into account the 2/5 ratio of m-H's leads to a mole ratio $[Fe(SPh)_4]^{2-}/[Fe_4(SPh)_{10}]^{2-}$ = 1.5 for the 4PhSH/$FeCl_3$ system in 90/5/5. If no equilibrium such as 19 were operative, a mole ratio $[Fe_2S_2(SPh)_4]^{2-}/[Fe_4S_4(SPh)_4]^{2-}$ = 0.75 would be expected upon reaction with S assuming transformations via the $2[Fe(SPh)_4]^{2-} \sim [Fe_2S_2(SPh)_4]^{2-}$ and $[Fe_4(SPh)_{10}]^{2-} \sim [Fe_4S_4(SPh)_4]^{2-}$ pathways. The higher ratios of Figure 14 obtained in 90/5/5 mean that reaction with S must shift equilibrium 19 to the right, regardless of which cation is present. This conclusion is consistent with the results of Figure 26. A reaction mixture identical to that used for Figure 28 but containing 0.1 M n-Bu_4NBr gave no NMR spectrum in the region of -10 to -30 ppm. This result suggests that n-Bu_4N^+ induces tighter association of $[Fe_4(SPh)_{10}]^{2-}$ and $[Fe(SPh)_4]^{2-}$ with Triton micelles and/or formation of larger detergent aggregates which, because of longer correlation times, lowers T_2 sufficiently to prevent observation of the NMR resonances. This interpretation is fully consistent with the results discussed in previous sections.

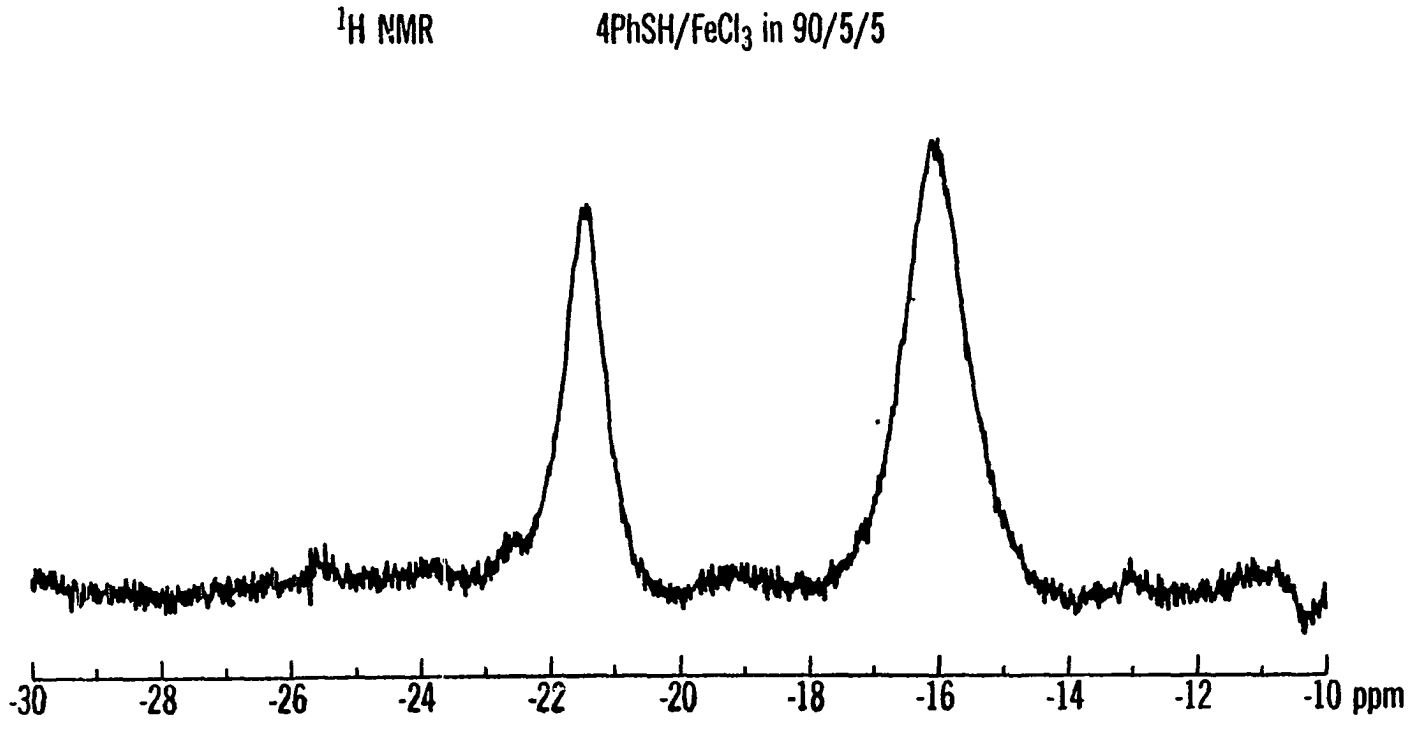

Figure 28. ^{1}H NMR spectrum in the m-H region at 278K of the reaction system 4PhSH/$FeCl_3$ in 90/5/5 prepared using the general procedure but omitting S and R_4N^+ and containing 20% D_2O. 2859 transients were collected. Each accumulation was preceded by a 3s presaturation pulse at -4.80 ppm. No other resonances were observed further downfield to -60 ppm

In order to take advantage of improved resolution and lack of solvent interference, we substituted p-fluorobenzenethiol (R_FSH) for PhSH and used ^{19}F NMR. Thus, a reaction mixture consisting of 4 $R_FSH/FeCl_3$ in 90/5/5 prepared according to the general procedure (substituting 1.55 ml R_FSH for 1.5 ml PhSH) but omitting S and R_4NBr gave the ^{19}F NMR spectrum shown at the bottom of Figure 29. Five major resonances are observed. On the basis of previous published ^{19}F NMR studies, we assign the -9.2 and 61.6 ppm resonances to $[Fe(SR_F)_4]^{2-}$ and R_FS^-, respectively. The corresponding chemical shifts in N-methyl-formamide (NMF) are -9.0 and 64.2 ppm, respectively.[128] We have found that bis-(p-fluorophenyl)disulfide (R_FSSR_F) gives a single ^{19}F resonance at 51.9 ppm in CD_3CN at 297K. On this basis, we assign the resonance at 50.5 ppm to R_FSSR_F, generated from reaction of Fe^{3+} and R_FS^-. The remaining resonances at 11.5 and 20.2 ppm we assign to the bridging and terminal thiolates, respectively, of $[Fe_4(SR_F)_{10}]^{2-}$. These assignments are based on observations of ^{19}F resonances at 11.9 and 23.0 ppm in CD_3OD of $(Et_4N)_2[Fe_4(SR_F)_{10}]$ prepared independently (see Figure 30). The ratio of the integrated intensity of the -9.2 ppm resonance to the sum of the integrated intensities of the 11.5 and 20.2 ppm resonances of Figure 29 is 0.50, close to the corresponding ratio of 0.61 for the m-H ^1H resonances of Figure 28. These data further support the existence in 90/5/5 of equilibrium 19 which, although facile, is apparently slow on the NMR time scale. Additional ^{19}F NMR studies show that at pH 6 the resonance assigned to $[Fe(SR_F)_4]^{2-}$ disappears, consistent with protonation of R_FS^- causing a shift of the equilibrium analogous to 19.

Figure 29. ^1H NMR spectra at 297K of (bottom) a portion of a reaction mixture in 90/5/5 containing 4 $R_FSH/FeCl_3$ (R_F = p-C_6H_4F) prepared according to the general procedure but omitting S and R_4N^+ and (top) a portion of the same reaction mixture a few minutes after addition of 1 mol S/mol Fe. The aqueous phase contained 1 mol LiOH/mol R_FSH, pH ~8. 512 transients were collected for each spectrum, which took ~ 6 min

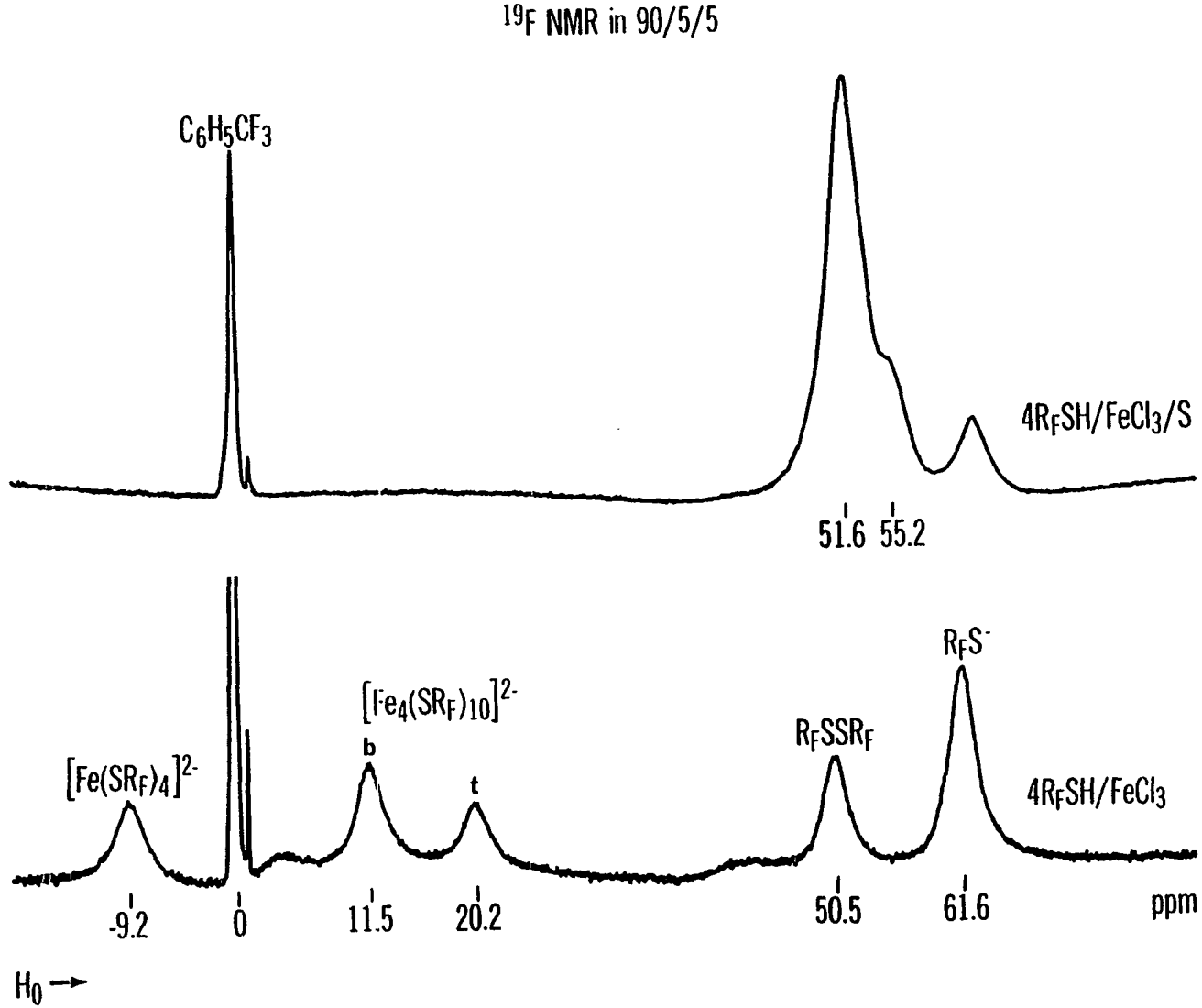
^{19}F NMR in 90/5/5
$C_6H_5CF_3$
$4R_FSH/FeCl_3/S$
51.6
55.2
R_FS^-
$[Fe_4(SR_F)_{10}]^{2-}$
b
t
R_FSSR_F
$[Fe(SR_F)_4]^{2-}$
$4R_FSH/FeCl_3$
-9.2
0
11.5
20.2
50.5
61.6
ppm
H_0 →

Figure 30. ^{19}F NMR spectrum in CD_3OD of a crude sample of $(Et_4N)_2[Fe_4(S\text{-}p\text{-}C_6H_4F)_{10}]$ prepared by the following reaction: To 160 mL methanol were added in order and anaerobically 1.01 g (3.76 mmol) $FeCl_3 \cdot 6H_2O$, 0.72 g (13 mmol) NaOMe, 3.36 g (16 mmol) Et_4NBr and 1.45 mL (13.2 mmol) p-fluorobenzenethiol. After stirring 2 h at ambient temperature, the solvent was removed in vacuo. The resulting solid, when dissolved in CD_3OD, gave this spectrum and the ^1H NMR spectrum shown in Figure 31. The signal just upfield of 0 ppm is due to an impurity in the $C_6H_4CF_3$ reference. The intense signal at 52.1 ppm is due to R_FSSR_F (R_F = p-C_6H_4F). The small signals which accompany the upfield resonances are probably due to shimming error. The signals at 11.9 and 23.0 ppm are assigned respectively to the bridging and terminal thiolates of the cluster dianion

1-24-85 FLUORINATED PHENYL ADAMANTYL

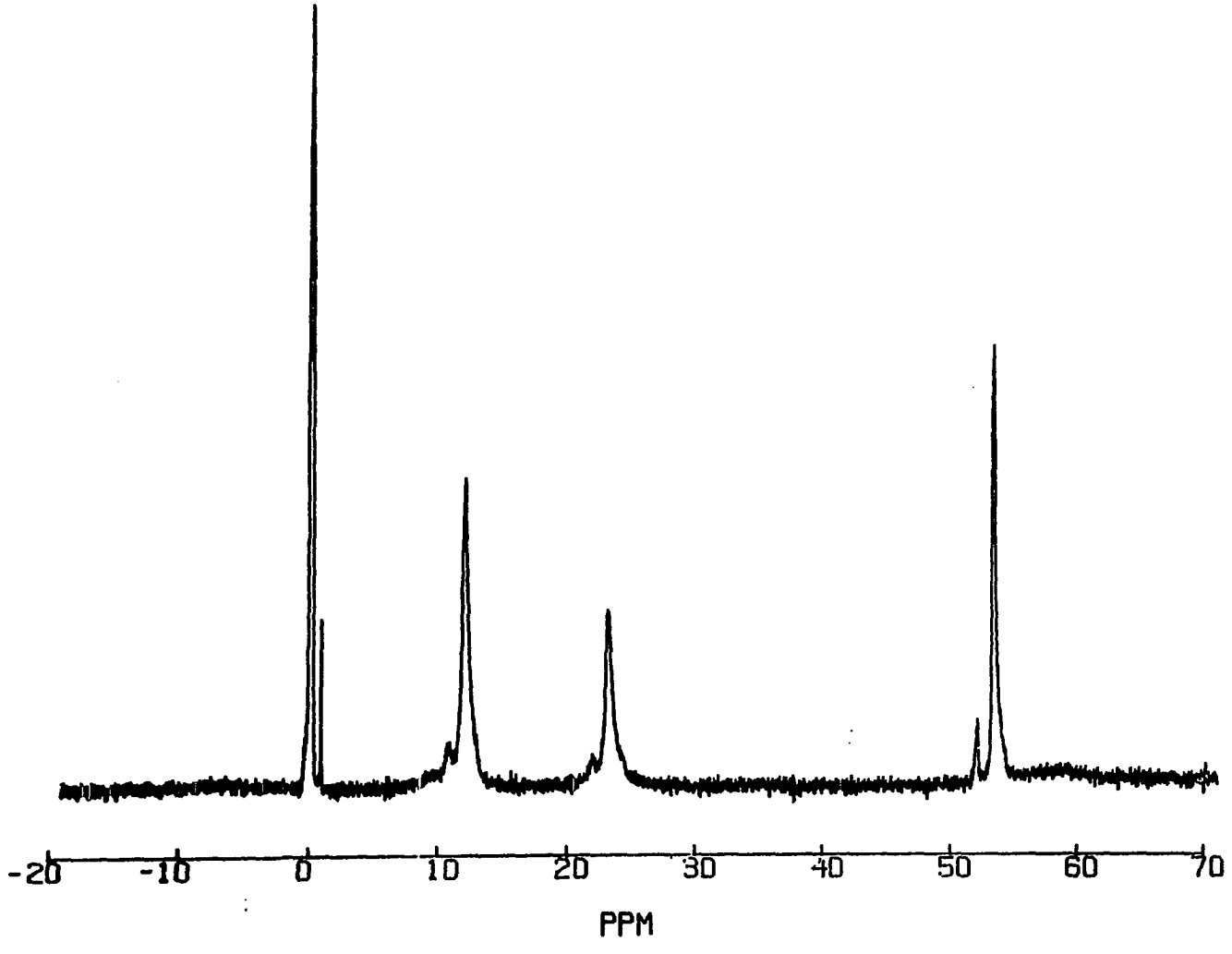

Figure 31. ^1H NMR spectrum in CD_3OD at ~ 22°C of crude $(Et_4N)_2[Fe_4(S\text{-}\underline{p}\text{-}C_6H_4F)_{10}]$. The preparation is given with the preceding figure. The doublet at -7.5 ppm is due to R_FSSR_F (R_F = $\underline{p}$-C_6H_4F). The $\underline{m}$-H region (above) attests to the formulation of the compound and to the absence of other $Fe\text{-}SR_F$ species

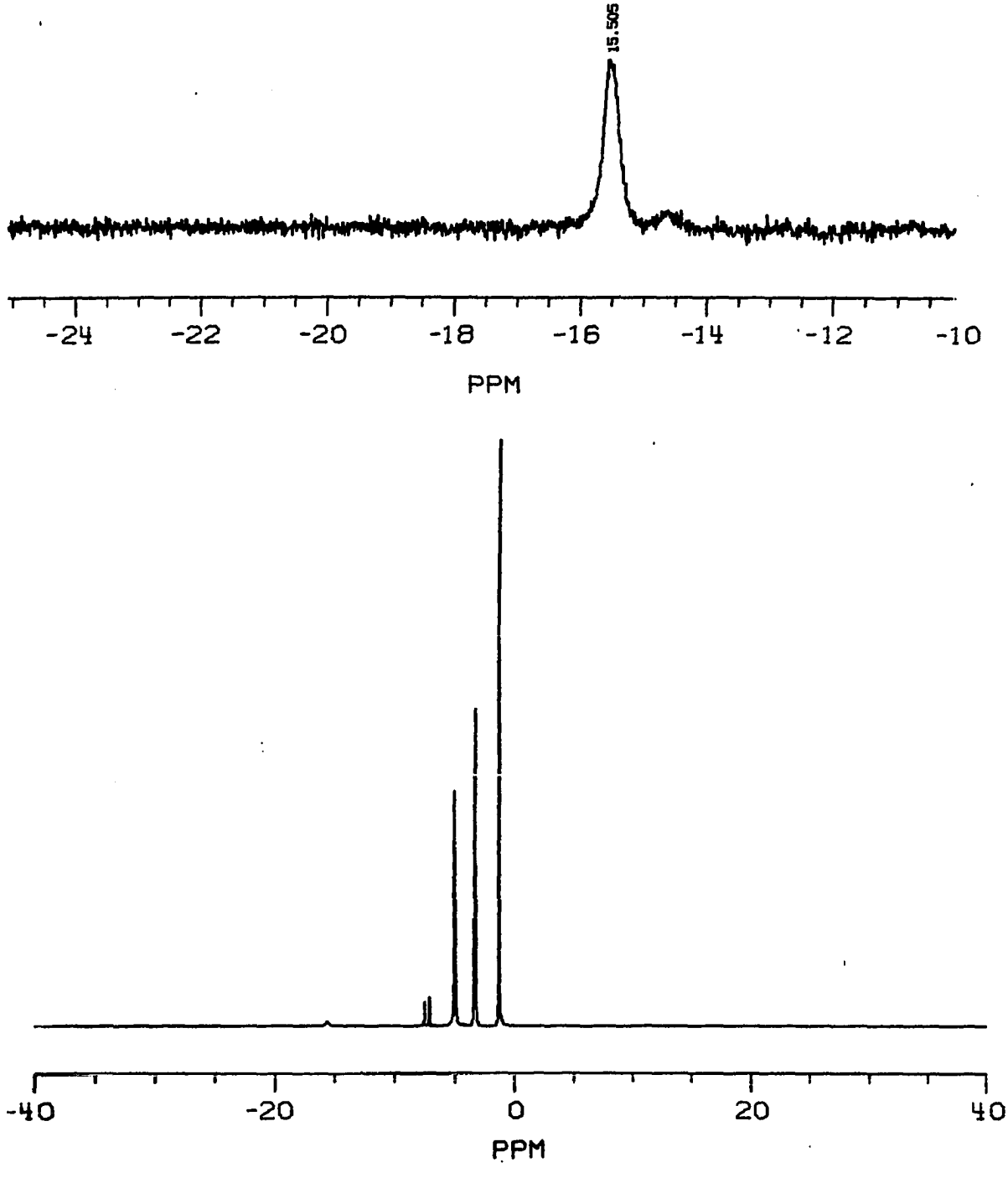
-15.505
-24
-22
-20
-18
-16
-14
-12
-10
PPM
-40
-20
0
20
40
PPM

Addition of 1 mol S/mole Fe to the reaction mixture causes complete loss of the $[Fe(SR_F)_4]^{2-}$ and $[Fe_4(SR_F)_{10}]^{2-}$ signals within the few minutes between addition of S and collection of the top spectrum of Figure 29. This rapid disappearance is probably caused by a combination of Fe(II) to Fe(III) oxidation, which would tend to shift the resonances out of the spectral window, and conversion of $[Fe(SR_F)_4]^{2-}$ to $[Fe_2S_2(SR_F)_4]^{2-}$ and $[Fe_4(SR_F)_{10}]^{2-}$ to $[Fe_4S_4(SR_F)_4]^{2-}$. The resonance at 51.6 ppm is likely due to a combination of R_FSSR_F and $[Fe_2S_2(SR_F)_4]^{2-}$ with the shoulder at 55.2 ppm due to $[Fe_4S_4(SR_F)_4]^{2-}$. (The ^{19}F chemical shifts of $[Fe_2S_2(SR_F)_4]^{2-}$ and $[Fe_4S_4(SR_F)_4]^{2-}$ in NMF are 50.5 and 54.6 ppm, respectively.[128])

A reaction conducted according to the general procedure with $R_4N^+ = Et_4N^+$ but substituting 1.55 mL R_FSH for PhSH and 1 mol LiOH/mol R_FSH for buffer led to a solid whose ^1H NMR spectrum in CD_3CN (shown in Figure 32) gave m-H resonances at -8.9 ppm assigned to $[Fe_2S_2(SR_F)_4]^{2-}$ (d_F^{2-}) and -7.9 ppm assigned to $[Fe_4S_4(SR_F)_4]^{2-}$ (t_F^{2-}). Integrations of these resonances gave a ratio of $d_F^{2-}/t_F^{2-} = 4.0$ compared to the analogous ratio of 1.5 when PhSH is used (cf. Figure 14). Thus, the general features ofthe $4PhSH/FeCl_3/S$ and $4R_FSH/FeCl_3/S$ reactions in 90/5/5 are similar to each other.

Summary

Figure 11 summarizes most of the results discussed above. Many features of the ≥ 3.5 $PhS^-/FeCl_3/S$ reaction system in 90/5/5 are similar to those observed or expected in organic solvents.[59] These include

Figure 32a. ^1H NMR spectrum in CD_3CN at ~22°C of solid isolated from a reaction performed according to the general procedure but in which 1.55 mL p-FC_6H_4SH replaced PhSH and equimolar LiOH replaced buffer. No other signals were observed outside the region shown. Signals not due to Et_4N^+, CD_2HCN, $[Fe_nS_n(SR_F)_4]^{2-}$ or R_FSSR_F are due to solvent impurities

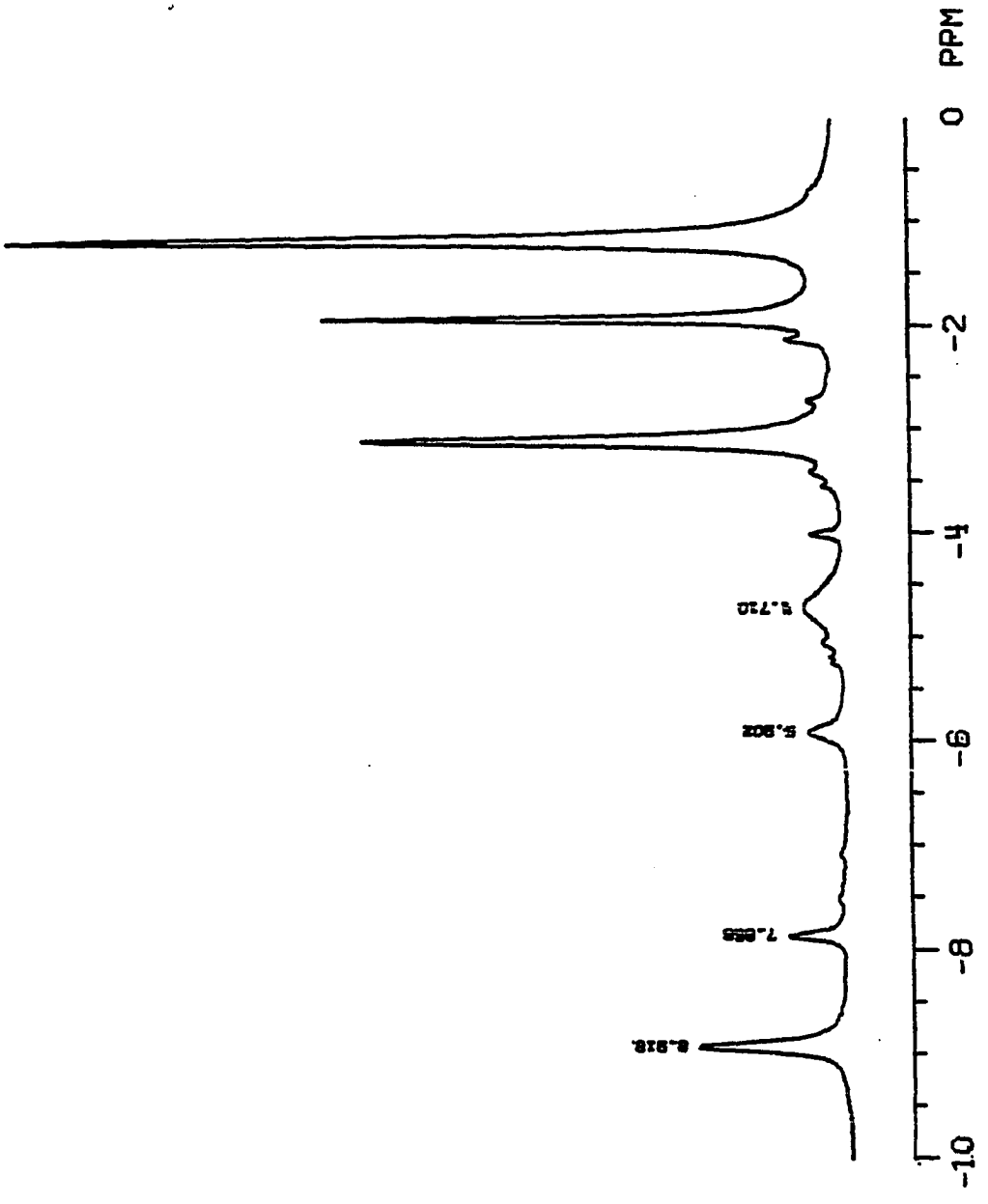
8.818
7.885
5.802
5.730
0 PPM
-2
-4
-6
-8
-10

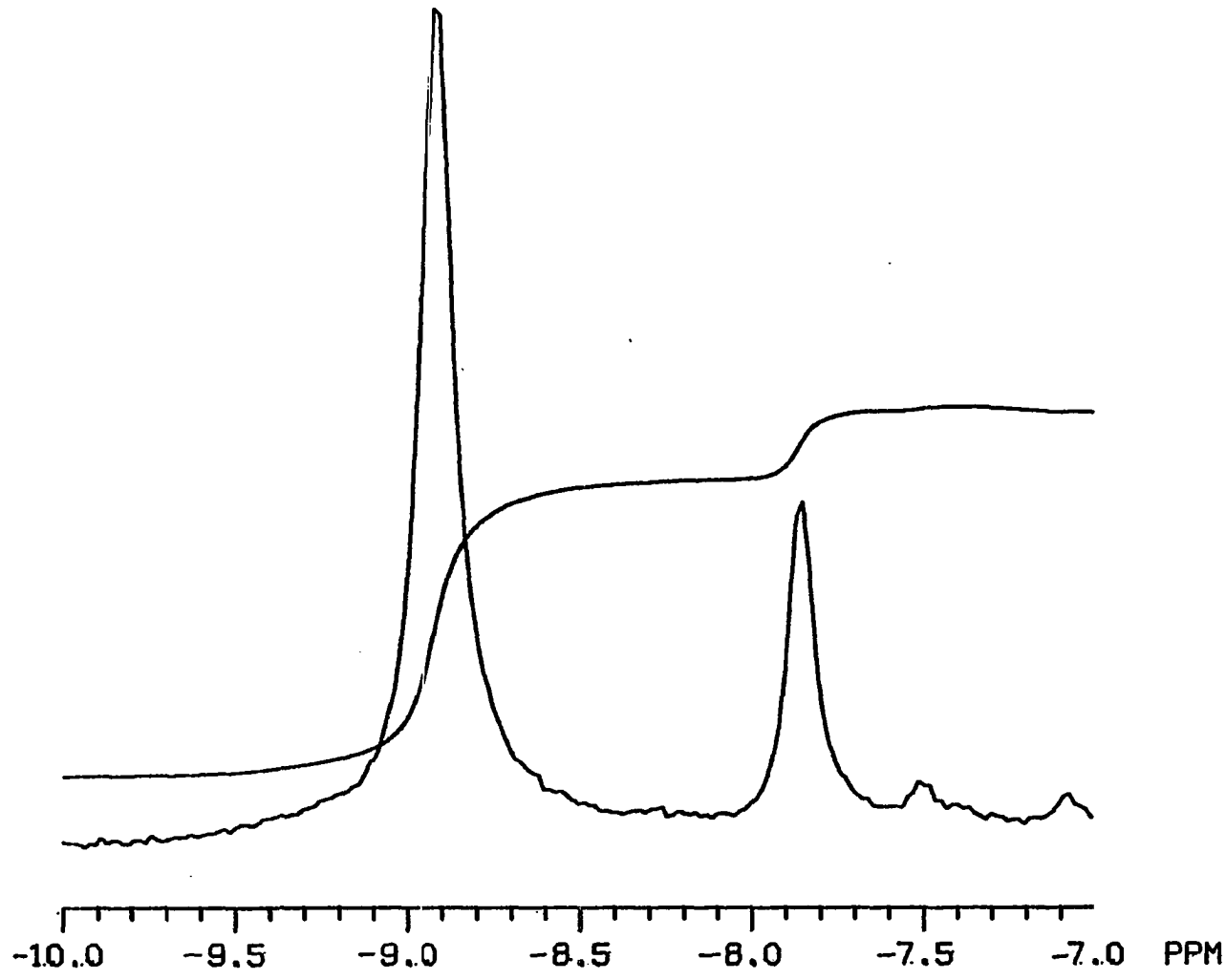

Figure 32b. Expansion of the m-H region of the preceding figure

occurrence of both the $[Fe(SPh)_4]^{2-} \rightarrow [Fe_2S_2(SPh)_4]^{2-} \rightarrow [Fe_4S_4(SPh)_4]^{2-}$ and $[Fe_4(SPh)_{10}]^{2-} \rightarrow [Fe_4S_4(SPh)_4]^{2-}$ pathways at $4PhS^-/FeCl_3$, favoring of the former pathway at > $4PhS^-/FeCl_3$ ratios, nearly quantitative formation of $[Fe_4S_4(SPh)_4]^{2-}$ in the absence of R_4N^+ and the trapping of $[Fe_2S_2(SPh)_4]^{2-}$ by addition of R_4N^+ at the outset of the reaction. The two most prominent unique features in 90/5/5 are (i) the facility with which equilibria 19-21 can be shifted, and (ii) the ability of detergent aggregates to shield $[Fe_2S_2(SPh)_4]^{2-}$ from water in the presence of relatively hydrophobic R_4N^+, thereby inhibiting conversion to $[Fe_4S_4(SPh)_4]^{2-}$. The foremost consequence of these unique features is the essentially quantitative production of either $[Fe_2S_2(SPh)_4]^{2-}$ or $[Fe_4S_4(SPh)_4]^{2-}$ from the same $4PhSH/FeCl_3/S$ reagent ratio. A second unique consequence is the production of substantial proportions of $[Fe_2S_2(SPh)_4]^{2-}$ upon reaction of $[Fe_4(SPh)_{10}]^{2-}$ with S (Figure 26). Thus, equilibrium 19 can be shifted to the right either by reaction with S or by ion pairing with relatively hydrophobic R_4N^+ (Figures 22 and 23). That equilibrium 19 can be shifted to the left in 90/5/5 is supported by the isolation of only $(Et_4N)_2[Fe_4(SPh)_{10}]$ from the $12PhS^-/FeCl_3$ mixture and by the increased proportion of $[Fe_4S_4(SPh)_4]^{2-}$ obtained at lower pH (Table 11). A third consequence is that pHs below the pK_a of PhSH are no deterrent to the production of ~50% yields of $(R_4N)_2[Fe_nS_n(SPh)_4]$ (n = 2,4).

At least for simple ferredoxins $[Fe(S\text{-}Cys)_4]^{2-} \rightarrow [Fe_2S_2(S\text{-}Cys)_4]^{2-} \rightarrow [Fe_4S_4(S\text{-}Cys)_4]^{2-}$ is an attractive (though unproven) pathway for [4Fe-4S] site assembly since all three sites are known to occur

naturally, and since most ferredoxins contain fewer than 10 Cys per molecule.[63,129,130] However, if similarly facile equilibria such as 19-21 occur when Fe^{2+} is inserted into an apoferredoxin, then, even if species such as $[Fe_4(S\text{-}Cys)_{10}]^{2-}$ or, perhaps more likely, $[Fe_2(S\text{-}Cys)_6]^{2-}$ form initially, small changes in protein conformation or in pH could tend to favor $[Fe(S\text{-}Cys)_4]^{2-}$. Furthermore, if as our results suggest, reaction with S shifts equilibria 19-21 to the right, then $[Fe(S\text{-}Cys)_4]^{2-}$ need not necessarily be the predominant species prior to incorporation of core sulfide.[131] Finally, our results suggest that a hydrophobic site would tend to favor $[Fe_2S_2(S\text{-}Cys)_4]^{2-}$ over $[Fe_4S_4(S\text{-}Cys)_4]^{2-}$ if assembled from $[Fe(S\text{-}Cys)_4]^{2-}$.

REFERENCES

1. Holm, R.H. Acc. Chem. Res. 1977, 10, 427-434.

2. San Pietro, A.; Lang, H.M. J. Biol. Chem. 1958, 231, 211-229.

3. Appella, E.; San Pietro, A. Biochem. Biophys. Res. Commun., 1962, 6, 349-354.

4. Fry, K.T.; San Pietro, A. Biochem. Biophys. Res. Commun. 1962, 9, 218-221.

5. Mortenson, L.E.; Valentine, R.C.; Carnahan, J.E. Biochem. Biophys. Res. Commun. 1962, 7, 448-452.

6. Tagawa, K.; Arnon, D.I. Nature 1962, 195, 537-543.

7. Bartsch, R.G. Bacterial Photosynthesis 315, Gest, H.; San Pietro, A.; Vernon, L.P., Eds.; Antioch Press: Yellow Springs, Ohio, 1963.

8. Massey, V. J. Biol. Chem. 1957, 229, 763-770.

9. a. Lovenberg, W.; Sobel, B.E. Proc. Nat. Acad. Sci. U.S. 1965, 54, 193-199. b. Lovenberg, W.; Sobel, B.E. Federation Proc. 1965, 24, 233.

10. Lovenberg, W.; Buchanan, B.B.; Rabinowitz, J.C. J. Biol. Chem., 1963, 238, 3899-3913.

11. a. Malkin, R.; Rabinowitz, J.C. Biochemistry 1966, 5, 1262-1268. b. Rabinowitz, J.C. Meth. Enzymol. 1972, 24, 431-446.

12. Bayer, E.; Eckstein, H.; Hagenmaier, H.; Josef, D.; Koch, J.; Krauss, P.; Roder, A.; Schretzmann, P. Eur. J. Biochem. 1969, 8, 33-49.

13. Gillum, W.O.; Mortenson, L.E.; Chen, J.-S.; Holm, R.H. J. Am. Chem. Soc. 1977, 99, 584-595.

14. Averill, B.A.; Bale, J.R.; Orme-Johnson,W.H. J. Am. Chem. Soc. 1978, 100, 3034-3043.

15. Wong, G.B.; Kurtz, D.M., Jr.; Holm, R.H.; Mortenson, L.E.; Upchurch, R.G. J. Am. Chem. Soc. 1979, 101, 3078-3090.

16. Coles, C.J.; Holm, R.H.; Kurtz, D.M., Jr.; Orme-Johnson, W.H.; Rawlings, J.; Singer, T.P.; Wong, G.B. Proc. Nat. Acad. Sci. U.S.A. 1979, 76, 3805-3808.

17. Kurtz, D.M., Jr.; McMillan, R.S.; Burgess, B.K.; Mortenson, K.E.; Holm, R.H. Proc. Nat. Acad. Sci. U.S.A. 1979, 76, 4986-4989.

18. Lovenberg, W.; Williams, W.M. Biochemistry 1969, 8, 141-148.

19. Rao, K.K.; Cammade, R.; Hall, D.O.; Johnson, C.E. Biochem. J. 1971, 122, 257-265.

20. Moulis, J.M.; Meyer, J. Biochemistry 1982, 21, 4762-4771.

21. Benson, A.M.; Mower, H.F.; Yasunobu, K.T. Proc. Nat. Acad. Sci. U.S., 1966, 55, 1532-1535.

22. Tanaka, M.; Nakashima, T.; Benson, A.; Mower, H.; Yasunobu, K.T. Biochemistry 1966, 5, 1666-1681.

23. Tsunoda, J.N.; Yasunobu, K.T.; Whitely, H.R. J. Biol. Chem. 1968, 243, 6262-6272.

24. Christou, G.; Ridge, B.; Rydon, H.N. J. Chem. Soc. Chem. Commun. 1979, 20-21.

25. Sugiura, Y.; Ishuzu, K.; Kimuro, T. Biochem. Biophys. Res. Commun. 1979, 60, 334-340.

26. Hong, J.-S.; Rabinowitz, J.C. Biochem. Biophys. Res. Commun. 1967, 29, 246-252.

27. Yang, C.S.; Huennekens, F.M. Biochemistry 1970, 9, 2127-2133.

28. Herskovitz, T.; Averill, B.A.; Holm, R.H.; Ibers, J.A.; Phillips, W.D.; Weiher, J.F. Proc. Nat. Acad. Sci. U.S.A. 1972, 69, 2437-2441.

29. Carter, C.W., Jr.; Freer, S.T.; Xuong, Ng.H.; Alden, R.A.; Kraut, J. Cold Spring Harbor Symp. Quant. Biol. 1971, 36, 381-385.

30. Averill, B.A.; Herskovitz, T.; Holm, R.A.; Ibers, J.A. J. Am. Chem. Soc. 1973, 95, 3523-3534.

31. Mayerle, J.J.; Frankel, R.B.; Holm, R.H.; Ibers, J.A.; Phillips, W.D.; Weiher, J.F. Proc. Nat. Acad. Sci. U.S.A., 1973, 70, 2429-2433.

32. Mayerle, J.J.; Denmark, S.E.; DePamphilis, B.V.; Ibers, J.A.; Holm, R.H. J. Am. Chem. Soc. 1975, 97, 1032-1045.

33. Gibson, J.F.; Hall, D.O.; Thornley, J.H.M.; Whatley, F.R. Proc. Nat. Acad. Sci. U.S. 1966, 56, 987-990.

34. Brintzinger, H.; Palmer, G.; Sands, R.H. Proc. Nat. Acad. Sci. U.S. 1966, 55, 397-404.

35. Buchanan, B.B.; Lovenberg, W.; Rabinowitz; J.C. Proc. Nat. Acad. Sci. U.S. 1963, 49, 345-353.

36. Mortenson, L.E. Biochim. Biophys. Acta 1964, 81, 71-77.

37. Eaton, W.A.; Lovenberg, W. in Iron-Sulfur Proteins Vol. II, Lovenberg, W., Ed.; Academic Press: New York, 1973; Chapter 3.

38. Herriott, J.R.; Sieker, L.C.; Jensen, L.H.; Lovenberg, W. J. Mol. Biol. 1970, 50, 391-406.

39. Watenpaugh, K.D.; Sieker, L.C.; Herriott, J.R.; Jensen, L.H. Cold Spring Harbor Symp. Quant. Biol. 1971, 36, 359.

40. Holah, D.G.; Coucouvanis, D. J. Am. Chem. Soc. 1975, 97, 6917-6919.

41. Coucouvanis, D.; Hollander, F.J.; West, R.; Eggerding, D. J. Am. Chem. Soc. 1974, 96, 3006-3008.

42. Lane, R.W.; Ibers,J.A.; Frankel, R.B.; Holm, R.H. Proc. Nat. Acad. Sci. U.S. 1975, 72, 2868-2872.

43. Lane, R.W.; Ibers, J.A.; Frankel, R.B.; Papaefthymiou, G.C.; Holm, R.H. J. Am. Chem. Soc. 1977, 99, 84-98.

44. Watenpaugh, K.D.; Sieker, L.C.; Jensen, L.H. J. Mol. Biol. 1979, 131, 509-522.

45. Watenpaugh, K.D.; Seiker, L.C.; Jensen, L.H. J. Mol. Biol. 1980, 138, 615-633.

46. Shethna, Y.I. Biochim. Biophys. Acta 1970, 205, 58-62.

47. Yoch, D.C.; Arnon, D.I. J. Biol. Chem. 1972, 247, 4514-4520.

48. Sweeney, W.V.; Rabinowitz, J.C.; Yoch, D.C. J. Biol. Chem. 1975, 250, 7842-7847.

49. Howard, J.B.; Lorsbach, T.; Que, L., Jr. Biochem. Biophys. Res. Commun. 1976, 70, 582-588.

50. Private communication by W.V. Sweeney quoted in Orme-Johnson, W.H. and Orme-Johnson, N.R. in Iron-Sulfur Proteins T. Spiro, Ed.; John Wiley & Sons: New York, 1982; Chapter 2.

51. Stout, C.D.; Ghosh, D.; Pattaldri, V.; Robbins, A. J. Biol. Chem., 1980, 255, 1797-1800.

52. Hunah, B.H.; Moura, J.J.G.; Moura, I.; Kent, T.A.; LeGall, J.; Xavier, A.V.; Munck, E. J. Biol. Chem., 1980, 255, 3242-3244.

53. Morgan, T.V.; Stephens, P.J.; Burgess, B.K.; Stout, C.D. FEBS Lett. 1984, 167, 137.

54. Emptage; M.H.; Dreyer, J.-L.; Kennedy, M.C.; Beinert, H. J. Biol. Chem. 1983, 258, 11106-11111.

55. Schrauzer, G.N.; Keifer, G.W.; Trano, K.; Doemeny, P.A. J. Am. Chem. Soc. 1974, 96, 641-652.

56. Christou, G.; Ridge, B.; Rydon, H.N. J. Chem. Soc. Dalton 1978, 1423-1425.

57. Christou, G.; Garner, C.D. J. Chem. Soc. Dalton, 1979, 1093-1094.

58. Reynolds, J.G.; Holm, R.H. Inorg. Chem., 1980, 19, 3257-3260.

59. Hagen, K.S.; Reynolds, J.G.; Holm, R.H. J. Am. Chem. Soc. 1981, 103, 4054-4063.

60. Millar, M.; Lee, J.F.; Koch, S.A.; Fikar, R. Inorg. Chem., 1982, 21, 4105-4106.

61. Holm, R.H.; Ibers, J.A. In "Iron-Sulfur Proteins", Vol. III, W. Lovenberg, Ed.; Academic Press: New York, 1977; Chapter 7.

62. Ibers, J.A.; Holm, R.H. Science 1980, 209, 223-235.

63. Berg, J.M.; Holm, R.H. In "Iron-Sulfur Proteins", T.G. Spiro, Ed.; John Wiley & Sons: New York, 1982; Chapter 1.

64. Coucouvanis, D.; Swenson, D.; Baenziger, N.C.; Holah, D.G.; Kostikas, A.; Simopolous, A.; Petrouleas, V. J. Am. Chem. Soc., 1976, 98, 5721-5723.

65. Shulman, R.G.; Eisenberger, P.; Teo, B.-K.; Kincaid, B.M.; Brown, G.S. J. Mol. Biol. 1978, 124, 305-321.

66. Bobrik, M.A.; Hodgson, K.O.; Holm, R.H. Inorg. Chem. 1977, 16, 1851-1858.

67. Que, L., Jr.; Bobrik, M.A.; Ibers, J.A.; Holm, R.H. J. Am. Chem. Soc. 1974, 96, 4168-4177.

68. Laskowski, E.J.; Frankel, R.B.; Gillum, W.O.; Papaefthymiou, G.C.; Renaud, J.; Ibers, J.A.; Holm, R.H. J. Am. Chem. Soc. 1978, 100, 5322-5337.

69. Carrell, H.L.; Glusker, J.P.; Job, R.; Bruice, T.C. J. Am. Chem. Soc. 1977, 99, 3683-3690.

70. Hagen, K.S.; Berg, J.M.; Holm, R.H. Inorg. Chim. Acta 1980, 45, L17-L18.

71. Holm, R.H.; Phillips, W.D.; Averill, B.A.; Mayerle, J.J.; Herskovitz, T. J. Am. Chem. Soc. 1974, 96, 2109-2117.

72. Bobrik, M.A.; Que, L., Jr.; Holm, R.H. J. Am. Chem. Soc. 1974, 96, 285-286.

73. Dukes, G.R.; Holm, R.H. J. Am. Chem. Soc. 1975, 97, 528-533.

74. DePamphilis, B.V.; Averill, B.A.; Herskovitz, T.; Que, L., Jr.; Holm, R.H. J. Am. Chem. Soc. 1974, 96, 4159-4167.

75. Que, L., Jr.; Anglin, J.R.; Bobrik, M.A.; Davison, A.; Holm, R.H. J. Am. Chem Soc. 1974, 96, 6042-6048.

76. A study of equilibrium formation constants of related complexes is presented in Burt, R.J.; Ridge, B.; Rydon, H.N. J. Chem. Soc. Dalton, 1980, 1228-1235.

77. Hong, J.-S.; Rabinowitz, J.C. J. Biol. Chem. 1970, 245, 6582-6587.

78. Reynolds, J.G.; Holm, R.H. Inorg. Chem. 1981, 20, 1873-1878.

79. Bobrik, M.A.; Laskowski, E.J.; Johnson, R.W.; Gillum, W.O.; Berg, J.M.; Hodgson, K.O.; Holm, R.H. Inorg. Chem. 1978, 17, 1402-1410.

80. Reynolds, J.G.; Holm, R.H. Inorg. Chem. 1980, 19, 3257-3260.

81. Reynolds, J.G.; Coyle, C.L.; Holm, R.H. J. Am. Chem. Soc. 1980, 102, 4350-4355.

82. Wong, G.B.; Bobrik, M.A.; Holm, R.H. Inorg. Chem. 1978, 17, 578-584.

83. Stevens, W.C.; Kurtz, D.M., Jr. unpublished work, Chemistry Department, Iowa State University, Ames, IA (pereant qui ante nos nostra dixerunt)

84. Pearson, R.G.; Songstad, J. J. Am. Chem. Soc. 1967, 89, 1827-1836.

85. Pearson, R.G.; Sobel, H.; Songstad, J. J. Am. Chem. Soc. 1968, 90, 319-326.

86. Complexes $[Fe_4X_4(SePh)_4]^{2-}$ (X=S,Se) have been prepared by reaction of $[Fe_4X_4(S\text{-}\underline{t}\text{-}Bu)_4]^{2-}$ and PhSeSePh.[79] These reactions suggest the initial step of thiolate dissociation followed by
2 $\underline{t}$-BuS$^-$ + PhSeSePh → $\underline{t}$-BuSS-$\underline{t}$-Bu + 2 PhSe$^-$.

87. Johnson, R.W.; Holm, R.H. J. Am. Chem. Soc. 1978, 100, 5338-5344.

88. Coucouvanis, D.; Kanatzidis, M.; Simhon, E.; Baenziger, N.C. J. Am. Chem. Soc. 1982, 104, 1874-1882.

89. Hagen, K.S.; Holm, R.H. J. Am. Chem. Soc. 1982, 104, 5496-5497.

90. Hagen, K.S.; Holm, R.H. Inorg. Chem. 1984, 23, 418-427.

91. Cambray, J.; Lane, R.W.; Wedd, A.G.; Johnson, R.W.; Holm, R.H. Inorg. Chem. 1977, 16, 2565-2571.

92. Hagen, K.S.; Watson, A.D.; Holm, R.H. J. Am. Chem. Soc. 1983, 105, 3905-3913.

93. Schick, M.J., Ed., "Nonionic Surfactants"; Marcel Dekker: New York, 1967.

94. Bailey, F.E., Jr.; Koleske, J.V. "Poly(ethylene oxide)"; Academic Press: New York, 1976.

95. Gratzel, M.; "Micellization and Microemulsions", Mitell, K.L., Ed.; Plenum Press: New York, 1977; Vol. 2, p. 531.

96. Fendler, J.H. "Membrane Mimetic Chemistry" Chem. and Eng. News, Jan. 2, 1984, 25-38.

97. Robson, R.J.; Dennis, E.A. Acc. Chem. Res. 1983, 16, 251-258.

98. Gratzel, M. Acc. Chem. Res. 1981, 14, 376-384.

99. Fendler, J.H. Acc. Chem. Res. 1980, 13, 7-13.

100. Calvin, M. Acc. Chem. Res. 1978, 11, 369-374.

101. Becker, P., Ed., "Nonionic Surfactants"; Marcel Dekker: New York, 1967; pp. 478-515.

102. Ray, A.; Nemethy, G. J. Am Chem. Soc. 1971, 93, 6787-6793.

103. Robson, R.J.; Dennis, E.A. J. Phys. Chem. 1977, 81, 1075-1078.

104. Paradies, H.H. J. Phys. Chem. 1980, 84, 599-607.

105. Mandel, A.B.; Ray, S.; Biswas, A.M.; Moulik, S.P. J. Phys. Chem. 1980, 84, 856-859.

106. Ribeiro,A.A.; Dennis, E.A. Biochemistry 1975, 14, 3746-3755.

107. Podo, F.; Ray, A.; Nemethy, G. J. Am. Chem. Soc. 1973, 95, 6164-6171.

108. Ribeiro,A.A.; Dennis, E.A. J. Phys. Chem. 1977, 81, 957-963.

109. Kurtz, D.M., Jr. Biochem. Biophys. Res. Commun. 1982, 104, 437-442.

110. Bonomi, F.; Kurtz, D.M., Jr. Biochemistry 1982, 21, 6838-6843.

111. Kurtz, D.M., Jr. Inorg. Chim. Acta 1983, 80, L75-L76.

112. Bruice, T.C.; Maskiewicz, R.; Job, R. Proc. Nat. Acad. Sci. U.S.A. 1975, 72, 231-234.

113. Job, R.C.; Bruice, T.C. Proc. Nat. Acad. Sci. U.S.A. 1975, 72, 2478-2482.

114. Hill, C.L.; Renaud, J.; Holm, R.H.; Mortenson, L.E. J. Am. Chem. Soc. 1977, 99, 2549-2557.

115. Simon, J.; LeMoigne, J.; Markovitski, D.; Dayantis, J. J. Am. Chem. Soc. 1980, 102, 7247-7252.

116. Cole, G.M., Jr. In "Inorganic Reactions in Organized Media" ACS Symposium Series 117, Holt, S.L., Ed.; American Chemical Society: Washington, D.C., 1982; pp. 157-163.

117. Pramauro, E.; Pelizetti, E.; Diekmann, S.; Frahm, J. Inorg. Chem. 1982, 21, 2432-2436, and references therein.

118. Foreman, T.K.; Sobol, W.M.; Whitten, D.G. J. Am. Chem. Soc. 1981, 103, 5333-5336.

119. Brugger, P.A.; Infelta, P.P.; Brown, A.M.; Gratzel, M. J. Am. Chem. Soc. 1981, 103, 320-326.

120. Shriver, D.F. The Manipulation of Air-Sensitive Compounds; McGraw-Hill: New York, 1969.

121. Kurtz, D.M., Jr.; Stevens, W.C. J. Am. Chem. Soc. 1984, 106, 1523-1524.

122. Chau, M.M.; Kice, J.L. J. Am. Chem. Soc. 1976, 98, 771-7716.

123. Hereafter this solvent will be referred to as 90/5/5.

124. (a) Jencks, W.P.; Salveson, K. J. Am. Chem. Soc. 1971, 93, 4433-4436. (b) Moss, R.A.; Dix, F.M. J. Org. Chem. 1981, 46, 3029-3035. (c) Daneny, J.P.; Parameswaran, K.N. J. Chem. Eng. Data 1968, 13 386-389.

125. Maclay, W.N. J. Colloid Sci. 1956, 11, 272-285.

126. The cloud point is the sudden onset of turbidity of an aqueous nonionic surfactant solution upon exceeding a certain critical temperature. The hydration of the oxyethylene chains accounts for the solubility of the surfactant and increased temperature is believed to cause partial dehydration of the chains. At the cloud point, the solution separates into two isotropic phases, one enriched and the other depleted in surfactant.[97]

127. The reverse process constitutes a possible pathway for assembly of $[Fe_4(SPh)_{10}]^{2-}$ from $[Fe(SPh)_4]^{2-}$.

128. Mascharak, P.K.; Smith, M.C.; Armstrong, W.H.; Burgess, B.K.; Holm, R.H. Proc. Nat. Acad. Sci. U.S.A. 1982, 79, 7056-7060.

129. Yasunobu, K.T.; Tanaka, M. in Iron-Sulfur Proteins Vol. 2, Lovenberg, W., Ed.; Academic Press: New York, 1972; pp. 27-130.

130. Howard, J.B.; Lorsbach, T.W.; Ghosh, D.; Melis, K.; Stout, C.D. J. Biol. Chem. 1983, 258, 508-522.

131. The source of core sulfide in vivo is unknown. It has recently been found that the outer sulfur of $S_2O_3^{2-}$ in the presence of the enzyme rhodanese and lipoic acid will furnish core sulfide during assembly of $[Fe_4S_4(SPh)_4]^{2-}$ in 90/5/5.[132] This enzymatic system has been shown to reconstitute apoferredoxins in vitro.

132. Bonomi, F.; Werth, M.; Kurtz, D.M., Jr., Inorg. Chem. 1985, 24, 4331-4335.

133. Pagani, S.; Bonomi, F.; Cerletti, P. Eur. J. Biochem. 1984, 142, 361-366.

134. Bonomi, F.; Pagani, S.; Kurtz, D.M., Jr. Eur. J. Biochem. 1985, 148, 67-73.

ACKNOWLEDGEMENTS

Thanks are due Drs. Dee-Hua Huang and R. David Scott for obtaining the NMR spectra of aqueous solutions and for their helpfulness with other things. Mark T. Werth and Wayne K. Jones contributed experimentally to this work, for which I am grateful.

My major professor, Dr. Donald M. Kurtz, Jr., has had to endure years of disquietude owing, in no small way, to a certain recalcitrance on my part. As he will be leaving ISU shortly after me, with him go my sincere best wishes for success and happiness.

My committee, Drs. Robert E. McCarley, John G. Verkade, Thomas J. Barton and Dennis K. Ross, deserve my gratitude for not throwing me out of here years ago. In particular, Tom Barton has been a friend and confidant to whom I owe much. I will not soon forget our motorcycle trip to Minneapolis: our olfactory acuity having located every small-town bar on route 13, we failed to recognize the Twin Cities and were some distance north of St. Paul before realizing our mistake.

My parents, Robert and Jean Stevens, have sacrificed greatly in helping me to achieve this degree and they have been driven nearly insane waiting for me to finish it. My thanks, apologies and love to them.

My running partners, Tom Weber, Charlie Hammer and, until recently, Russ Pounds, have been a daily source of irritation to me. Their encouragement, effectively disguised as ridicule, is acknowledged.

Dr. John W. Patterson has been a special friend owing to our similar intellectual interests and capacities for beer. His wife, Shirley, deserves my thanks for the many times Jack brought me home with him on little or no notice and for the many meals she prepared for me. Though I am sure to stay in touch, I will miss our frequent challenging conversations on ethics, religion and thermodynamics.

Those conversations took place, for the most part, in Tork's Pub and Dugan's Deli. Many of the denizens of those establishments have become cherished friends who are partly responsible for whatever measure of sanity I have left. They will be missed.

The chemistry department depends upon the skills and hard work of a lot of support personnel and can do so with great confidence. I am pleased to say that I've made many friends among them and would now like to thank them for what usually felt like special attention. Thanks go particularly to Sue Cafferty for her expert work on this manuscript.

Finally, a special acknowledgement to a fine friend, Roger D. Murphy, whose companionship has seen me through some difficult times. When things seemed darkest for me, there would always be some discernible extra effort in the grilled T-bones and martinis he provided. When I ran out of money near the end, he took me into his home. It seems unlikely to me that this work would have ever been finished without his selfless friendship.